MASS DEPENDENT STABLE ISOTOPE FRACTIONATION OF MERCURY DURING ITS MICROBIAL TRANSFORMATIONS

by

KRITEE

A dissertation submitted to the Graduate School-New Brunswick

Rutgers, The State University of New Jersey

and

The Graduate School of Biomedical Sciences

University of Medicine and Dentistry of New Jersey

In partial fulfillment of the requirements

For the degree of

Doctor of Philosophy

Graduate Program in Microbiology and Molecular Genetics

Written under the direction of

Prof. Tamar Barkay

And approved by

New Brunswick, New Jersey

May 2008

ABSTRACT OF THE DISSERTATION

Mass Dependent Stable Isotope Fractionation of Mercury during its Microbial Transformations

By KRITEE

Dissertation Director:

Prof. Tamar Barkay

Mercury (Hg) is often cited in fish consumption advisories across the world due to the extreme neurotoxicity of its methylated forms. Given the complex biogeochemical cycling of Hg, a differentiation between local vs. global and natural vs. anthropogenic sources of Hg(0) and determination of transformations that are dominant in a given ecosystem is critical. Mercury has seven stable isotopes and Hg isotope ratios can become a novel biogeochemical tool to track sources and transformations of Hg in the environment. However, development of a stable isotope based tool requires the determination of the extent of fractionation during individual biotic and abiotic transformations that can occur in the environment. This thesis reports the extent of fractionation of Hg isotopes during two biological transformations: 1) degradation of monomethyl-Hg (MMHg) via the mercury resistance (*mer*) pathway in *Escherichia coli* JM109/pPB117 and 2)

Hg(II) reduction by four Hg(II) reducing strains, including three Hg(II) resistant strains (*E. coli* JM109/pPB117, *Bacillus cereus* Strain 5 and *Anoxybacillus* spp. FB9) and a Hg(II) sensitive strain (*Shewanella oneidensis* MR-1). Using a multi-collector inductively coupled plasma mass spectrometer, it was found that MMHg and Hg(II) that remained in the reactors became progressively heavier (increasing δ^{202}Hg) with time and underwent mass dependent Rayleigh-type fractionation with average fractionation factors of 1.0004 and 1.0016, respectively. Mass independent fractionation (MIF) was not observed and based on the nature of microbe-Hg interactions, it is suggested that the nuclear spin dependent MIF is unlikely to occur during biological processes. A multi-step framework for understanding the extent of fractionation seen during the *mer* mediated MMHg degradation and Hg(II) reduction experiments is provided, and based on the biochemistry and kinetics of the steps involved in the two pathways, the steps in the process that could contribute to the observed extent of fractionation are suggested in the thesis. A clear effect of Hg(II) bioavailability on the extent of fractionation of Hg was observed and is also discussed. The framework discussed here can guide future experiments on Hg isotope fractionation during other transformations in its biogeochemical cycle, and ultimately facilitate a more rigorous development of a Hg isotope based geochemical tool.

Acknowledgements

I have been extremely honored to have the chance to work with two excellent research mentors and wonderful human beings as my co-advisors. In the course of my doctoral years, I must have exchanged hundreds of emails with Profs. Tamar Barkay and Joel Blum and they have guided me very closely. However, they have both patiently given me the time, support and encouragement that I needed to 'grow' at my own pace and enjoy my research. They have always been gracious and warm even in periods when I was apparently not making any progress. I consider myself very lucky to have their unfailing confidence in both my capabilities as a researcher and the potential of this relatively new area of collaborative research from the very beginning. Because I spent much more time at Rutgers than at Univ. of Michigan, I have had the chance to interact much more frequently with Tamar on a day today basis. I am indebted to her for the generous time, friendly attention and deep warmth that she has given me even when she was tired or very preoccupied. She has a wonderful knack of constantly pointing out the strengths of her students and I am grateful to her for the encouragement and inspiration that she has given me throughout these years.

I am also very thankful to my doctoral thesis and qualifying committee members: Drs. Paul Falkowski, Max Haggblom, John Reinfelder, Robert Sherrell, and Costantino Vetraini who have inspired me to work hard and think deeply. They have always provided enthusiastic support to this research effort and have always been available to comment on my manuscripts, answer my questions and make their laboratory resources available for my use.

I would not have completed any of my experiments without continuous expert advice from all members of the Barkay lab. Drs. Jonna Coombs and Jeffra Schaefer were instrumental in introducing me to numerous laboratory techniques during my first few months in Barkay lab. I could not have finished my experiments with *Shewanella oneidensis* MR-1 and *Anoxybacillus* spp. Strain FB9 in time without constant help and generous time from Dr. Heather Wiatrowski and Aspassia Chatziefthimiou, respectively. Matthew Meredith, a senior from Colby College in Maine and Richard Pescatore, a freshman from NSF's Undergraduate Research Centre at Rutgers helped a great deal to perform some early mercury reduction experiments. Melitza Crespo-Medina and Zachary Freedman have helped me to use MINEQL software; Sharon Crane, Heather and Aspa have helped troubleshoot problems with our Leeman Hg analyzer and trace-metal level cleaning protocols; Riqing Yu and Dr. Yanping Wang have helped with their expertise in molecular techniques; together with Rachel Ward, Pat Lu Irving, Jane Yagi, Ria John, Jackie Deitz and Reena Gupta, they have all contributed to insightful discussions in our weekly lab meetings and creating a wonderfully warm learning environment in our lab.

I have also received tremendous support from the members of Prof. Joel Blum's research group at University of Michigan (UM). I am especially indebted to Marcus Johnson in the Department of Geological Sciences at University of Michigan for his expert help in carrying out the isotopic analysis using Multi-collector ICPMS and diligent work on my data files. He arranged a large quantity of data collected during ICPMS runs very meaningfully and made it very easy for me to analyze the data in the carefully prepared files that he sent me. I am also very thankful Dr. Bridget Bergquist, who is currently at University of Toronto but was a post-doctoral research fellow at UM between

2005 and 2007. Her constant and keen inputs were indispensable while I was writing the manuscript for my first publication. Drs. Bjorn Klaue, Abir Biswas and Chris Smith were also excellent hosts and always eager to make me comfortable during my visits to Ann Arbor.

Drs. Neal Woodbury (Arizona), Steve Snetzer (Physics, Rutgers), Charles Grissom (Utah), Anne Summers (Georgia) and Sue Miller (UCSF) have obliged me by giving me time to discuss and clear my lingering doubts about mass independent effects, membrane potentials and the nature of Hg-microbe interactions. I am especially full of gratitude towards Chris Irving, a friend with training as a physicist for the time he gave me to critique on my analysis of possibility of observing Hg magnetic isotope effects during biological transformations of mercury. During these doctoral years, I have also received much needed inputs from many Hg biogeochemists including Drs. William Fitzgerald (Connecticut), Carl Lamborg (WHOI) and Janina Benoit (Wheaton), Alex Poulain and Stephanie Hamelin (Montreal), and isotope geochemists including Donald Canfield (Denmark), Ariel Anbar (Arizona), Thomas Johnson (UIUC) and Daniel Sigman (Princeton).

I have greatly enjoyed learning research and teaching skills from the community of ecologists, microbiologists and environmental scientists at Cook campus in Rutgers University. I am thankful to Drs. Lily Young, Peter Morin, John Ehrenfeld, Peter Storm, Jerome Kukor, Nathan Yee, Donna Fennell, Doug Eveleigh, Diane Davis, Lee Kerkhof and Craig Phelps along with their lab members for creating a vibrant and warm community at Rutgers and personally encouraging me in my research and teaching efforts.

I am indebted also to Drs. David Ehrenfeld (Ecology, Rutgers), Beth Ravit (Environmental Law Clinic, Rutgers) and Kurt Spellmeyer (English, Rutgers) for their warm combination of mentorship and friendship. They have actively encouraged me to 'keep going' and not quit the research efforts during the most difficult times in these years.

No single time period in my doctoral years was as intellectually exciting, physically strenuous and scientifically productive as the time spend at Marine Biological Laboratory at Woods Hole, Cape Cod, MA for the Microbial Diversity summer course in 2007. I am very thankful to the faculty (Drs. Tom Schmidt, Bill Metcalf and Jared Leadbetter), teaching assistants and colleagues (including Adam Mumford from Rutgers) for the memorable and intense learning experience.

Many collegues at Rutgers have become lifelong friends and I would especially like to express my thankfulness to Priya Narasingarao, Qaiser Tarique, Gunaseelan Alagappan, Emilie Stander, Kristen Gilmore, Jay Kelly, Samriti Sharma, Bhuvnesh Parekh, and Maya Panangadan for their friendship and help in making this doctoral journey a joy.

I am indebted to Carolyn Ambrose and Diane Murano from Microbiology and Molecular Genetics Graduate Program; Eileen Glick, Arleen Nebel, Kathy Maguire and Jessie Maguire from the Department of Biochemistry and Microbiology; and Sarah Kozak from Eagleton Institute of Politics is helping me cruise through the bureaucratic entanglements at Rutgers so smoothly. Peter Anderson has been extremely gracious with his time and in helping me recover the data from my crashed computers.

I thank everyone in the extended community of friends and family in India and New Jersey that I have been extremely blessed to have. No words can express my gratitude towards my mother who has let me leave her vicinity and in this case our country to pursue my goals. She has been an unusually strong, caring and devoted single parent who has never wavered in her belief about my capabilities and has always put my all-rounded development before her social, professional and health interests. I also could not have surmounted the difficulties encountered in these years without the constant loving and generous support of my wonderful colleague, friend and husband, Imtiaz Rangwala. His warmth, sense of humor and excellent culinary skill have all always been delightful, especially in the last few weeks of dissertation writing!

Table of contents

List of tables

Page

List of illustrations and figures Page

Chapter 1: Introduction

Overview:

1. Mercury: A globally distributed pollutant

    a. Importance of tracking sources and transformations of mercury and potential applications of stable isotope systematics

    b. Role of microbes in biogeochemical cycling

2. Definitions

        a. Isotope effects, Fractionation, Isotope systematics

        b. Kinetic and thermodynamic fractionation

        c. Mass-independent fractionation: Magnetic & Nuclear volume effects

        d. Fractionation factors

            1. Inter-relationship of kinetic and thermodynamic effects

            2. Rayleigh equations

3. Importance of advent of Multi collector Inductively coupled mass spectrometry

4. Stages in the development of mercury isotope systematics

    a. Importance of experimental approach to determining fractionation factors

1. Mercury: a toxic global pollutant

1a. Importance of tracking sources and sinks

Mercury (Hg) pollution and monomethylmercury (MMHg) exposure are worldwide concerns for human[1] and wildlife[2] health. Hg is often cited in fish consumption advisories across the world because high exposure to MMHg during the fetal and neonatal periods leads to a variety of developmental problems affecting motor skills such as walking and speech, and may cause mental retardation and death in humans[1].

Mercury is a trace element in the lithosphere (<1 ppm) and hydrosphere (<1 ppb) and its ores such as cinnabar, metacinnabar and hypercinnabar[3] are relatively insoluble. However, since the beginning of the industrial age, the transfer of Hg present in these ores, from deep geological stores to the Earth's surface to the more soluble, bioavailable, toxic and comparatively easily distributable forms, has lead to huge increases in the concentrations of Hg in the planet's atmosphere and oceans. Because of the volatility and relatively long atmospheric life-time of elemental mercury (Hg(0)), Hg is referred to as a global pollutant.

Following wet deposition of inorganic Hg [Hg(II)] (See Fig. 1.1), formed in the atmosphere by oxidation of Hg(0), and dry deposition of particulate [Hg_p] to aqueous ecosystems, inorganic Hg is converted to MMHg which is then accumulated in local food webs. Because Hg mostly enters the environment in its inorganic forms[4-7], the accumulation of MMHg is controlled by the dynamics of the microbiological and abiotic processes that control MMHg synthesis, degradation and transfer in the environment. These dynamics are best understood in the context of the Hg biogeochemical cycle where

reactions, both microbial and (photo)chemical, that directly and indirectly affect Hg speciation are integrated[4,7].

More than 50 years of research into the possible biotic and abiotic sources, sinks and transformations of Hg have greatly enhanced the understanding of Hg's global and watershed cycling. Microbial processes are known to play a crucial role in 1) the formation and degradation of MMHg[7] and, 2) redox transformation of inorganic Hg potentially controlling the concentration of the substrate for methylation[8] and evasion of Hg(0) from open waters[9]. However, we do not have a high degree of confidence regarding the absolute and relative contributions of these processes to the formation of MMHg. Issues such as the clear identification of sources and sinks for Hg in the environment, the *in situ* pathways leading to toxicity, and the nature and evolution of redox reactions are key to the understanding of Hg biogeochemistry in both modern and paleo environments and also vitally pertinent to the development of a management policies for the control of environmental Hg contamination[6].

From a policy standpoint, there is a 27 to 50% uncertainty in the total amount of Hg emissions from different continents[10,11] and given the fact that many countries around the globe (e.g. Sweden) are trying to become Hg-free, it is vital to know the contribution of different continents and countries to total Hg emissions. Also, the assessment of truly "natural" Hg sources and their relative importance compared with direct anthropogenic emissions and (re)emissions from natural surfaces is a fundamental problem in studying the global cycling of Hg. It has been estimated that anthropogenic emissions account for two thirds of the total global emissions but there are about ±30% uncertainties in the total amount of anthropogenic Hg emissions[6] on a global scale. It is also not known what

percentage of these emissions are deposited locally close to the source as opposed to entering the global atmospheric pool that may be deposited at pristine locations far-away from the source; the error margin of estimates is ±50%[6].

Additionally, it is known that total Hg loadings to all systems which are far from immediate sources of Hg(II) are generally dominated by atmospheric inputs (either to water body directly or to the watersheds)[7]. However, it is neither totally clear nor straightforward to predict which sources of Hg(0) emission (local vs. far-off; biotic vs. abiotic; natural vs. anthropogenic) dominate Hg deposition at a given location[6]. From the standpoint of agencies interested in developing a remediation plan, e.g., an *ex-situ* bioremediation or bioaugmentation strategy, it might be sufficient to know if the pathways leading to reduction of Hg(II) or degradation of MMHg are microbiological. It might be crucial to know if the biotic transformation is mediated by an enzyme (e.g. organomercurial lyase (MerB), see below) or it is dissolved organic carbon (DOC) mediated non-specific co-metabolic process. Among some other unanswered questions related to the global Hg cycle and relevant to the promise of developing Hg stable isotope systematics are: What are the sources of MMHg in open ocean waters and in marine fish? What is the significance of hydrothermal vents in the marine cycling of Hg? What is the relative importance of photoreduction vs. enzymatic reduction in Hg(0) evasion or supersaturation of lakes and oceans?

A panel of international experts on Hg cycling was convened before the Eighth International Conference on Mercury as a Global Pollutant in Madison, Wisconsin in 2006 to ascertain the relative importance of different sources of Hg emissions. The panel felt that answers are forthcoming from two primary approaches: direct measurements and

models, both of which are subject to uncertainty[6]. The ability to determine the accuracy of current models used to predict the relative importance of different sources is severely limited by the lack of dry deposition measurements, uncertainties in the altitudinal distributions of Hg species, uncertainties in atmospheric reaction rates, emission profiles of various Hg chemical species, Hg emission rates by developing nations, and meteorology. The panel recognized that the application of measurement using isotopic signatures required intensive high-resolution sampling efforts but held promise as analytical technology improves. Because Hg has seven stable isotopes (^{196}Hg, ^{198}Hg, ^{199}Hg, ^{200}Hg, ^{201}Hg, ^{202}Hg and ^{204}Hg) with a relative mass difference of 4%, and it undergoes redox transformations involving compounds with a high degree of covalent character, measurable stable isotope fractionation of Hg could occur during its transformations in the environment.

1b. Role of microbes in biogeochemical cycling

Microbes play vital roles in the biogeochemical cycling of Hg[7,8] by mediating redox transformations of Hg and formation and degradation of methylmercury in aquatic environments. The following is a brief discussion of the contribution of biotic and corresponding abiotic transformations to the cycling of Hg in the environment.

Hg(II) reduction (Hg(II) → Hg(0)): Reduction of Hg(II) to Hg(0) results in the partitioning of Hg into the air due to the product's low aqueous solubility (60 μg/L water at 25 ^{0}C) and high volatility. Biological reduction of Hg(II) to Hg(0) significantly contributes to this process. The best documented mechanism of Hg biological reduction is mediated by the inducible bacterial enzyme mercuric reductase (MerA). Microbes

expressing MerA remove Hg(II) from contaminated aquatic environments leading to a decrease in the availability of the substrate of methylation. Concentrations of total Hg in most natural environments are at pM – fM levels, which might not be sufficient for induction of MerA. In these environments Hg(II) may be reduced by photosynthetic organisms. Another process that reduces Hg(II) in environments with low Hg concentrations is the Fe(II)-dependent reduction among acidophilic thiobacilli (reviewed in[8]).

Abiotically Hg(II) is reduced as a result of photochemical transformations as well as dark reactions. Photoreduction is mostly due to the formation of reducing organic free radicals that are produced by photolysis from dissolved organic carbon (DOC)[12], dissolved oxygen and organic carbon complexes, and Fe(III) organic acids coordination compounds[13]. In the dark, Hg may be reduced by fulvic[14] and humic acid-associated free radicals. Finally, two molecules of mercurous ion (Hg(I)) formed by weak reductants from Hg(II), may disproportionate to Hg(0) and Hg(II)[15].

MMHg degradation (MMHg → Hg(0)/Hg(II) + CH_4/CO_2): There are two known pathways for the microbial degradation of MMHg: a reductive pathway whose products are CH_4 and Hg(0) and an oxidative pathway whose products are CO_2, a small quantity of CH_4, and an as of yet unidentified Hg product. The mechanism for the reductive pathway is protonolysis by the bacterial organomercury lyase (MerB) resulting in CH_4 and Hg(II). The later is then reduced by MerA to Hg(0)[16]. Diverse bacteria from diverse environments carry MerB and their activities limit MMHg production in contaminated environments[17]. Oxidative demethylation is likely a co-metabolic by-product of

methylotrophic metabolism in anaerobic bacteria[18]. A pure culture that oxidatively degrades MMHg has not been identified limiting the knowledge of the biochemical details of this process.

Abiotically MMHg is degraded by sunlight at a wavelength range of 280 – 400 nm[19]. Suda et al (1993) reported production of inorganic Hg during photo-degradation while Hg(0) was identified as the major mercuric product of photo-degradation in wetlands (D. Krabbenhoft, Personal communication). While in light exposed environments, such as wetlands and lakes, photo-degradation may be the major mechanism for MMHg degradation[20], in sediments and bottom waters, where MMHg accumulates following methylation, this process may have little impact on demethylation and microbial processes most likely dominate.

Hg(II) methylation (Hg(II) → MMHg):

Hg(II) is methylated by microbes in anaerobic sediments and incubations of anaerobic sediments with specific metabolic inhibitors and substrate additions have clearly implicated sulfate reducing bacteria (SRB) in this process[21-23]. The soluble neutral HgS is most likely the substrate for methylation by SRB[24-26]. Later and recent work[27,28] has shown also methylation by iron reducing bacteria that belong to the *Deltaproteobacteria*.

Abiotic methylation occurs by humic and fulvic acids[29], carboxylic acids[30], and alkylated tin compounds[31]. The importance of these abiotic processes to MMHg production is contested and experiments clearly evaluating their role relative to the well-documented role of SRB have not been reported.

Hg(0) oxidation (Hg(0) → Hg(II)): Elemental Hg is oxidized to Hg(II) in the atmosphere[32], natural waters[33] and soils[34]. Smith et al (1998) showed Hg(0) oxidation mediated by peroxidases in common soil microbes suggesting a potential role in the cycling of Hg in the environment[35].

Abiotically, oxidation of Hg(0) is photo-induced and is mediated by O_2 in the presence of excess chloride[36], by hydrogen peroxide and ozone[37], sulfhydral compounds[38], by free radicals of Br and Cl[32,39], and by UV-B in the presence of Cl radicals and photoreactive compounds such as benzoquinone[40]. Dark oxidation of Hg(0) in the presence of chloride, most likely by O_2 in seawater is also known[41].

2. Definitions

2a. Isotope effects, Fractionation & Isotope systematics

The word isotope is derived from a Greek word meaning "in the same place" (Bigelstein, 2006). As they have the same atomic number, stable isotopes are placed at the same spot in the periodic table and they participate in the same chemical reactions. But since they do have different atomic masses, the molecules made up of different stable isotopes have different vibrational frequencies which in turn lead to differences in heat capacities, entropies, diffusivities, velocities, free energies and rates of reaction of the molecules[42]. These deviations from the perfect physico-chemical equivalence amongst stable isotopes are called isotope effects[43]. The isotope effects come into play during chemical transformations and lead to isotope fractionation - the differential partitioning of stable isotopes among reactants and products.

Out of 108 naturally occurring elements, 87 have more than one stable isotope(s) and although the total abundance of each of the stable isotopes of any element is constant on Earth (unless lost to space), a variety of causes (i.e. isotope effects) lead to changes in the relative amounts of the isotopes at different places on earth (i.e. isotope fractionation). The measurement of the relative amounts of stable isotopes of an element, in the form of stable isotope ratios in any natural sample, allows us to track the origin and history of that sample. A priori and systematic knowledge of processes that cause fractionation, i.e. development of isotope systematics, of a particular element is vital for interpreting isotope data in natural samples. Mercury has seven stable isotopes (^{196}Hg, ^{198}Hg , ^{199}Hg , ^{200}Hg , ^{201}Hg , ^{202}Hg , and ^{204}Hg) with the maximum relative mass difference of 4% between ^{196}Hg and ^{204}Hg (see Table 1.1 for relative abundance and spins of these isotopes).

Hg isotopes ratios for various samples are reported in delta notation, in units of parts per thousand or 'per mil (‰)', referenced to an internationally recommended Hg standard (i.e. NIST SRM 3133). δ^{xxx}Hg refers to δ^{xxx}Hg/^{198}Hg[44] and is calculated as:

$$\delta^{xxx}\mathrm{Hg} = \left(\frac{(^{xxx}\mathrm{Hg}/^{198}\mathrm{Hg})_{\mathrm{sample}}}{(^{xxx}\mathrm{Hg}/^{198}\mathrm{Hg})_{\mathrm{SRM}}} - 1 \right) \times 1000$$

Hereafter, ^{202}Hg/^{198}Hg will be referred to as R. It is recommended that the ratios (R) used in the delta notation define ratios as heavy over light isotope so that a positive delta value indicates that the sample is isotopically enriched in heavier isotope and a negative value indicates that the sample is depleted in the heavier isotope as compared to the standard[44,45]. However, some Hg isotope studies[46] have used the ratios with the isotope

^{202}Hg as denominator because it is the most abundant isotope (see Table 1.1), but the use of common nomenclature and standards is encouraged[44].

2b. Mass dependent fractionation: Kinetic vs. Thermodynamic effects

Molecules made of lighter isotopes have weaker intra-molecular and inter-molecular bonds as compared to "heavy" molecules. Therefore, at a given temperature, whenever a chemical transformation involves bond cleavage, the lighter molecules break more readily. They react (and might diffuse) faster and therefore preferentially accumulate in the product as compared to the heavier isotopes leaving the heavier ones in the product. This leads to kinetic fractionation – partial separation of isotopes due to kinetic isotope effects (KIE), i.e., difference in kinetics (rates) of reaction of light vs. heavy reactants.

However, if the products have not been isolated from the original reactant (i.e. the system is closed) and the reaction is reversible, it is not necessarily true that the product will be enriched in lighter isotopes. In such cases, the ratio (R) in the product and the reactant depends on the extent of free energy change (ΔG) in the reactant or product molecules with changing isotopic content. 'Heavier' molecules have less reserve of free energy than 'lighter' molecules (see reasons below) and hence are more stable. However, the amount of change in free energy levels due to isotopic substitution is different for the reactant and product. Therefore, to attain minimum free energy for the whole system (see notes on the second law of thermodynamics below) a redistribution of isotopes in reactant and product is required. This leads to thermodynamic or equilibrium fractionation – partial separation and exchange of isotopes due to equilibrium isotope effects (EIE), i.e.,

difference in a thermodynamic property of the reactants and products existing in equilibrium.

2c. Mass independent fractionation: Nuclear spin vs. Nuclear volume effects

Numerous processes, especially abiotic pathways, related to Hg biochemistry (see above) involve participation of radicals or paramagnetic ion pairs in the reaction pathway. The reaction products and rates of such reactions depend on the orientations (singlet vs. triplet) of the electronic spin of one radical with respect to the other radical in the pair. In isotopes with nuclear spins, the interaction of the spin (i.e. magnetic moment) of the nucleus with that of the electron, leads to change in the orientation of the electronic spins. The rates and course of a chemical reaction involving radical pairs may thus depend on the occurrence and orientation of nuclear spins in the pair[47]. This leads to magnetic isotope fractionation – separation of isotopes due to the magnetic isotope effect i.e. difference in the magnetic property of their nucleus which is independent of the mass of the isotope.

Stable isotopes, as noted above, have the same amount of positive charge in their nuclei but the strength of the interaction between the negatively charged electrons and the positively charged nucleus depends on the nuclear radius and volume of an isotope. Therefore, isotopes with smaller nuclei occupy those electronic configurations where electronic charge density is higher close to the nucleus[48]. This leads to nuclear volume fractionation - separation of isotopes due to the nuclear volume effects that is based on the nuclear volume of the nucleus, which too does not scale linearly with mass.

2d. Fractionation factors

Kinetic effects during processes involving transformation of an element are due to the differences in the stiffness of bonding of the isotopic atom in the transition state relative to the substrate, whereas equilibrium effects compare the stiffness of bonding of product and substrate. The stiffness is related to the mass of the molecule and both of them can be mathematically described by partition functions (see Appendix). In each case, the heavy isotope enriches in the more stiffly bonded position (Cleland in[49]). Kinetic effects during processes such as diffusion are due to differences in the diffusion rates of the molecules. Fractionation factors (α or ε, see below) quantify the extent of fractionation during any process. For a reaction A → B, the fractionation factor ($\alpha_{reactant-product}$) is simply equal to $R_{reactant}/R_{product}$..

For kinetic fractionation, $\alpha_{reactant-product}$ is also equal to the ratio of the rates of the forward reaction for light and heavy isotopes, e.g., for the reaction Hg(II) → Hg(0)

$$(\alpha_{202/198})_{r-p} = k_{198}/k_{202} = (^{202}Hg/^{198}Hg)_{reactant}/(^{202}Hg/^{198}Hg)_{product} = R_{reactant}/R_{product}$$

where k_{202} is the forward rate constant for the reaction $^{202}Hg(II) \rightarrow {}^{202}Hg(0)$

For thermodynamic/equilibrium fractionation, $\alpha_{reactant-product}$ is equal to the equilibrium constant for the exchange reaction symbolizing the isotopic distribution in two compounds, e.g. for the conversion $HgCl_4^{2-} \rightarrow HgCl_2 + 2Cl^-$, the exchange reaction will be $^{198}HgCl_4^{2-} + {}^{202}HgCl_2 \leftrightarrow {}^{202}HgCl_4^{2-} + {}^{198}HgCl_2$

$$\alpha_{r\text{-}p} = 1/K = \frac{[^{198}HgCl_4^{2-}][^{202}HgCl_2]}{[^{202}HgCl_4^{2-}][^{202}HgCl_2]} = R_{reactant}/R_{product} = \frac{[^{198}HgCl_4^{2-}]/[^{202}HgCl_4^{2-}]}{[^{198}HgCl_2]/[^{202}HgCl_2]}$$

where K is the equilibrium constant for the isotopic exchange reaction above. If the isotopic exchange reaction involves transfer of 'n' atoms (i.e., more than one Hg atoms) the $\alpha_{r\text{-}pr} = (1/K)^{1/n50}$.

Different definitions of fractionation factors

Development of any new stable isotope systematics (i.e., development of a stable isotope based geochemical tool) requires determination of isotope ratios in representative sources and fractionation factors for individual biotic and abiotic transformations that are possible within an element's biogeochemical cycle. Different researchers prefer to use different definition of fractionation factors and one must be careful to notice the definition of the fractionation factor for any given study . Three common ways to express extent of difference between two compounds A and B are:

$$\alpha_{A\text{-}B} = R_A/R_B; \qquad \varepsilon_{A\text{-}B} = (R_A/R_B - 1)*1000; \qquad \Delta_{A\text{-}B} = \delta_A - \delta_B$$

A value of 1.02 for $\alpha_{A\text{-}B} = 1.02$ or 0.98 for $\alpha_{B\text{-}A}$ or 20 for $\varepsilon_{A\text{-}B}$ or 19.6 for $\Delta_{A\text{-}B}$ imply the same extent of fractionation. $\alpha_{A\text{-}B}$ is unitless but, $\varepsilon_{A\text{-}B}$ and $\Delta_{A\text{-}B}$ are measured in units of per mil (‰). Some Hg isotope studies have defined alpha (α) such that it reports $R_{product}/R_{reactant}$[51], while others have defined α such that the reported α =

$R_{reactant}/R_{product}$[52]and it is essential to use same definition of fractionation factor in order to compare them meaningfully..

2d. i) Inter-relationship of the kinetic and equilibrium effects

Kinetic isotope fractionations (KIF) are of the most interest for microbiologists because most biological transformations are unidirectional and non-equilibrium processes with incomplete isotope exchange[50]. Nevertheless, equilibrium isotope fractionations (EIF) are also important because they can act as calibration points for interpretation of KIF and the theory of equilibrium effects with some modification can be used to explain kinetic effects[53]. Most importantly, at the limit when external or internal conditions (substrate limitation, steady state, accumulation of product in the vicinity of reactant etc.) lead to conversion of a mostly unidirectional reaction to a bidirectional reaction because of thermodynamic constraints, the resultant fractionation factor is close to the equilibrium factor but not to the kinetic fractionation factor, as explained below[54].

Kinetic fractionation is usually larger than equilibrium fractionation for the same reaction at the same temperature. This is because unidirectional processes where the product gets physico-chemically separated from the reactant and back reactions can not occur, the kinetic fractionation factor (KFF) takes only the differential rates of the "light" and "heavy" reactants into account. On the other hand, the equilibrium fractionation factor (EFF) incorporates the backward reaction as well[54] . In other words, equilibrium fractionation factors depend on the imbalance between forward rate constants and reverse rate constants for different isotopes; kinetic factors depend only on the forward rates.

Both rates are likely to be faster for light isotopes, so the reverse reaction diminishes the fractionation. Therefore, EFF = $(KFF)_{forward}$ - $(KFF)_{backward}$[54].

2d. ii) The Rayleigh Equation

The isotope ratios (R) for a reactant or product can depend on the extent of reaction completion. In those cases, it is not feasible to determine the value of fractionation factors using the definitions above that assume that the values of R (and hence the values of δ) for compounds A and B remain constant. In such cases, α is defined as $R_{instantaneous\ reactant}$/ $R_{instantaneous\ product}$ instead of $R_{reactant}/R_{product}$. The Rayleigh equations can be used to describe such cases if: 1) the product is continuously removed from a well mixed and finite reservoir of reactant/substrate molecules consisting of two or more isotopic species (e.g., $HgCl_2$ molecules consisting of $^{202}HgCl_2$ and $^{198}HgCl_2$ being reduced to Hg(0) such that the product does not re-react with the $HgCl_2$ pool), 2) the fractionation accompanying the removal process at any instance is described by the fractionation factor α, and 3) α does not change during the process[55].

In a strict sense, the term "Rayleigh fractionation" should only be used for chemically *open* systems where the isotopic species removed at every instant were in thermodynamic and isotopic equilibrium with those remaining in the system at the moment of removal. However, Rayleigh equations are followed for processes with kinetic (unidirectional reactions with quantitative conversion to product where back reaction is prohibited due to loss of product but the initial fractionation at the time of product formation occurs due to difference in rates) and equilibrium (the process takes place under equilibrium conditions but the product escapes the vicinity of the substrate

and doesn't remain in physical contact with the reactant preventing isotopic exchange) control.

Many microbiological reactions (e.g., sulfate reduction, methane oxidation, ammonia oxidation & volatilization, nitrification, and denitrification) can also be modeled with Rayleigh-type models[55,56]. This thesis shows that microbial Hg(II) reduction and MMHg degradation can also be modeled using Rayleigh equations[52], (see region 1 in Fig. 5.1). But it is important to note that not all biological processes cause kinetic fractionation (see example of equilibrium dissimilatory reduction of Fe(III) below) and not all processes causing kinetic fractionation follow the predictions made by Rayleigh curves (i.e. SeO_4^- reduction). In the case of selenium reduction, fractionation can not be modeled based on Rayleigh equations because the value of α (or ε) changes during the course of the reaction[57].

Some mathematical treatments of the Rayleigh equation indicate that this equation holds only when one of the isotopes is very rare[58] as compared to the other but this is not necessary and the only requirement for the Rayleigh equation to hold is that alpha should be small (close to 1). It is also noteworthy that similar values of fractionation factors for two processes do not necessarily imply similar cause of fractionation (see *merA* vs. MerB discussion below) that depends on the experimental conditions and the nature of the rate limiting steps.

3. High precision Isotopic Ratio Measurement of Hg by Cold vapor Generation MC-ICP-MS:

Because Hg is so heavy (average molecular weight 200 amu) and the percentage mass difference between its different isotopes is lower (4%) as compared to percentage mass difference between isotopes of lighter elements (e.g. carbon) and the zero point energy (ZPE, see Appendix) differences between its isotopes would be small, very little Hg fractionation was expected to be seen in natural environments. Moreover, like other heavy metals including molybdenum, iron, selenium and uranium, it is present in trace quantities in the environment. Therefore, very sensitive and precise determination of isotopic ratios is needed to establish Hg fractionation during transformations. First conceived in early 1990s, the magnetic sector mass spectrometers with plasma based ion sources and multiple-collector cups (MC-ICPMS) have provided an excellent tool for measurement of heavy stable isotope ratios in recent years[45]. Up until the use of high precision mass spectrometers[59] became common, it was commonly believed that the phenomenon of isotopic fractionation is limited to elements with low atomic mass. But recently very heavy elements have been shown to fractionate both biologically (Hg with Average molecular weight of 200 (this thesis)[52] and uranium with molecular weight of 238[60]) and abiotically (Hg[51] and thallium with molecular weight of 204[61]).

The details of mercury isotope analysis are presented in Chapter 2 of this thesis (for more details, see[44,52,62,63]). Briefly, a NU Plasma (NU Instruments, UK) MC-ICP-MS in the laboratory of Prof. Joel Blum in the department of Geological Sciences at the University of Michigan equipped with 12 Faraday cups and 3 ion counters was used in my biological Hg(II) reduction and MMHg degradation studies to simultaneously

measure the ratios of isotopes with masses of 196, 198, 200, 201, 202, 203, 204, 205, and 206. MC-ICPMS allows high efficiency of ionization of Hg and a very rapid sample throughput. Mercury is introduced by continuous-flow cold vapor generation (CV) with Sn(II). This reagent reduces only Hg(II) in the liquid samples to Hg(0), a volatile species, and provides specific analyte-matrix separation in the gas-liquid separator. All samples are evaluated against standard reference material NIST 3133 (Hg standard solution at 10000±10 ppm) diluted to match the sample concentration. Internal inter-element mass bias correction is achieved using the NIST 997 isotopic thallium (Tl) standard with a certified value for $^{205}Tl/^{203}Tl$ and by applying the exponential mass bias law. All δ values for a sample are calculated based on standard-sample-standard bracketing runs after the Tl exponential law mass bias correction.

Mercury's volatility and high ionization potential make isotopic measurements by thermal ionization mass spectrometry (TIMS) impractical. Moreover, typical instrumental mass bias varies during the course of a TIMS analysis session making the use of standard-sample-standard bracketing technique for mass bias correction impossible. Analysis by single-collector inductively coupled mass spectrometry or gas source mass spectrometry are typically limited to a precision of 1‰, which is insufficient for the expected levels of natural isotopic fractionation of Hg.

Future mercury isotope research in modern freshwater and marine ecosystems can contribute greatly to tracing Hg's sources and transformations, but at this time direct Hg isotope analysis of many of the samples from these ecosystems is very difficult due to extremely low concentrations (pM for Hg) (Fitzgerald, 2007)[64,65].

4. Role of microbial studies in development of isotope systematics

A large body of knowledge is available for consideration of the various processes that may affect Hg isotopic fractionation. Such considerations will help us to establish a comprehensive view of how Hg isotope systematics can be integrated into the Hg biogeochemical cycle (See Fig. 1.1 and 1,2).

Since microbes play a vital role in Hg biogeochemical cycling, studying of the extent of change in isotope ratios during microbial processes is indispensable to the development of Hg isotope systematics. This thesis provides 1) experimental results of microbial fractionation studies of Hg stable isotopes (Chapters 2,3 and 4); 2) a framework for the understanding microbial fractionation of Hg, especially during the reduction of Hg(II) and degradation of MMHg, along the lines of work by the sulfur isotope community (Chapter 3 and 4)[66]; and 3) on the basis of the provided framework and synthesis of conclusions drawn from biotic and abiotic Hg fractionation studies, suggests future experiments that could help advance Hg isotope systematics (Chapter 5)[54,67]. In Chapter 5, given the thermodynamic underpinnings of the isotopic fractionation presented above in this chapter and changing internal and external environment of the cell, indicate the complexities faced in the interpretation of isotopic data from biological experiments, and discuss why in spite of these complexities, the study of Hg stable isotope fractionation during microbial transformations can be an important biogeochemical tool.

4a. The importance of experimental approaches to isotope systematics

Since the development of precise Hg isotope measurements by MC-ICPMS, significant Hg isotope variations in natural samples have been reported in hydrothermal ores[63,65], sediment cores[68], fish tissues[51] and other components of the aquatic food chain[46]. Interpretation of the isotopic data thus recovered depends on the precise determination of fractionation factors (see section 2) for individual biotic and abiotic Hg transformations that can occur in the environment. It is critical that such fractionation factors be determined experimentally. This is because although theoretical calculation of kinetic and equilibrium fractionation factors (i.e. α) is possible in principle[50,53,69-71], it is limited in its scope especially with reference to fractionation by biotic processes. Accurate calculation of α values depends on the precise knowledge of vibrational frequencies for each of the isotopically substituted molecules in a reaction. Even when the vibrational frequencies have been determined experimentally (infrared or Raman spectroscopy) and/or estimated by *ab initio* force field calculations[50], only equilibrium fractionation factors can be confidently estimated. Determination of kinetic fractionation factors requires detailed knowledge of reaction mechanism and transition state structures[50,72]. Because it is difficult, although not impossible, to predict the structures of transition states, it is very challenging to come up with partition functions and reduced masses for transition states and to estimate the fractionation factors associated with enzymatic reactions. Moreover, microbiological processes are usually multi-step processes where the net extent of fractionation observed is a function of the forward and backward rates of, and fractionation by, all the constituting steps involved ([54]; see Chapters 3 and 4). The rates of all the steps, in turn, can depend on the physiological

properties of the microbe such as the rate of gene expression and enzyme turnover numbers (Chapter 3 and 4) and external environmental parameters like pH, temperature, redox potential and the concentration of electron donors and acceptors[67,71]. Therefore systematic experimental determination of fractionation factors during all kinetically controlled (unidirectional and fast) processes is essential for rigorous development of Hg isotope systematics.

Chapter 2: Mercury stable isotope fractionation during reduction of Hg(II) to Hg(0) by mercury resistant microorganisms

Abstract:

Mercury (Hg) undergoes systematic stable isotopic fractionation; therefore, isotopic signatures of Hg may provide a new tool to track sources, sinks and dominant chemical transformation pathways of Hg in the environment. I investigated the isotopic fractionation of Hg by Hg(II) resistant (Hg^R) bacteria expressing the mercuric reductase (MerA) enzyme. The isotopic composition of both the reactant Hg(II) added to the growth medium and volatilized product (Hg(0)) was measured using cold vapor generation and multiple collector inductively coupled plasma mass spectrometry. I found that exponentially dividing pure cultures of a Gram negative strain *E. coli* JM109/pPB117 grown with abundant electron donor and high Hg(II) concentrations at 37 °C, 30 °C and 22 °C, and a natural microbial consortium incubated in natural site water at 30 ^{0}C after enrichment of Hg^R microbes, preferentially reduced the lighter isotopes of Hg. In all cases, Hg underwent Rayleigh fractionation with the best estimates of $\alpha_{202/198}$ values ranging from 1.0013 to 1.0020. In the cultures grown at 37 ^{0}C, below a certain threshold Hg(II) concentration, the extent of fractionation decreased progressively. This study demonstrates mass dependent kinetic fractionation of Hg and could lead to development of a new stable isotopic approach to the study of Hg biogeochemical cycling in the environment.

Introduction

Mercury (Hg) is often cited in fish consumption advisories across the world due to the extreme neurotoxicity of its methylated forms. Because Hg is globally distributed by atmospheric transport as Hg(0)[73], a differentiation between local vs. global and natural vs. anthropogenic sources of Hg(0) is critical. Moreover, since Hg enters the environment mostly in its inorganic form and transformations within the environment determine its toxicity, it is important to determine which transformations are dominant in a given ecosystem[8]. Methods that provide insight into the sources, redox cycling, and other chemical transformations of Hg in ecosystems are therefore needed to better understand Hg bioavailability, the mechanisms for production and degradation of methylated Hg compounds, and the resultant toxicity of Hg.

Stable isotope ratios of many light elements (*i.e.,* C, N, O, S) have proven useful as proxies for determining sources, sinks and dominant transformation pathways of nutrients and toxic substances in present and paleo environments (see review[70]). The measurement and application of stable isotope fractionation of heavier elements such as Fe, Cr, Se, Cu and Zn has recently become possible with the advent of new instrumentation and analytical techniques (see review[45])[57,74]. Because Hg has seven stable isotopes (^{196}Hg, ^{198}Hg, ^{199}Hg, ^{200}Hg, ^{201}Hg, ^{202}Hg and ^{204}Hg) with a relative mass difference of 4%, and it undergoes redox transformations involving compounds with a high degree of covalent character, measurable stable isotope fractionation of Hg could occur during its transformations in the environment. Indeed, significant Hg isotope variations in natural samples from hydrothermal ores[63,65], sediment cores[75], and fish tissues[51] have recently been reported, but the causes of the observed fractionations have

not yet been explored. This study reports one process that can lead to Hg isotopic fractionation seen in natural samples.

Development of any new stable isotope proxy for addressing complex biogeochemical phenomena requires the determination of fractionation factors for individual biotic and abiotic transformations that occur in the environment. For Hg, one such transformation is the reduction of Hg(II) to Hg(0), which is an important pathway in its biogeochemistry as it adds to the pool of Hg(0) available for atmospheric global transport[76], and also reduces the amount of Hg(II) available for MMHg synthesis[17,77]. I hypothesized that bacteria expressing the enzyme mercuric reductase (MerA), an enzyme found in a broad range of Hg-resistant (Hg^R) bacteria from diverse environments, would lead to measurable preferential uptake and reduction of lighter isotopes of Hg and demonstrate kinetic fractionation. MerA is part of an elaborate resistance mechanism that is mediated by the mercury resistance (*mer*) operon. This Hg(II) inducible operon has evolved to protect microorganisms from the toxicity of Hg(II) by removing it from their environment in the form of Hg(0), and mediates the most efficient biological reduction of Hg(II). At their optimum growth conditions, actively growing MerA expressing bacterial cultures (~10^5-10^6 cells/ml) can reduce 99% of a 50 micromolar Hg(II) in less than an hour. In natural uncontaminated environments between 1 to 10%, and in Hg contaminated environments up to 50%, of the culturable microbes are Hg^R and likely have a functional MerA[8].

The extent of stable isotope fractionation during microbial transformations can change with the bacterial species involved, the quantity and quality of nutrients, and other environmental factors including pH, temperature, and redox conditions that can change

reaction pathways or rate-limiting steps and the degree of reaction completion[71]. Therefore, before isotope ratios can be interpreted within the complexity of environmental samples, controlled laboratory experiments are required to assess the effect of individual variables on the extent and expression of isotopic fractionation. Here, in collaboration with Professor Joel Blum's laboratory at University of Michigan, I performed high precision Hg stable isotope measurements by cold vapor generation coupled with multiple collector inductively coupled plasma mass spectrometry (MC-ICPMS) to show fractionation of Hg isotopes during the reduction of Hg(II) by a pure culture at differing temperatures and by natural microbial communities.

Materials and methods

All experiments were performed in an autoclaved glass or Teflon apparatus that was cleaned by soaking in either 8N HNO_3 or 10% BrCl overnight followed by rinsing 5 times in 18 MΩ deionized water. All inoculated and un-inoculated control experiments were carried out in the dark in order to isolate biological reduction from possible photochemical reduction pathways. Details of the reagents used, the experimental set-up, sample collection and preservation, Hg concentration and isotopic composition analyses, mathematical treatment of data and approximations employed are described below (also see supplement).

Mercury reduction by Hg^R Gram negative pure culture: *Escherichia coli* strain JM109 carrying the mercury resistance plasmid pPB117 (hereafter *E. coli* JM109/pPB117) was used in Hg(II) reduction experiments. The plasmid pPB117 originated in the soil bacterium *Pseudomonas stutzeri*[78]. *E. coli* JM109/pPB117 was

grown in M9 defined medium[79] supplemented with 1% pyruvate at 37 ^{0}C, 30 ^{0}C or 22 ^{0}C. This medium was used in order to achieve very slow bacterial growth rates of about 1.5 hours per generation at 37 ^{0}C[80] (typical growth rate in rich media is ~ 20 minutes per generation) and consequently decrease the rate of Hg(II) reduction. Bacterial cultures grown overnight at 37 ^{0}C were diluted to an optical density (OD) of 0.05 at 660 nm and incubated at the selected growth temperature in the presence of 600 ng Hg(II) per g of the growth medium until the OD increased to 0.2. About 30 minutes before using it as a inoculum, another dose of 600 ppb (see end of Appendix for conversions of interconversion of concentration units) Hg(II) was added to induce *merA*[8]. Cultures were then diluted 1:1000, yielding a cell density of ~10^5 colony forming units per ml (CFU/ml), into a Pyrex glass reactor wrapped with aluminum foil (100 or 1000 ml) connected to traps with a Hg(0) trapping solution (0.05M $KMnO_4$ [Hg grade] and 5% H_2SO_4 [Fisher Trace Metal Grade]) via a soda lime drying tube. NIST SRM (Standard Reference Material) 3133 available as $Hg[NO_3]_2$ (with a certified Hg concentration of 10.00 ± 0.02 mg/g) was added to the reactor to reach a final concentration of 600 ppb , and the Hg(0) volatilized during the growth was purged into the trapping solution by sparging the culture solution with Hg-free air at a rate of 35 ml/min. The cells remained in exponential growth phase throughout the length of the experiments. Experiments with *E. coli* JM109/pPB117 were done multiple times in 100 ml reactors at all three growth temperatures. In addition, experiments were done twice at 37 ^{0}C and once at 30 ^{0}C in a larger 1L reactor that allowed for sample withdrawal from the reactor and isotopic analysis of the remaining reactant [Hg(II)], as well as the analysis of the collected product [Hg(0)] as a function of time.

Mercury reduction by Hg^R and Hg(II) 'sensitive' (Hg^S) natural microbial communities:

Water samples from a freshwater pond, Passion Puddle (on the grounds of Rutgers University, New Brunswick), with no known point sources of mercury, were pre-exposed to $HgCl_2$ to adapt the indigenous microbial community to Hg(II) and enrich for Hg^R microbes[81]. Mercuric chloride was added to 300 ml of site water to achieve a final concentration of 225 ppb and incubated at 30 ^{0}C. After four days, cells were harvested by centrifugation (at 4,300 x g for 25 minutes in a Sorvall RC-5B Superspeed centrifuge) and re-suspended in 300 ml of filtered (0.2 μm pore size Millipore Durapore membrane filter) site water containing 225 ppb Hg(II) (NIST 3133 standard) in a 1L reactor wrapped with aluminum foil. The reactor solution was constantly sparged with Hg free air and the Hg(0) stripped from solution was trapped as described above for pure culture experiments.

The acclimation to Hg(II) was followed by counting the number of total heterotrophic and Hg^R colonies during the four days of the pre-exposure period. Water samples withdrawn from the reactor were diluted serially in 0.85% NaCl and plated on modified LB medium (3 g yeast extract, 5 g NaCl, 6 g trypton and 15g agar in 1L water) with and without 20 μM (4 μg/g) Hg(II) in Petri plates. Plates were incubated for 3 days at room temperature, after which the number of visible colonies were counted and CFU/ml of total and Hg^R microorganisms present were calculated. Another experiment with the un-adapted natural Hg^S microbial community consisted of an un-exposed Passion Puddle water sample in a 1L reactor supplemented with 25 ppb Hg(II). A dark

abiotic control experiment was performed by purging filter sterilized (0.2 μm filter) Passion Puddle water sample containing 225 ppb Hg(II).

Sample collection

In order to determine the change in isotopic composition of the product Hg(0) as a function of the fraction of added Hg(II) that remained in the reactor (f), traps were replaced periodically to collect the volatilized Hg(0). For experiments done with *E. coli* - JM109/pPB117 at 37 ^{0}C, traps were replaced every ~35 min for a period of ~300 min, for those at 30 ^{0}C, traps were replaced every ~60 minutes for a period of ~550 minutes, for those done at 22 ^{0}C, traps were replaced every ~90 minutes for a period of ~800 minutes, and for the experiments with natural microbial community, traps were replaced every 10-12 hours for a period of 50-60 hours. The isotopic composition of the trap sample thus collected does not represent the isotopic composition of instantaneous product but rather a time integrated product (see below).

To determine the isotopic composition of the reactant Hg(II) in the reactor as a function of "f", ~20 ml samples were withdrawn from the 1 L reactor at the same time that the traps were replaced and were preserved by the addition of 0.2% HCl (w/w) and 10% BrCl (w/w).

Mercury concentration and stable isotopic composition analysis:

Concentrations of Hg(II) in the reactor and trap solutions were measured using atomic absorption spectroscopy (AAS; Hydra AA, Leeman Labs) at Rutgers University as soon as the experiments were completed. Preserved reactor and trap samples were

analyzed for their Hg isotopic composition using a Nu Instruments MC-ICPMS at the University of Michigan. Samples were introduced into the mass spectrometer using cold vapor generation with Sn(II) reduction, which ensures complete reduction of Hg(II) in the sample and does not cause any fractionation (Bridget Bergquist, unpublished data). Instrumental mass bias was corrected using both a thallium (NIST 997) internal standard and standard-sample bracketing with the NIST SRM 3133 standard[62]. The Tl internal spike was added to the Hg vapor after cold vapor generation via an Aridus desolvating nebulizer[62]. Prior to introduction to the cold vapor generator and MC-ICPMS, samples were partially reduced with hydroxylamine hydrochloride to reduce excess $KMnO_4$ (in trap samples) or excess BrCl (in reactor samples) and diluted to a final concentration of 35 ppb or less. About 7 ml of solution was used for each individual analysis. Sample concentrations were matched within 10% to the bracketing standard (NIST SRM 3133), and the matrix of the bracketing standard was matched to the samples (either $KMnO_4$ or BrCl). In addition, on-peak zero corrections were applied to all masses and the ^{204}Pb interference on ^{204}Hg was corrected by monitoring ^{206}Pb. All procedural blanks were routinely analyzed for Hg. For a typical 7 ml sample, reactor and trapping solution blanks had Hg concentrations of < 0.75 ppb and < 0.15 ppb, respectively, which were too low to be accurately analyzed for isotopic composition.

Mercury isotopes are reported here in delta notation, in units of per mil (‰), referenced to a Hg standard (NIST 3133) and unless otherwise indicated, $\delta^{202}Hg$ refers to $\delta^{202}Hg/^{198}Hg$ and is calculated as:

$$\delta^{202}Hg = \left(\frac{(^{202}Hg/^{198}Hg)_{sample}}{(^{202}Hg/^{198}Hg)_{NIST}} - 1 \right) \times 1000$$

To ensure that the measured fractionation observed was mass dependent and that the isotope ratios measured were free of interferences, multiple isotope ratios (i.e., $^{200}Hg/^{198}Hg$, $^{201}Hg/^{198}Hg$, $^{202}Hg/^{198}Hg$ and $^{204}Hg/^{198}Hg$) were measured.

The typical internal (instrumental) precision for natural samples was better than ±0.003% (RSE) for all measured ratios. The uncertainty (external precision) for $\delta^{202}Hg$ in this paper has been estimated in two different ways: 1) the 2SD of repeated analyses of the in-house Almaden Standard prepared in the same matrix as the samples [$\delta^{202}Hg$ = -0.54 ± 0.09‰ (2SD, BrCl matrix, n=14) and -0.58 ± 0.19‰ (2SD, $KMnO_4$ matrix, n=13)], and 2) the 2SE of replicate analyses of each sample. To be conservative, error bars on Rayleigh plots and uncertainties used during linear regression of data (using Isoplot add-on function from Microsoft Excel software)[82] are based on the larger of these two values for each sample.

Calculations:

The kinetic fractionation factor ($\alpha = {}^{202}Hg/^{198}Hg_{reactant}/{}^{202}Hg/^{198}Hg_{product}$) was determined from the results of the experiments using the following two forms of the Rayleigh Distillation Equation as described by Hoefs[71] and Scott et al[83]. These equations were used to infer the value of α using the relative isotope ratio data from the reactor

(containing the liquid phase) and traps (containing samples corresponding to the time integrated product in the vapor phase), respectively.

$$\ln(R_{Li}/R_{Lo}) = ((1/\alpha) - 1)\ln(f) \quad \textbf{(1)}$$

$$\ln(R_{Vi}/R_{Lo}) = ((1/\alpha) - 1)\ln(f) + \ln(1/\alpha) \quad \textbf{(2);}$$

where

R = Relative isotope ratio $^{202}Hg/^{198}Hg_{\text{sample}}/^{202}Hg/^{198}Hg_{\text{NIST 3133}}$;

V = Vapor phase [Hg(0) in trap];

L = Liquid phase [Hg(II) in the reactor]

$\alpha = {}^{202}Hg/^{198}Hg_{\text{instantaneuos reactant}}/^{202}Hg/^{198}Hg_{\text{instantaneous product}}$

f = fraction of added Hg(II) remaining

$f^R = [Hg]_{Li}/[Hg]_{Lo}$

$f^T = ([Hg]_{Lo} - \Sigma[Hg]_{Vi})/[Hg]_{Lo}$

0 = 0 minutes; i = i minutes; [Hg] = Total amount of mercury (ng).

Both the slope [$(1/\alpha) - 1$] of the linear Rayleigh plots for Eq. 1 and 2 and the intercept [$\ln(1/\alpha)$] of the plot for Eq. 2 were used to calculate the value of $\alpha_{202/198}$. Linear regressions were carried out by the York method[82] in which each data point is weighted according to its uncertainty. In the absence of replicate analyses (for 100 ml reactor experiments), 0.09‰ and 0.19‰ were used as uncertainties for reactor and trap samples, respectively (see uncertainty discussion above).

Best estimates of alpha value: An $\alpha_{202/198}$ value based on the reactor isotope and concentration data is considered the best estimate of $\alpha_{202/198}$ value for that individual experiment. This is because reactor isotope data give the true instantaneous isotopic composition of the reactor at any given time (R_{Li} in Eq. 1 above), calculation of 'f^R' does not involve any estimations, and the reproducibility (external precision) for the reactor samples (BrCl matrix) is better than for trap samples ($KMnO_4$ matrix).

Approximation used to calculate f^T: For the trap samples, an effective f^T was calculated as the average of f before and after the interval of time during which a particular trap accumulated the product Hg(0) because the isotopic composition of the traps represents a time integrated product rather than the true instantaneous product composition (R_{Vi} in Eq. 2 above). Moreover, values of f^R calculated from reactor Hg concentration data are considered more reliable than f^T from the trap data (see supplement), and whenever possible (for all the experiments done using 1L reactor), the values of averaged f^R were used in preference to averaged f^T as the effective f for traps (see above).

Results and Discussion

In all experiments, the trapped Hg(0) had a lower δ^{202}Hg, i.e. was isotopically lighter, than the reactant Hg(II)(e.g. Fig. 2.1). Both the product Hg(0) and reactant Hg(II) followed mass dependent (Fig. 2.2) Rayleigh fractionation (Fig. S1-S4) as the experiments progressed, i.e., the Hg became isotopically heavier with the increasing extent of completion of the reaction.

Table 2.1 summarizes the estimates of the fractionation factors ($\alpha_{202/198}$ = $^{202}Hg^{/198}Hg_{reactant}/^{202}Hg^{/198}Hg_{\ product}$) based on the isotopic composition of the reactant Hg(II) remaining in the reactor and Hg(0) trapped in successive traps in these experiments, as modeled with the Rayleigh fractionation equation. The isotopic compositions of the reactant Hg(II) and product Hg(0) formed during microbial reduction (Tables S1-S4) and the Rayleigh plots (Fig. S1-S4) are provided as a part of the online supplementary material.

I discuss below the results of individual experiments in light of the well understood Hg(II) uptake and reduction mechanism in Gram negative Hg^R bacteria[8,84]. MerA mediated Hg(II) reduction is a complex process that includes diffusion through outer membrane, active transport (by *MerT* and *MerP*) across the periplasm and the inner membrane and interactions with thiol compounds[8]. Thus, I suggest that, similarly to the model that explains net sulfur fractionation during sulfate reduction by sulfate reducing bacteria (SRB)[67], the Hg fractionation observed will be the net effect of the fractionation at all of the individual steps before, and including, the rate-limiting step. It is important to note, however, that the reduction of the Hg(II) is an energy-requiring detoxification mechanism and therefore, is fundamentally different from the dissimilatory reduction of sulfate where SRB depend on sulfate for their growth[67] (or microbial reduction of terminal electron acceptors like nitrate[70], Se(VI)[57] and Fe(III)[74]).

Fractionation of Hg by *E. coli* JM109/pPB117 at its optimum growth temperature

Repeat experiments with *E. coli* JM109/pPB117 were performed at its optimal growth temperature (37 ^{0}C) (Fig. 2.1, see Appendix: supplement to Chapter 2:Table S1

and Fig S1, excluding data with f <0.3, see discussion on the suppression of fractionation below) in either 100 ml or 1 L reactors. All experiments yielded similar or overlapping values of fractionation factors (based on the isotopic composition of either the Hg(II) that remained in the reactors or the Hg(0) in the successive traps) with the $\alpha_{202/198}$ values (Table 2.1) ranging from 1.0014 to 1.0020, demonstrating that the $\alpha_{202/198}$ values are reproducible regardless of reactor size.

Dark abiotic controls volatilized only 1.2% or less of the added Hg(II) in the reactor, and the δ^{202}Hg of the reactor did not change over the length of the experiments (0.05 ± 0.05‰). Thus, the small amount of Hg(II) that was reduced abiotically in the growth medium is unlikely to have had a significant effect on the observed biological reduction in the experimental setup. Purging of Hg(0) formed after abiotic reduction of Hg(II) by addition of $SnCl_2$ did not cause any fractionation (Bridget Bergquist, unpublished data) demonstrating that the fractionation observed in the biological reduction experiments was due to biological uptake and/or reduction of Hg(II) rather than fractionation during purging and transport of Hg(0) between the reactor and trap.

Concentration dependent suppression of Hg fractionation

For the two pure culture experiments done at 37 ^{0}C in a 1L reactor (Table S1), I observed that when the fraction of added Hg(II) remaining in the reactor (f) fell below 0.3 (<180 ppb), there was a progressive suppression in the amount of fractionation compared to the prediction of the Rayleigh model (Fig. 2.1). Because all bacterial cells reducing Hg(II) were in the exponential growth phase (see methods) and there was an ample

supply of nutrients in the bacterial growth medium throughout the length of the experiments, the suppression in fractionation was unlikely to have been due to changes in the bacterial growth phase or nutrient limitation. Moreover, since this suppression was not observed for experiments done at 30 ^{0}C and 22 ^{0}C (see Rayleigh plots in Appendix: Supplement to Chapter 2), where f was always > 0.3 (with the exception of one point; Supplement to Chapter 2: Table S2) due to a slower growth rate of *E. coli*, this may be due to reactant [Hg(II)] limitation, as has been observed for some other stable isotope systems. There is considerable evidence that Hg(II) uptake is the rate limiting step in the MerA mediated reduction of Hg(II) ([84] and references therein). For sulfur, it is thought that at low sulfate concentrations (<1 mM) sulfate exchange across the cell membrane is rate limiting, leading to lesser exchange of sulfate back out of the SRB and suppression in apparent sulfur isotope fractionation[67]. I do not fully understand why there is drastic suppression in fractionation only after the Hg(II) concentration falls below 180 ppb in the reactor. Nevertheless, I suggest that as the experiments progressed, the concentration and availability of the Hg(II) in the reactor decreased to the point where the molar ratio of reactant Hg(II) to 'activated' Mer proteins became so low that it led to uptake and reduction of all the toxic Hg(II) in the cell's environment, diminishing the extent of fractionation. It is also plausible that as the cell density inside the reactor increased, the increasing amount of cell exudates sorbed Hg(II), further limiting the bioavailability of Hg(II) for uptake and reduction[85].

Effect of growth temperature on Hg fractionation: The effect of growth temperature on the extent of isotopic fractionation by strain *E. coli* JM109/pPB117 was tested by incubating the reactor at 30 ^{0}C and 22 ^{0}C. A decrease in growth temperature from 37 ^{0}C

to 30 ^{0}C increased the generation time of the bacterium from 90 minutes to 195 minutes, decreasing the rate of Hg(0) volatilization and necessitating a doubling of the time interval between two consecutive sampling points relative to that at 37 ^{0}C (Appendix: Supplement to Chapter 2: Table S2). Nevertheless, both the product Hg(0) and reactant Hg(II) followed Rayleigh fractionation (Appendix: Supplement to Chapter 2: Fig. S2) and the fractionation factors ($\alpha_{202/198}$) obtained were similar in range to those obtained for experiments at 37 ^{0}C (Table 2.1). When *E. coli* JM109/pPB117 was grown at 22 ^{0}C, the generation time of the bacterium increased to 300 minutes or more (Table S3, Fig S3) and the $\alpha_{202/198}$ values obtained using the reactor data are similar to those obtained at higher temperatures. The trap data from experiments done at 22^{0}C implied slightly higher values of $\alpha_{202/198}$, but with much larger uncertainties (Table 1, see supplementary text).

It is generally accepted that since bacterial metabolism slows down at lower temperatures[67], preference for the lighter isotope and the extent of fractionation should increase. Moreover, MerA is a thermophilic enzyme[86] and the lowered activity of MerA at low temperatures could potentially introduce another rate limiting step (in addition to the Hg(II) uptake step) in the processing of Hg(II) by Hg(II) reducing bacteria. Possibly, the absence of a significant increase in fractionation (and alpha values) at lower temperatures is due to the increased fractionation by MerA, balanced by an equal decrease in fractionation during the uptake/transport steps. A similar rationale has been accepted as the reason for lack of any change in sulfur fractionation when a naturally occurring SRB community growing with lactate as an electron donor experienced change in incubation temperatures from 25 ^{0}C to 5 ^{0}C[87]. Low temperatures decrease the fluidity of the membrane[87] and could limit the Hg(II) exchange reactions occurring within the

outer membrane and/or transport across the inner membrane of the Gram negative cell, thereby decreasing the fractionation during the Hg(II) uptake step.

Fractionation of Hg by Hg^R and Hg^S natural microbial communities

To expand the observations on the isotopic fractionation of Hg(II) during its biological reduction from pure bacterial cultures to the activities of natural microorganisms *in situ*, I obtained a natural microbial community from a freshwater pond and enriched the indigenous Hg^R bacteria by pre-exposure (see methods) to 225 ppb Hg(II). During this pre-exposure period, the majority of Hg^S microorganisms died while the Hg^R microbes increased in biomass; at the end of the pre-exposure period all culturable surviving cells were Hg^R (Fig. 2.3) and very likely carried and expressed *mer* operons[81]. I did not supplement the site water with nutrients at any stage of this experiment but it is possible that the death of Hg^S microbes resulted in the release of significant amounts of organic electron donors available for use by the Hg^R microbes during pre-exposure[81]. Since the enriched cells were harvested by centrifugation before re-suspension in filter sterilized site water, excess electron donors were not carried over from the pre-exposure period.

When the re-suspended enriched cells volatilized Hg from site water containing 225 ppb NIST 3133 Hg(II), the δ^{202}Hg of the Hg(II) remaining in the reactor followed Rayleigh fractionation with $\alpha_{202/198}$ value (1.0013 ± 0.0004), within the range of alpha values for the pure culture experiments (Fig. 1.4 and Appendix: Supplement to Chapter 2: S4 and Table S4). I expected to observe more noise in this data because even though all

the microbes in the 'adapted' natural microbial consortium are Hg^R, they must belong to diverse lineages, have differing metabolic potentials and the microbial community composition can change during the length of the experiment (60 hours).

In order to compare the extent of Hg fractionation by a Hg^R microbial consortium with a natural Hg^S community, microorganisms from the same water source were exposed to 25 ppb Hg(II) (NIST 3133) without preceding pre-exposure. This lower level of Hg(II) exposure for the un-adapted community, as compared to the adapted Hg^R consortium, was necessitated by the Hg(II) sensitivity of un-adapted microbes such that higher levels of Hg(II) in the reactor would have resulted in cell death. In this cell suspension less than 10% of the colony forming units (CFU) were Hg^R. During the length of the experiment, the un-adapted Hg^S community reduced 0.16 pg/g Hg(II) per CFU, in contrast to the Hg adapted consortium that reduced a thousand-fold more Hg(II) (0.162 ppb per CFU). Reduction by the un-adapted community resulted in a very small Rayleigh fractionation with $\alpha_{202/198} = 1.0004 \pm 0.0002$ (Tables 2.1 and Appendix: Supplement to Chapter 2: Table S4).

A very low extent of Hg(II) loss during dark abiotic control experiments consisting of filtered water from the same site (<2% of the added Hg(II) volatilized) indicated that the loss of Hg(II) from the reactor in the experiment with the un-adapted Hg^S community was due primarily to biological activity and not abiotic processes. The small amount of Hg reduced in the dark abiotic control experiments along with the smaller isotopic fractionation observed for the un-adapted community, suggests that dark biological reduction mechanisms that are likely unrelated to MerA activities do not cause

significant Hg stable isotope fractionation. These mechanisms possibly include Hg(II) reduction by Hg^S microbes and/or their metabolic products[88]. It is also possible that the reduced extent of fractionation by Hg^S community is partially due to suppression of fractionation at lower Hg(II) concentrations.

Implications and future of Hg isotope systematics

Mercury resistant bacteria preferentially reduced lighter isotopes of Hg as expected from past studies on microbial fractionation of traditional[70] and non-traditional stable isotopes[45]. The total range of δ^{202}Hg observed in the Hg transformations examined in this study is ~6‰ (Appendix: Supplement to Chapter 2:Table S1) and is similar to the maximum fractionation per atomic mass unit (Appendix: Supplement to Chapter 2:Table S5) observed for fractionation of much lighter elements including Fe and Mo[45]. As pointed out by Smith et al. (2005) (Fig. 4 in[63]), this large range of isotopic fractionation (i.e. δ^{202}Hg) of these heavy elements, including Hg, may be due to predominance of kinetic effects and redox sensitivity. A slightly smaller range of δ^{202}Hg (~5‰) was observed in hydrothermal ores[63] and sediments[68]. Although Smith et al. (2004) suggested that high temperature inorganic mechanisms may be responsible for Hg isotope fractionation in hydrothermal ores[63], the present study suggests that MerA-expressing Hg^R thermophilic bacteria[86] could also contribute to the isotopic fractionation observed in hydrothermal deposits.

The overlapping range of $\alpha_{202/198}$ values (best estimates from each experiment ranging from 1.0013 to 1.0020) observed for one Hg^R pure culture as well as a natural consortium of Hg^R microbes, and the non-dependence of the fractionation factor on

growth temperature, imply that bacterial Hg(II) uptake and reduction via the ubiquitous and efficient *mer* pathway could yield a consistent isotopic signature under differing experimental conditions. The progressive suppression in Hg(II) fractionation observed when the Hg(II) concentration in the reactor falls below ~180 ppb in both 1 L experiments done at 37 ^{0}C (Table S1) is interesting. In naturally occurring aquatic environments, the Hg(II) concentrations are lower than 180 ppb but since the induction of *mer* operon is quantitatively related to the concentration of bioavailable Hg(II)[8], the molar ratio of reactant Hg(II) to Mer proteins, including MerA, will not become as low as it possibly became during the experiments. Therefore, the environmental relevance of this decrease in the extent of fractionation at lower concentrations of Hg(II) could depend on a variety of factors that must be explored in future studies. It is highly probable that even though I found a narrow range of alpha values at differing temperatures for one exponentially growing Gram negative pure culture of bacteria grown with abundant electron donor and high Hg(II) concentrations, other growth conditions and/or other Hg^{R} bacterial species will not lead to similar extent of Hg fractionation because of differences in number and kind of rate limiting steps in the reduction pathway.

I also note that these experiments were carried out using ppb levels of Hg while in most natural waters, where the accumulation of MMHg in biota is of public health concern, Hg concentrations are often in the sub-ppb range. Currently the analysis is limited by the size of the reactor and the sensitivity of high-precision MC-ICPMS measurements. Future analytical developments are likely to enable determination of Hg stable isotope ratios in experimental products with lower concentrations of Hg.

This study, along with additional studies of similar and other Hg redox transformations, could give insights into Hg accumulation in natural sediment samples which typically contain abundant Hg (high ppb levels) and are easily measured archives of the Hg isotopic composition of aquatic systems[68,75]. I expect that further experimentation will reveal multiple mechanisms leading to Hg isotope fractionation, but nevertheless it seems likely that isotopic measurements will prove helpful in tracking changes in the redox state of Hg in aquatic and terrestrial environments in a manner analogous to the isotope systematics of other heavy elements such as Cr[74] and Fe[57].

In summary, I have provided clear evidence of systematic mass dependent kinetic fractionation of Hg isotopes. Hg is one of the heaviest elements for which significant biological fractionation has been observed, and the work adds to the growing number of heavy elements for which stable isotope systematics has been successfully developed in the past decade (see review[45]). This chapter suggests that Hg isotopes might have the potential for distinguishing between different sources of Hg(0) emissions based on the extent of Hg isotope fractionation. Thus this work is an important initial step in the development of Hg isotope systematics for the purpose of identifying Hg sources and sinks in the environment, for determining in situ pathways affecting Hg toxicity, and for investigating the nature and evolution of Hg redox reactions in both modern and paleo environments.

Chapter 3: Mercury stable isotope fractionation during MerB mediated biological degradation of methylmercury

Abstract

The extent of fractionation of mercury stable isotopes during degradation of monomethylmercury (MMHg) via the mercury resistance (*mer*) pathway in *E. coli* JM109/pPB117 was investigated in this study. The *mer* mediated degradation is a multi-step process that involves two enzymes, organomercurial lyase (MerB) and mercuric reductase (MerA). It was found that the MMHg remaining in the reactor became progressively heavier (increasing δ^{202}Hg) with time and underwent mass dependent Rayleigh fractionation with a fractionation factor $\alpha_{202/198} = 1.0004 \pm 0.00002$. A clear effect of cell density on the extent of fractionation of Hg both during reduction of Hg(II) and degradation of MMHg via the *mer* pathway was also seen. I discuss the implications of the effect of cell density on fractionation and the absence of mass independent fractionation during biological degradation via the *mer* pathway. I also provide constraints on the steps which could cause the extent of fractionation seen during experiments reported in this paper based on what is known about the rates at which different steps in the *mer* mediated MMHg degradation pathway.

Introduction

Significant variations in stable isotope ratios of Hg have been reported in natural samples including hydrothermal ore deposits[63], sediment cores[68,75,89] and fish

tissues[51]. But the ability to meaningfully interpret the stable isotope data from these studies hinges upon precise determination of isotope ratios in representative sources and quantification of the extent of change in isotopic ratios (i.e. fractionation factors) during individual biotic and abiotic transformations. For Hg, the mechanistic causes of the fractionation observed in natural samples and fractionation factors are beginning to be understood and quantified, respectively[51,52,90]. This paper reports experiments done to quantify the extent of fractionation during degradation of methylmercury (MMHg) by microorganisms that express the organomercury lyase (MerB) enzyme. This activity is specified by the mercury resistance (*mer*) operon in broad spectrum[8] Hg resistant bacteria. Here, I used strain *Escherichia coli* JM109 which carried the broad spectrum *mer* operon of the soil denitrifying bacterium *Pseudomonas putida* OX[78] plasmid on plasmid pPB117, a strain for which I had previously conducted reduction experiments[52].

$$\mathbf{CH_3Hg(I)} \xrightarrow{\text{MerB}} \mathbf{[CH_4 + Hg(II)]} \xrightarrow{\text{MerA}} \mathbf{Hg^0}$$

The *mer* mediated degradation of MMHg compounds is a multi-step process that involves transport of MMHg inside the cell (see below) and two enzymatic steps 1) breakage of the organo-mercury bond by organomercurial lyase (MerB) leading to formation of Hg(II) and methane and 2) reduction of Hg(II) to Hg^0 by the mercuric reductase (MerA). MerB and MerA are part of an elaborate Hg resistance mechanism that is specified by the inducible *mer* operon[8]. Both MerA and MerB are cytosolic enzymes[8,16]. It has been

shown that MerB mediated degradation can control MMHg accumulation in highly contaminated natural waters by reducing the concentration of MMHg[17].

I studied the extent of Hg isotope fractionation during degradation of monomethylmercury (MMHg) via MerB and MerA and discuss the data below in the context of what is known about the nature of Hg-microbe interactions. I consider diffusion of various mercury species that are involved in the uptake into, and release from, a microbial cell, as I have done for MerA mediated Hg(II) reduction in various microbial strains (Chapter 4). Finally, I discuss the results in light of what is known about the extent of fractionation that occurs during photo-degradation of MMHg.

Methods

***E. coli* JM109/pPB117 experiments**: Growth medium and conditions were those previously described in the study on fractionation during reduction of Hg(II) by *E. coli* JM109/pPB117[52]. Briefly, cultures were grown overnight in M9 based medium to an optical density (OD_{660}) of 0.8, diluted 1:10 in fresh medium, and exposed to 30 ng/ml (i.e. 150 nM) MMHg (Brookrands catalogue no: 06602, Lot 05-278-02E: stock supplied as 1000 ppm Hg in the form of methylmercury hydroxide) which, given the chloride concentration (pCl = 1.36) in the medium used[52], should speciate into methylmercury chloride[91]. After 4 hours of incubation at 37 ^{0}C, the OD_{660} of the pre-exposed starter culture increased to 0.3. This exponentially growing culture was used to inoculate the reactor at a ratio of 1:20 for the low cell density experiment and 1:40 for the high cell density experiment. The M9 based medium containing 30 ng/ml MMHg was used and samples were collected from the reactor at regular intervals to determine the

concentration and isotopic composition of mercury remaining in the reactor. Preliminary experiments (not presented) showed the pre-exposure of the starter culture led to higher growth rates in the reactor as compared to using an unexposed inoculum (see Appendix: supplement to Chapter 3). The cell concentration in the reactors was determined by plating on solid media as described earlier[52].At time = 0 minutes for the "low cell density" experiment was $1*10^6$ CFU/ml and for the "high cell density" experiment was $4*10^6$ CFU/ml, respectively (see results and Table 2.1 for details). An experiment to measure the change in isotopic composition during reduction of Hg(II) by *E. coli* JM109/pPB117 at a "high cell density" (~$4*10^6$ CFU/ml) was performed using Hg(II) (NIST SRM 3133) at ~30 ng/ml.

Mercury concentration and isotope analyses: Total Hg concentration and isotopic composition of the reactant MMHg and Hg(II) remaining in the growth medium was measured using cold vapor generation and multiple collector inductively coupled plasma mass spectrometry as described elsewhere[52]. Hg isotopes ratios are reported in delta notation, in units of per mil (‰), referenced to Hg standard (NIST SRM 3133). δ^{xxx}Hg refers to $\delta^{xxx}Hg/^{198}Hg$[44]and is calculated as:

$$\delta^{xxx}Hg = \left(\frac{(^{xxx}Hg/^{198}Hg)_{sample}}{(^{xxx}Hg/^{198}Hg)_{SRM}} - 1 \right) \times 1000$$

The MMHg stock used as a substrate in the experiments had an average δ^{202}Hg value of -0.4 ‰ with respect to SRM3133. Fractionation factors ($\alpha_{202/198} = [^{202}Hg/^{198}Hg]_{instantaneous\ reactant}/[^{202}Hg/^{198}Hg]_{instantaneous\ product}$) were calculated using methods described earlier[52].

Results

For the "low cell density" experiment, the isotopic composition of Hg in the reactor became progressively heavier indicating preferential degradation of the lighter isotopes of MMHg by the MerB mediated degradation by *E. coli* JM109/pPB117. The reactant MMHg followed mass dependent Rayleigh fractionation (Fig. 3.1) with a fractionation factor ($\alpha_{202/198}$) equaling 1.0004 ± 0.0002 (Fig. 3.1A and Table 3.1). As compared to the live control, where 30% of the added MMHg was lost in the first 8 hours of incubation and 60% after 18.5 hours (Table 3.1), loss of MMHg from the dark abiotic control reactor did not occur in the first 8 hours and less than 5% (1±0.5 ppb out of a total of 30 ppb) was lost by the end of the experiment. This loss was too small to allow determination of isotopic fractionation during abiotic degradation of MMHg under these conditions (see methods).

For the "high cell density" experiment (Fig. 3.2), however, no progressive change in the isotopic composition of Hg in the reactor was seen in spite of loss of MMHg from the reactor that was comparable to the loss during the "low cell density" experiment (Table 3.1). In fact, for the bulk of the experiment the isotopic composition of the reactor remained constant. The only reactor sample for the high cell density experiment that had a significantly different isotopic composition, as compared to consecutive samples in the experiment, was the sample taken immediately following the addition of MMHg (i.e. sample corresponding to f = 0.856 for the high cell density experiment in Table 3.1) (Fig. 3.2, Table 3.1). This suggests a small "start-up effect" occurring before a steady state (with respect to the concentration of intermediate species) was established in the system (see discussion below)

A qualitatively similar start-up effect along with a lack progressive change in isotopic composition was also seen when *E. coli* JM109/pPB117 reduced Hg(II) via the *mer* mediated pathway at high cell densities (Fig. 3.2). This complete dampening of fractionation at high cell densities is in stark contrast with the near perfect Rayleigh fractionation seen at low cell densities for both the reduction of Hg(II) (38) and degradation of MMHg (Fig. 3.1). The possible reasons for this dampening of isotopic fractionation with increased cell density are discussed below.

Discussion

The *mer* mediated degradation of MMHg: a multi-step process

The multi-step process of the *mer* mediated MMHg degradation includes (Fig. 3.3): 1) diffusion through the cell's boundary layer (see below), 2) uptake across the cell membrane 3), catalysis by 4) MerB and 5) MerA, 5) diffusion of Hg^0 out of the cell, and 6) diffusion of Hg^0 from the aqueous phase into the gaseous phase. Microbes are believed to be surrounded by a diffusion boundary layer (DBL) or diffusion sphere[92] that is not affected by the surrounding turbulence or bubbling[92,93]. Therefore, transport of substrate molecules from the aqueous environment to the bacterial cell surface takes place by molecular diffusion through the DBL. Genetic, uptake and biochemical studies show that, once at the cell surface, MMHg passes through the cell's outer membrane via passive diffusion in its neutral/hydrophobic form(s)[8,91,94,95]. In spite of some suggestions[96,97], there is no evidence suggesting a clear role of a specific protein transporter (Mer or otherwise) in uptake of MMHg compounds from the periplasm/inner membrane to the interior of the bacterial cell[95]. Studies of MMHg transport across mammalian cells

indicate that MMHg is transported as a complex with molecules containing –SH groups (i.e. cysteine or glutathione) via transporter specific to these molecules but this kind of MMHg co-transport is very unlikely to be relevant to the study because of the media composition and growth requirements of *E. coli*. The medium used in the study does not contain any molecules with –SH groups and *E. coli* can synthesize these molecules inside its cytoplasm After MMHg crosses the cell membranes and is in the cytoplasm, MerB breaks the C-Hg bond in MMHg and transfers the Hg(II) directly to MerA[98]. The product of MerA, Hg(0), diffuses through the cell membrane into the aqueous medium subsequently crossing the liquid-air interface.

Mechanism of fractionation

It is now well established that the net isotopic fractionation observed during a multi-step process is a function of fractionation by all the steps unto and including the rate limiting step[54,67]. In the following sections, I argue that at low cell concentrations, breakage of the C-Hg bond by MerB is the rate limiting, and very likely the only, fractionation contributing step because the preceding two steps do not cause fractionation. At higher cell concentrations, however, uptake of MMHg by the cell becomes the rate limiting step but does not cause significant fractionation. Although the substrate specificity and turnover number of MerB that are encoded by pPB117 are not known, the turnover rates of MerA are generally known to be much higher at k_{cat} = 400-800 min^{-1}[99,100], than those of MerB, k_{cat} = 0.7-20 min^{-1} for alkylmercurials including MMHgCl[101]. The significant fractionation that was reported to occur during the diffusion of Hg(0) from the aqueous to the gaseous phase[90] was unlikely to impact the results

because the reactors were continuously bubbled, so that the diffusion of the MerA product, Hg(0) out of the aqueous phase, could not be the rate limiting step under the employed experimental conditions. Therefore, I have assumed that the steps following the catalysis by MerB were not rate limiting in the overall process of the *mer* mediated degradation of MMHg (Fig. 2.3) and did not add to net fractionation.

1. Estimates of the rate of diffusion across DBL: The total diffusion flux (J) to the cell surface of a bacterium with a radius R, and assuming a substrate present at a concentration in the bulk medium of C_∞ (See Fig. 3.3) and with a diffusion coefficient (D) at a given temperature, is $J = 4\pi DR(C_\infty - C_{out})$[92]. The thickness of the DBL for a spherical cell is approximately equal to the cell's radius[93]. Although *E. coli* cells are short elliptical rods rather than spheres, the use of this equation is not likely to significantly change the approximate estimation of diffusion or uptake rates (see below). In order to calculate the maximum possible diffusion rate, I use the values of $R = 0.5*10^{-4}$ cm (typical half length for an *E. coli* cell), C_∞ = 30 ppb (i.e. the maximum concentration of MMHg in the medium: $0.15 *10^{-9}$ moles/cm^3), $D = 1.3 *10^{-5}$ cm^2/sec at 25^0C[102] and assume C_{out} *(*substrate concentration immediately outside the cell surface) ~ 0. These numbers imply a maximum diffusion flux (J_{max}) of $1.22*10^{-18}$ moles/sec ($7.4*10^5$ molecules of MMHg per second) at the beginning of the experiment. Naturally, J would become much lesser than J_{max} when MMHg concentration in the bulk medium (C_∞) decreases. I think that C_{out} will remain ~ 0 because cell is likely to be uptake limited most of the time (see below).

2. Estimates of the uptake rate across the bacterial membrane: The maximum uptake rate of a chemical species that permeates the cell membrane by passive diffusion, *V* (mol $cell^{-1}sec^{-1}$), can be estimated by the equation $V = P*C_{out}*A$, where *P* is the ability of the substrate to permeate the membrane (cm/s), C_{out} is substrate concentration immediately outside the cell surface (mol/cm^3) with the intracellular concentration being neglected, and A ($=4\pi R^2$) is the area of the cell surface (cm^2 $cell^{-1}$). In the medium pCl equals 1.35[52], which according to results of a previous study (Fig. 2 in[91] implies that over 96% of the total MMHg molecules in the medium were present as MMHgCl. Therefore, using the values of $P = 7.2*10^{-4}$ as permeability of MMHgCl[91] and $R = 0.5*10^{-4}$ cm , and assuming the maximum value of concentration of MMHg on the surface of the cell (Fig. 2.3)C_{out} = 30 ppb ($0.15 *10^{-9}$ $moles/cm^3$), the maximum possible uptake rate (V_{max}) equals $3.48*10^{-21}$ moles/sec (or $2.1*10^3$ MMHg molecules/second per cell). Under experimental conditions, C_{out} will be lower than 30 ppb and consequently V will be significantly lower than V_{max}. Nevertheless, V will always be 1-2 orders of magnitude less than J (see above) and hence the uptake rate across bacterial membrane will always be less than the rate of diffusion across DBL and cell will remain uptake limited.

3. Estimates of the rate of breakage of the C-Hg bond: The rate of breakage of C-Hg bond in a cell is the product of the total number of MerB enzyme molecules in a single cell (N_{merB}) and the turnover rate of an enzyme molecule (k_{cat}) and I do not precisely know either of these quantities for a number of reasons (see Appendix) . Previous research has shown that a single MerB enzyme molecule encoded by a plasmid unrelated to the one used in the study, but the only case for which turnover rates have been

reported, can process MMHgCl at the rate of 0.011 MMHg molecules/sec (k_{cat} = 0.7 min^{-1})[101]. I suggest the following two methods for estimating N_{merB}:

3a. Based on maximum possible known levels of MerA: It is known that at the height of induction of Tn501, a well characterized transposon carrying *mer* operon, MerA may account for a maximum of 0.7% (w/w) of the total wet weight of a cell[103]. The total number of MerA molecules in a cell (N_{merA}) would be equal to $W_{wet\text{-}cell}*f_{merA}*N_A/W_{MerA}$ where $W_{wet\text{-}cell}$ is the wet weight of an *E. coli* cell in grams; f_{merA} is the fraction of cell weight in the form of MerA; N_A is the Avogadro's number and W_{MerA} is the molecular weight of one mole of MerA molecules in grams. Using $W_{wet\text{-}cell} = 1*10^{-12}$[104], f_{merA} = 0.007 , $N_A = 6.023*10^{23}$ and $W_{MerA} = 1.2*10^5$ g, the maximum possible N_{merA} would be ~$3.5*10^4$. If I assume that MerB would also be expressed at that level inside a cell, the maximum number of N_{merB} will be close to N_{merA} i.e. $3.5*10^4$. This approach to calculate N_{merB} is not perfect because the arrangement and sequence of genes and promoters within *mer* operon of the plasmid pPB117 is quite different from arrangement in Tn501[78]. However, it has been observed that at low Hg concentrations number of transcripts of MerA and MerB are similar [17] and it is reasonable to assume that they could be expressed at similar levels.

3b. ***Based on the number of merB mRNA molecules and their average rate of translation:*** The total number of MerB mRNA molecules in a cell would be equal to $t_{merB/RNA}* W_{wet\text{-}cell}*f_{total\text{-}RNA}* N_p$ where $t_{merB/RNA}$ is the number of MerB transcripts per unit weight of total RNA per plasmid; $W_{wet\text{-}cell}$ is the wet weight of a single actively dividing

E. coli cell; $f_{total\text{-}RNA}$ is the fraction of cell wet weight in the form of total RNA; and N_p is the number of copies of the plasmid in the strain being used. At concentrations of Hg comparable to those used in this study, it was shown that there are ~100 transcripts of MerB per pg of total RNA for the low copy plasmid from which pPB117 was derived and that the number of mRNA transcripts for MerA and MerB are the same during induction at low mercury concentrations[17]. Using a value of 100 as the copy number (N_p) of plasmid pPB117 and $\sim 1*10^{-12}$ g as $W_{wet\text{-}cell}$ and 0.14 as $f_{total\text{-}RNA}$[104], the total number of MerB transcripts in a single *E. coli* JM109/pPB117 cell is estimated at $\sim 1.4*10^{3}$. It has also been estimated that in *E. coli* there are about $\sim 10^{2}$ protein molecules per transcript that encodes for this protein[105], implying that the maximum number of MerB molecules (N_{merB}) present in a *E. coli* JM109/pPB117 cell at any point is $\sim 1.4*10^{5}$. High copy number, however, does not necessarily imply proportional increase in the number of active Mer proteins and some Mer proteins could be "cryptic" i.e. non-functional in a high copy number plasmid[106] suggesting that this estimate for N_{merB} might be on the higher side.

The rate limiting step: Enzymatic turnover vs. substrate uptake at low vs. high cell densities

In this section, I would like to consider the role of decreased bioavailability of MMHg and decreased rate of MMHg uptake across the cell on the extent of fractionation during 'low cell density' ($\alpha_{202/198}$ = 1.0004) and 'high cell density' (no apparent fractionation) experiments.

The turnover rate (k_{cat}) of 0.011 MMHg molecules/sec (see above) implies that for a cell to be uptake limited at uptake rate (V_{max}) of $2.1*10^3$ molecules/sec/cell (see above), a single bacterial cytoplasm should have more than $1.9*10^5$ active MerB enzymes molecules. Both estimates of the maximum number of MerB enzymes per cell (see above) suggest that, at least at the beginning of the experiment, the uptake rates might be slightly higher than the rate of breakage of the C-Hg bond. Based on these numbers, I suggest that at low cell densities, ample MMHg is bioavailable for diffusion and uptake into the cell and the activity of MerB is the rate limiting step in the overall process of MMHg degradation by the *mer* mediated pathway.

At higher cell concentrations, however, the MMHg concentration available per unit cell is lower than during the low cell density experiment. Although the distribution coefficients (K_D) for MMHg compounds are 1-2 orders of magnitude lower than for Hg(II)[107], this change in bioavailability of MMHg could be further exacerbated by enhanced sorption of MMHg to the bacterial cell surface, a process known to decrease bioavailability of Hg(II) to intracellular processes[85,108]. The rate of MMHg degradation for the low cell density experiment is significantly higher (as determined by the Tukey-Kramer method for unplanned comparison of regression coefficients at 95% confidence level) than the rates of its degradation in the experiment starting with high cell density (see Appendix: supplement to chapter 3). This change in the rate of reduction at higher cell densities suggests that at high cell concentrations, the process of MMHg degradation via the *mer* pathway could have been uptake limited[108]. It has been shown that the diffusion of molecules including heavy elements like Fe and Zn in water based solutions

did not cause significant fractionation over distances as small as the length of a cell's diffusion boundary layer[109]. Studies of stable isotope fractionation during sulfate reduction have relied on the maximum and minimum observed extent of fractionation during the overall process of sulfate uptake and reduction to estimate the extent of fractionation possible during individual steps in that multi-step process[54,67]. Similarly, I suggest that the absence of any change in isotopic composition of the reactor with time (Fig. 3.2), with the exception of the first data point (see start up effect below), at higher cell densities is due to MMHg diffusion through the DBL and the outer membrane becoming the rate-limiting step(s) that do(es) not cause fractionation (see also supplement to Chapter 3 in the Appendix).

Explanation for the "start-up effect"

In a multi-step process, intermediate species build up in concentration inside the cell and should eventually reach a steady state. Once the pools of intermediate species have reached a steady state, the extent of fractionation (α) should be fixed. However, at the beginning of an experiment when this has not yet been attained, the steady-state model does not yet apply leading to a deviation from the steady state behavior in the beginning of reaction. This phenomenon is referred to as a "start-up effect"[57]. This effect is usually ascribed to the understanding that the early product of the overall reaction, before the concentration and isotopic composition of the intermediates have become constant inside the cell, experiences the kinetic effects of all the steps occurring even beyond the rate limiting step, and is thus relatively more fractionated than the steady state product[57].

Since I observe start up effects in both the MMHg degradation (first time point at 3 hours) and the Hg(II) reduction experiments (first reactor time point at 25 minutes) (Fig. 3.2 and Table 3.1), I ascribe the initial change in isotopic composition of the reactor to the degradation of very light reactants in the first few minutes of the experiment when the amount of MMHg processed per cell was likely very low and the cell was not yet diffusion-limited. The experiments with higher Hg(II) concentrations and low cell densities[52] when the cells were not likely to be diffusion limited (See also discussion in Chapter 4), show higher fractionation with $\alpha_{202/198} \sim 1.0016$. This higher fractionation suggests that higher fractionation is possible when the step involving reduction by MerA, and not diffusion of the reactant, is the rate limiting step and thus provides explanation for the start-up effect (i.e., higher fractionation before establishment of steady state). The start up effect would not be seen if the time period after which the first sample was collected following the beginning the experiment was longer than the time required to reach steady state under those experimental conditions. This explains why a start up effect was not observed in experiments with low starting cell densities (Fig. 3.1A and Table 3.1; see also Chapter 2), where the time required to reach a steady state was likely short due to high mercury concentration available per unit cell. Therefore, in those experiments the steady state kinetic fractionation dominated the isotopic composition when the first samples were collected. Because natural systems are unlikely to experience abrupt changes in mercury concentrations they are probably closer than the pure cultures incubations to a steady state system with regard to the concentrations of intermediates inside the cell. Therefore it is not clear how significant the start-up effect will be in producing fluctuations in isotopic composition of MMHg in the environment.

Absence of mass independent fractionation during *mer* mediated degradation of MMHg

The value of fractionation factor that I determined for the biological degradation of MMHg ($\alpha_{202/198}$ = 1.0004 ± 0.0002) is much lower than the value determined by Bergquist and Blum[51] for the photo-degradation of MMHg ($\alpha_{202/198}$ = 1.0016 ± 0.0002) (Fig. 3.1A). In addition, biological *mer* mediated transformations[52,110] show no evidence for mass independent fractionation (MIF) as reported for photo-induced Hg(II) reduction and MMHg degradation[51] (Fig. 3.1B). The absence of MIF during biotic transformations of Hg clearly supports one of the important assumptions made by Bergquist and Blum[51] who, in calculating the relative importance of photo-degradation of MMHg in different lakes, assumed that only photochemical processes, and not biological transformations, would cause MIF of Hg in aquatic systems. Although it cannot be completely ruled out, I suggest that MIF, specifically the magnetic isotope effect (MIE), during other biologically mediated transformations is quite unlikely (see below). Below I list a number of conditions that must be satisfied for the manifestation of MIE (Chapter 5).

The MIF of mercury during photochemical transformations[51] may be ascribed either to the MIE or nuclear volume effect[48,51]. However, because of the involvement of radicals in DOC mediated reduction of Hg(II) and for other reasons[51], I suggest that the MIE is the likely reason for MIF. The MIE happens due to a higher spin inter-system crossing (ISC) (i.e. triplet ↔ singlet conversion rates) rate in radical pairs involving isotopes with nuclear spins (^{201}Hg and ^{199}Hg) as compared to those without nuclear spins (e.g. ^{198}Hg and ^{202}Hg). The interaction of nuclear spins with electronic spins is called

hyperfine coupling (HFC). The change in ISC rates can affect the reaction rate of different isotopes when a number of conditions are met[47].

Specifically, for MIE to be manifested during non-photochemical enzymatic reactions[47,111], there must be at least one step in the biological process that generates a relatively long lived *pair* of weakly coupled spin-correlated radicals, or paramagnetic particles, and a physical mechanism, i.e., hyperfine splitting in the absence of an external magnetic field, must exist to promote magnetic field-dependent ISC. However, currently there is no evidence available that suggests active involvement of radical pairs or paramagnetic species in non-photochemical biological reactions of mercury. On the contrary, biochemical investigations[16,112], insights from the three dimensional structure of MerB[113], and recent synthetic analog studies[114] clearly show involvement of –SH groups from at least three different cysteine residues in the proposed mechanism for the C-Hg bond cleavage and no evidence for radical formation. In fact, if radical pair formation and recombination was involved in MerB catalysis, cleavage of bi- and tri-cyclic organomercurial substrates, whose radicals can undergo rapid skeletal rearrangement, would have yielded multiple reaction products and this was not found to be the case[112]. Similarly, in spite of frequent interactions of Hg(II) with cysteine residues or -SH groups in all Mer proteins[115], no involvement of radicals, radical pairs or paramagnetic species, e.g., $Hg^{\bullet}$ or Hg^{+}, seems possible based on results from numerous biochemical studies that have elucidated the MerA reduction mechanism[116]. Specifically, exchange of cysteine residues (or -SH groups) by Hg(II) does not involve any radical reactions (Sue Miller, personal communication).

For MIE to manifest itself, rate of HFC dependent ISC should be also be much faster than the rates at which 1) the starting radical pair reacts and 2) the spin relaxation occurs[117]. Therefore, another important aspect that needs to be considered in the context of MIE for Hg isotopes is that due to an atomic number that is very high (Z = 80), Hg atoms exhibit a high magnitude of spin orbit coupling. High SOC can cause singlet-triplet transitions irrespective of the extent the HFC (i.e. the rate of SOC induced ISC is independent of the nuclear spins of the isotopes). High SOC can also cause faster paramagnetic/radical spin relaxation and can decrease the role of HFC in MIE and might even lead to complete quenching of MIE[117]. High SOC in heavy atoms causes high ISC not just of their own radicals (internal heavy atom effect) but also of other neighboring atoms (external solvent effect)[118,119] . Because they have an inherent quality of causing high rates of ISC, the presence of elements with high SOC such as Xenon (SOC constant of ~6000 cm^{-1}), in the solvent phase are able to induce ISC and possibly change electron transfer rates in zeolite[120] and enzyme bound radicals pairs[119]. Specifically for Hg (SOC constant range 4000-5000 cm^{-1}[1121]), it has been found that the complexation to a mercury compound leads to decreased lifetime of triplet states and decreased phosphorescence in three different organic compounds not known to phosphoresce on their own clearly demonstrating the effect of Hg's high SOC on ISC[121]. The effect of SOC can be minimized if either of the following conditions are met: 1) the heavy atom in the radical is very symmetrically bound to its ligands; 2) the electronic spin density on this atom is low; 3) the valence shell electrons of the heavy atom are effectively screened from the nucleus[117]; or 4) the rate of the reaction is faster that the rate of relaxation of spins due to high SOC (rate of relaxation is always $<10^9$ s^{-1})[111,117].

Ionic mercury can form very symmetrical linear complexes with two sulfur donor ligands but the Hg(II)-thiol bonds are labile especially during biological interactions and a single Hg atom is coordinated with more than two –SH ligands often with flexible and distorted trigonal or tetrahedral coordination figures ([122] and references therein). Therefore, it is difficult to comprehend how biological transformations of Hg compounds which are typically slow (k_{cat} for MerB $4*10^{1}$-$1.4*10^{4}$ s^{-1}, k_{cat} for MerA < $4.8*10^{4}$ s^{-1}[18] could allow minimization of SOC to allow the difference in nuclear spins of Hg and the resultant HFC to be dominant and cause significant magnetic isotope effect (Grissom, personal communication). On the other hand, although I can not be certain, significant MIE that has been recently observed by two groups[51,123] can possibly be explained by a number of characteristics of photon induced transformations of Hg compounds. Unlike biological pathways, which in the absence of light would lead to formation of singlet states, photon absorption permits efficient formation of triplet state radical pairs[111] and a single radical formation can trigger propagation of multiple chain events and might lead to lifetimes of radical pairs that are shorter than the time needed for SOC dependent spin relaxation[111,117] but slower than the time needed for HFC mediated ISC.

Because of the two reasons (absence of evidence of radical pairs and high SOC range) outlined above, I am puzzled by a study[124] which presents an experimental dataset supporting a high percentage of MIF (up to 20%, which is 25 fold higher than the range of MIF observed during photochemical processes) during *in vitro* binding of MMHgCl with a non-Hg transforming enzyme, creatine kinase, in the absence of any external magnetic field and light. Most elements which undergo MIE in spite of high SOC constant have a very small magnitude of MIE[117] which is only expressed during

photochemical transformations. Therefore, this high percentage of MIF[124] is quite unlikely given the extremely high SOC constant value of Hg (Charles Grissom, personal communication)(see above). Buchachenko *et al.*[124] present a reaction scheme based on a radical pair (methylmercury anion radical and R-cysteine cation radical) recombination that could, in principle, explain "escape" and enrichment of odd isotopes in an enzyme bound fraction due to their higher ISC rates as compared to the ISC rates in even-numbered isotopes[47,111]. However, as explained above, there is no evidence, in their paper or elsewhere, that supports either involvement of Hg-thiol interaction in binding of MMHg with creatine kinase or generation of long lived radical pairs during Hg-thiol interactions. Moreover, the isotopic abundance of Hg in methylmercury chloride used as starting material in the creatine kinase study is also difficult to reconcile with the known natural isotopic abundance variation of Hg leaving the validity of the isotope abundances measured in the study in question.

This discussion above suggests that evidence for MIF in natural samples (fish, sediments and water) can not be explained by the activity of Mer enzymes and very likely other dark biological pathways in degradation of MMHg and reduction of Hg(II). Of course, it is plausible that photo processes impart MIF to Hg species after they have been fractionated in a mass dependent manner by biological pathways, thus complicating interpretation of the isotope data. Because the presence or absence of MIF has important repercussions for the future use of Hg isotopes as a biogeochemical tool, more research is needed to ascertain the effect of the consecutive reprocessing of Hg compounds by different pathways (e.g. photo-chemically or reactive halogen species- induced oxidation

of Hg(0) that was originally produced by biological reduction of Hg(II)) on net fractionation.

I would also like to point out that the effectiveness of SOC in causing spin relaxation depends on magnetic quantum numbers of the isotopes and could also depend on the nuclear volume of the isotope. Smaller nuclear volume would likely increase the effectiveness of SOC in compounds where valence electrons are in the s orbital[48,117]. Therefore, if some photo-chemical pathways are slower as opposed to others and allow a different extent of manifestation of SOC, it could possibly explain the changing relationship between Δ^{199}Hg and Δ^{201}Hg as seen during photo-induced reactions of mercury[51]. Therefore, an understanding of the nature of the competing HFC and SOC interactions is crucial to understanding the efficiency and role of MIF (magnetic vs. nuclear volume effects) in natural reactions involving radical pairs containing heavy atoms[117].

Overall implications of this study

This study provides clear evidence for systematic mass dependent biological fractionation and absence of MIF of Hg isotopes during degradation of methylmercury by the organomercury lyase and also the other *mer* mediated functions. It supports the suggestion that Hg isotopes might have the potential for distinguishing between different sources of, and transformation pathways leading to Hg(0) emissions (abiotic vs. biotic) based on the extent of mass dependent and mass independent isotope fractionation. It also underscores the importance of the role of cell densities (and possibly other ligands that can reduce Hg bioavailability) in determining the extent of *mer* pathway mediated mass

dependent biological fractionation. It is plausible that a kinetic, i.e., time dependent, competition for Hg between ligands and the interior of the cell could play an important role in the extent of biologically mediated Hg fractionation. This thesis (this chapter and Chapter 4) makes it clear that net fractionation of Hg during a microbial process is a function of intracellular physiology of the cell (e.g., rates of gene expression and turnover number of proteins etc. that can control the nature of the rate limiting step in the multi-step process) and external environment of the cell (i.e., concentration of Hg compounds that can control the bioavailability of the Hg species). I provide a theoretical framework for understanding the net fractionation seen under various experimental conditions and this framework can be used to design experiments to confirm the steps within the *mer* mediated MMHg degradation pathway that cause fractionation.

I also point out that the two *mer* mediated processes, Hg(II) reduction and MMHg degradation, share a crucial step in the reduction of Hg(II) to Hg(0) and apparently have similar net extent of fractionation (Chapter 5). However, because of the different mode by which Hg(II) and MMHg are transported into the bacterial cell, the rate limiting and thus fractionation contributing step(s) are different in these two processes. A detailed comparison of the two processes is presented in Chapter 5.

Hence, this work is an important step in the development of Hg isotope systematics for the purpose of identifying Hg sources and sinks in the environment and for determining relative importance of *in situ* pathways affecting Hg toxicity.

Chapter 4: Constraints on the extent of mercury stable isotope fractionation during reduction of Hg(II) by different microbial species

Abstract

The extent of fractionation of mercury stable isotopes during reduction of Hg(II) by three different Hg(II) reducing strains (including two Hg(II) resistant strains with active *mer* pathway *Bacillus cereus* Strain 5 and *Anoxybacillus* spp. Strain FB9; and a Hg(II) sensitive strain, *Shewanella oneidensis* MR-1, that reduces Hg(II) at low concentrations by a non-*mer* mediated process) was investigated in this study. It was found that in all cases the Hg(II) remaining in the reactor became progressively heavier (increasing δ^{202}Hg) with time and underwent mass dependent Rayleigh fractionation with a fractionation factor $\alpha_{202/198} = 1.0016 \pm 0.0004$. An effect of cell density on the extent of fractionation of Hg both during reduction of Hg(II) was also seen. I discuss and provide constraints on the steps which could cause the extent of fractionation seen during experiments reported in this paper based on what is known about the rates at which different steps in the *mer* mediated Hg(II) reduction pathway and non-*mer* mediated Hg(II) reduction in MR-1.

Introduction

Reduction of ionic mercury [Hg(II)] to elemental mercury [Hg(0)] is one of the most important transformations in the mercury biogeochemical cycle because it competes for the substrate of methylation, i.e. Hg(II), and results in the removal of the

product Hg(0) from aquatic ecosystems. Both photo-chemical processes and specific and non-specific microbiological activities reduce Hg(II) but it is not clear which mechanisms lead to the reduction of Hg(II) in a given aquatic environment[7]. Because the atmospheric transport and distribution of Hg(0) remains a major source of Hg contamination, the sources and pathways for the formation of Hg(0) emissions are central to all regulatory efforts that are aimed at controlling this problem[6]. On a regional and global scale, the two primary approaches, direct measurements and modeling, which are used to assess sources of Hg(0) emissions are subject to high amounts of uncertainties[6]. Stable isotopic signatures hold great promise in differentiating between sources, elucidating pathways, and determining the relative contribution of each source to mercury deposition at a given location[6]. The ability to use stable isotope ratios of mercury as a reliable indicator of biogeochemical history of the mercury species for environmental management, however, depends on determination of the fractionation factors resulting from each individual transformation process known to be a part of the global and regional mercury biogeochemical cycle.

A previous chapter[52] showed that reduction of Hg(II) by the *mer* mediated pathway in a Hg(II) resistant Gram-negative bacterium, *Escherichia coli* JM109/pPB117, systematically reduced the lighter isotopes of Hg(II) with the best estimates of a fractionation factor ($\alpha_{202/198}$) ranging from 1.0014 to 1.0020 irrespective of incubation temperature. However, as noted earlier[52], it is likely that even though I found a narrow range of overlapping alpha values for one Gram-negative pure bacterial culture when grown at different temperatures (22 to 37 ^{0}C), other *mer* carrying bacteria may not lead to a similar extent of mercury fractionation because of differences in the nature of cell walls

and transport mechanisms, or the number and nature of the rate limiting step in the reduction pathway. In the case of selenium (Se) isotopes, experiments with a Gram positive and a Gram negative microbe each suggested that the extent of Se isotope fractionation changes significantly during selenate reduction to elemental selenium but not during selenite reduction to elemental selenium[57] but in the case of sulfur isotopes, a large dataset collected from studies with 32 different sulfate reducing microbes doesn't show any systematic effect of microbial phylogeny or physiology. Therefore, experimental studies such as this are vital for constraining the range of fractionation factors for Hg.

It is also vital to study fractionation during non-*mer* mediated biotic processes of Hg(II) reduction because microbial Hg(II) reduction is known to play an important role in the evasion of Hg(0) from marine waters, but it is unclear whether this is the result of *mer* mediated enzymatic reduction or non-specific biotic reduction pathways[9]. Previous experiments[52] with natural microbial communities suggested that the stable isotopic composition of Hg(II) that remained in the reactor could be used to differentiate between reduction by the *mer* mediated pathway (average $\alpha_{202/198}$ = 1.0013) from reduction of Hg(II) by a non-specific reduction in the dark by Hg(II) sensitive microbes (average $\alpha_{202/198}$ = 1.0004). This suggested that different Hg(II) resistant microbes, likely present in the natural consortium, caused a similar extent of fractionation as the pure *E. coli* JM109/pPB117 strain while the Hg(II) sensitive microbes did not. To confirm this suggestion, I attempted to constrain the extent of isotope fractionation by various Hg(II) reducing bacteria by measuring the extent of mercury isotopic fractionation during Hg(II) reduction by three bacterial strains known to reduce Hg(II) during their growth. We used

two Hg(II) resistant Gram-positive bacterial strains, a mesophilic soil bacterium, *Bacillus cereus* Strain 5[125] and thermophilic *Anoxybacillus* spp. Strain FB9[126], which grow at 30 and 60 ^{0}C, respectively, and a Hg(II) sensitive Gram-negative anaerobic bacterium, *Shewanella oneidensis* MR-1, that was recently shown to reduce Hg(II) at low concentrations by a non-*mer* mediated process likely associated with respiratory electron transport chains[108].

The *mer* mediated Hg(II) reduction mechanism is mediated by the mercury resistance (*mer*) operon which is found in a broad range of Hg-resistant bacteria and archaea from diverse environments[8,127]. There are three components central to the *mer* pathway in bacteria, Hg(II) transport, catalysis, and regulation. Specific and high affinity dedicated uptake of Hg(II) starts in bacterial periplasm (in Gram-negative bacteria) where MerP acts as an extra-cytoplasmic Hg(II) "sponge" and transfers the Hg(II) ion to trans-membrane alpha helical transporters like MerT, which transports it across the inner membrane. It has been suggested that in Gram-positive bacteria, which have a different cell wall structure and lack both the outer membrane (OM) and the periplasmic space, MerP is present outside the cell but attached to cytoplasmic/inner membrane[128]). Mercuric reductase (MerA), a disulfide oxidoreductase which uses NAD(P)H as a reductant mediates the catalytic reduction of Hg(II) to Hg(0). The regulatory components of the operon (e.g. MerR) regulate the induction of the operon in the presence of extracellular Hg(II).

There has been no systematic exploration of the Hg(II) reduction mechanism in anaerobes, but this might mainly involve cytochromes in anaerobic bacteria that are abundantly present in the periplasm or in the outer membrane and possibly encounter and

reduce Hg(II) before it enters the cytoplasm and becomes complexed to cytoplasmic thiols (Sue Miller, personal communication). This is supported by Wiatrowski *et al*[108] who have shown that Hg(II) reduction in MR-1 is dependent on the presence of both electron donor and acceptor. The fact that not all dissimilatory metal reducing anaerobic bacteria that were tested reduced Hg(II), suggested that this process is specific to those metal reducing strains that did reduce Hg(II)[108]. I discuss the results in light of the steps known or proposed to be involved in the multi-step processes of Hg(II) reduction by these three strains.

Materials and Methods

Bacterial strains and growth conditions: The overall strategy for the determination of fractionation factors during Hg(II) reduction experiments was described previously[52]. Cultures, available in the culture collection in Barkay laboratory, were grown in the dark under optimal conditions for each strain as described below:

1) *Bacillus cereus* Strain 5: *B. cereus* strain 5, a low GC Gram-positive soil organism[125] for which Hg(II) resistance is inducible and is encoded by an uncharacterized plasmid pGB130[129], was grown in M9 based defined medium[52] with the addition of 0.1% yeast extract. Cells were grown overnight at 30 ^{0}C with shaking to an optical density (OD_{660}) of 0.6. The overnight culture was diluted 1:10 in fresh medium containing ~600 ppb Hg(II) in the form of $HgCl_2$. After 3.5 hours when an OD_{660} of 0.35 was reached, another addition of 600 ppb Hg(II) was made to re-induce the culture and 15 min later, 300 μL of this starter culture was added to 300 ml of fresh M9 medium containing 600 ppb of

Hg(II) in the form of SRM NIST 3133 in a 1L reactor. An uninoculated reactor containing the same medium and level of Hg(II) addition was used an abiotic control. The starting cell density in the reactor as determined by spread plating on LB plates was $5*10^5$ CFU/ml. Samples were collected from the reactor at regular time intervals to determine the concentrations and isotopic composition of Hg(II) that remained in the reactor.

2) *Anoxybacillus* sp. Strain FB9: Strain FB9 is a low GC Gram-positive thermophilic facultative chemolithoautotroph that was isolated from a mercury rich geothermal spring in Tuscany, Italy[126]. The strain was grown under chemolithoorganotrophic conditions with 10 mM acetate at its optimum growth temperature of 60 ºC as described previously[126]. The cells were grown overnight at 60 ^{0}C to a cell count of $1.5*10^9$ CFU/ml as determined by direct microscopic counts[126]. The overnight culture was induced by the addition of 200 ppb Hg(II), incubated for additional 30 min, and diluted 1:10 into a 1L reactor which contained ~350 ml fresh medium with 500 ppb Hg(II). The strain *Anoxybacillus* spp. FB9 failed to grow in medium containing Hg(II) in the form of NIST SRM 3133 as starting material very likely because the bromine chloride (BrCl) which was used at 1% to preserve the secondary SRM 3133 stock is a strong oxidizing agent which could have been toxic to the strain. Therefore, instead of using this standard reference material I used a 5 ppm $HgCl_2$ stock preserved in 2% trace metal grade HCl that had an average δ^{202}Hg (see below) value of -0.85 ‰ with respect to NIST SRM 3133 as the source of Hg(II) in the growth medium. Two control incubations employing the same medium and condition were included: a control consisting of heat killed cells,

which had been placed at 90 ^{0}C for 40 minutes prior to inoculation of the reactor, and an abiotic control that was performed on a different date, which contained a higher starting Hg(II) concentration (~875 ppb). All incubations and sample collections were performed as described above for *B. cereus* strain 5.

3) *Shewanella oneidensis* MR-1: Strain MR-1 is a facultative anaerobe that grows on multiple electron acceptors and was recently shown to reduce Hg(II) by a non-inducible non-*mer* dependent pathway[108]. This strain was grown under fumarate reducing conditions as described previously[108]. Briefly, autoclaved medium components (except as noted below) were assembled aerobically in a pre-sterilized 1000 ml reactor and the reactor was bubbled with oxygen free air for 45 minutes to purge any dissolved oxygen. Anaerobic and filter sterilized stock solutions of sodium fumarate (electron acceptor), sodium lactate (electron donor), amino acids and sodium bicarbonate were added towards the end of this bubbling period. NIST SRM 3133 diluted to 50 ppb Hg(II) was added to the reactor before the addition of the starter culture. A fumarate reducing starter culture was grown to an OD_{660} of 0.07, corresponding to ~ 10^8 cells/ml (Wiatrowski *et. Al,* 2006), and diluted 1:1000 in fresh medium (that was prepared as described above) to start the experiment. A heat-killed control reactor consisted of same medium, incubation conditions, and Hg(II) concentration as above but instead of live cells, the same number of heat killed cells (heated at 80 ^{0}C for 30 minutes) were added. All incubations and sample collections were performed as described above for *B. cereus* strain 5.

Mercury concentration and isotopic determination: The concentration of total Hg and the isotopic composition of the reactant Hg(II) in growth medium samples were measured using cold vapor generation and multiple collector inductively coupled plasma mass spectrometry, respectively, as described previously[52,63]. Isotope ratios for all experiments are reported in delta notation, in units of per mil (‰), referenced to a standard (NIST SRM 3133)[44]. $\delta^{xxx}Hg$ refers to $\delta^{xxx}Hg/^{198}Hg$ and is calculated as:

$$\delta^{xxx}Hg = \left(\frac{(^{xxx}Hg/^{198}Hg)_{sample}}{(^{xxx}Hg/^{198}Hg)_{NIST}} - 1 \right) \times 1000$$

Fractionation factors ($\alpha_{202/198} = [^{202}Hg/^{198}Hg]_{instantaneous\ reactant}/[^{202}Hg/^{198}Hg]_{instantaneous\ product}$) were calculated using methods described earlier[52].

MINEQL modeling

The speciation of Hg(II) in both the anaerobic growth medium used for growing Strain MR-1 was determined using the chemical equilibrium speciation model, MINEQL+ (version 4.5)[130], using input parameters obtained from the MINEQL+ and the National Institute of Standards and Technology (NIST) database[131].

Results

Reduction of Hg(II) to Hg(0) by all Hg(II) reducing strains used in this study lead to enrichment of heavier isotopes in the reactor indicating preferential uptake and reduction of lighter isotopes of Hg and, barring the suppression of fractionation at lower Hg(II) concentrations and higher cell densities, caused mass dependent Rayleigh type

fractionation (Fig. 4.1-4.3; Tables 4.1-4.3) of Hg(II) in the reactor with the mean values of $\alpha_{202/198}$ ranging from 1.0012 to 1.0018.

For the experiment with *B. cereus* Strain 5 (Fig. 4.1, Table 4.1), the value of the fractionation factor (N = 4; see Table 4.4)($\alpha_{202/198}$) was 1.0012 ± 0.0001 (2SD). As compared to the live control, where 65% of the added Hg(II) was lost from the reactor in the first 6.5 hours (Table 3.2), only 2.5% was lost during that period from the dark abiotic control with an isotopic composition (δ^{202}Hg) of 0.07 ± 0.08 ‰ (2SD of repeat analyses of the in-house standard[52]). After ~3 hours of incubation, when cell density had increased to ~10^7 CFU/ml and Hg(II) concentration dropped to <520 ppb, a very clear (but slow) progressive suppression in fractionation was seen even though the growing cells continued to actively reduce Hg(II). If I include all the data points (N = 8) in the calculations for alpha factor (Fig. 4.1), the value of $\alpha_{202/198}$ is much lower (1.0006) but is not a good fit (lower R^2 values in Rayleigh plots, not shown). In my view, such a inclusion of all data points for calculation of fractionation factor will miss the clear trend of suppression of fractionation that is seen in the other experiments as well (see below and chapters 2 and 3).

For the experiment with *Anoxybacillus* sp. FB9 (Fig. 4.2, Table 4.2), the value of the fractionation factor ($\alpha_{202/198}$) was 1.0014 ± 0.0001 (2SD). As compared to the live control where 72% of the added Hg(II) was lost from the reactor in the first 9 hours of incubation (Table 3.3), only ~1% and <3% were lost in same amount of time from the dark abiotic and dark heat-killed controls, respectively, and the isotopic composition

(δ^{202}Hg) of both, especially for the dark abiotic control, remained very close (± 0.1 ‰) to the composition of the starting material. Since there are very large errors associated with the repeat isotope ratio measurements for the some data points (e.g., first time point for the heat killed control 2SD = 0.36 ‰), I can not ascertain if there is a systematic trend (i.e. a start up effect as seen earlier (Chapter 3) or a slow but continuous decrease in the δ^{202}Hg values) for these two controls. After ~4 hours and when cell density in the live control increased to ~10^9 CFU/ml and Hg(II) concentration in the reactor dropped to <180 ppb, a suppression in fractionation had clearly occurred (Fig. 4.2).

For the experiment with *S. oneidensis* MR-1, ~50% of the added Hg(II) was lost from the reactor in the first 12 hours of incubation (Fig. 4.3, Table 4.3) and the value of the fractionation factor ($\alpha_{202/198}$) was 1.0018 ± 0.0003 (2SD). A suppression in fractionation seems to have set in after ~5 hours when Hg(II) concentration in the reactor dropped to <30 ppb. The Hg(II) concentration and isotopic data from the dark heat killed control show no evidence of significant loss of Hg(II) from the reactor as reported earlier as well[108].

Discussion

Effects of cell wall composition and incubation temperature

All $\alpha_{202/198}$ values calculated based on the isotopic data from this study (Fig. 4.1–4.3) overlapped those obtained for the two experiments with *E. coli* JM109/pPB117 done at its optimum growth temperature[52] (Table 4.4). Based on what is known about the biochemistry and biophysics of the *mer* mediated Hg(II) reduction, I argue below that a) the fractionation seen in this thesis is due to kinetic fractionation by MerA, the central

and defining component of the *mer* system and b) diffusion and Hg(II) transport by the specific the Mer transporters very likely do not cause significant fractionation.

As noted above, the transport of Hg(II) inside the cell is an important component of the *mer* mediated resistance in bacteria. Most of what is known about the transport of Hg(II) by the *mer* system (see introduction) is based on studies with Gram-negative bacteria[8]. As compared to extended genetic, biochemical and structural characterization of Mer transport proteins from operons in Gram-negative bacteria, relatively little is known about the exact mechanism of Hg(II) transport in Gram-positive bacteria[8]. Nevertheless, gene encoding for MerP and MerT like trans-membrane transporters are found in *mer* operons in various Gram-positive bacteria[8,132] and at least two *Bacillus* strains express *merP* whose activity leads to Hg(II) sorption by cells[128,133]. Because phylogenetic analysis indicates that *merP* and *merT* might have coevolved[134], I believe that MerP and MerT like transporters are likely to be expressed and involved in Hg(II) transport in Gram-positive cells. This is especially likely to be the case for the *Bacillus cereus* Strain 5 used in this study, as it is resistance to very high levels of Hg(II) (~100 μM)[125] and a dedicated Hg(II) transport system should exist to make this level of resistance possible. Without dedicated transporters, Hg(II) resistance is significantly lowered[135,136] (also see below). The steps involved in the *mer* mediated reduction of Hg(II) by Gram-positive microbes might include: 1. diffusion of neutral Hg(II) species across the diffusion boundary layer (DBL) with a thickness similar to the cell's radius, 2. uptake of Hg(II) across the murein layer of Gram-positive cell wall possibly involving MerP[128], 3. transfer of Hg(II) to MerT (or an alternative trans-membrane transporter), and

transport across the cell membrane to –SH rich groups in the cytoplasm or the N-terminal domain of MerA[8,137], 4. MerA mediated Hg(II) reduction, 5. diffusion of volatile and lipid soluble Hg(0) across the cell membrane, and 6. diffusion of Hg(0) across the liquid-gas interface.

As mentioned earlier, the net fractionation in a multi-step reaction is the combined effect of fractionation by all steps up to and including the rate limiting step (Chapter 3). In Chapter 2 and based on an assertion by a recent paper[84] it was mentioned that Hg(II) uptake might be the rate limiting step in the chain of steps leading to Hg(II) reduction. Here, based on a re-assessment of *mer* mediated Hg(II) transport studies[135] (see below), I suggest that under some circumstances, Hg(II) reduction by MerA, rather than Hg(II) uptake, is the rate-limiting step.

The activity of Hg(II) transport protein(s) is(are) critical for maintaining cellular resistance to Hg(II), and in absence of MerA an active transport function leads to hypersensitivity[135,136]. Conversely, in their absence and consequently reduced specific uptake of Hg(II), MerA activity by itself does not lead to resistance to high levels of Hg(II) possibly because low concentrations of Hg(II) inside the cytoplasm lead to lower level of operon induction[138] and in the absence of high affinity dedicated transport system toxic interactions of Hg(II) with cell wall/membrane proteins can harm the cells[8]. Thus, some have argued that the Mer system is "uptake" limited[84,135,136]. I suggest that this reasoning only applies to an initial non-steady state lasting from about 30 seconds to 2-3 minutes following exposure to Hg(II)[8] prior to the full induction of *mer* operon expression. In a Gram-negative strain, due to the polarity in the expression of the *mer*

operon[139], once the operon is optimally induced, transcripts and the protein abundance of Hg(II) transporters is higher (10-20 times) than that of MerA. Although it has not been demonstrated, it is likely that in Gram-positive *Bacillus and Anoxybacillus* the expression of the Hg(II) transporters is similarly higher than MerA expression because transporter genes are located upstream of MerA in the *mer* operons in the *Firmicutes*[8] and are likely co-transcribed with *merA* from a single promoter upstream of the transport genes. Together, these observations suggest that Hg(II) reduction by a well induced Hg(II) resistant cell is not likely to be uptake limited when bioavailability of Hg(II) in the medium is high.

Having asserted above that in induced cells and under steady state conditions, Hg(II) transport is not the rate limiting step in Hg(II) reduction, I proceed with the assumption that diffusion and uptake steps do not contribute to isotopic fractionation, and that the fractionation seen in this thesis might be primarily due to kinetic effects during the MerA mediated reduction step.

Transport of Hg(II) across the cytoplasmic membrane

Although there is no direct experimental evidence so far, recent conserved sequence and motif analysis strongly suggest that the Mer transport proteins have 2-4 transmembrane α helical spanners and function by a simple channel-type mechanism to allow facilitative passive diffusion of Hg(II) in response to membrane potential as opposed to a carrier type mechanism[134]. I have argued earlier (Chapter 3) that there is insignificant fractionation of Hg during passive diffusion of neutral forms of Hg-ligand complexes (Chapter 3). Thus, I propose that it is unlikely that isotopic fractionation

occurs during transport via Mer specific transport systems (see also (Chapter 5)). There is evidence to suggest the mechanism of Hg(II) transport across the cytoplasmic membrane also involves successive transfer of Hg(II) between paired thiol residues within MerT like proteins ([8,115,134] and references therein) but I think that since transfer of Hg(II) from one thiol group to another thiol group does not involve change in redox state and might not involve significant change in the bonding environment of Hg(II), this will not cause significant fractionation. Rather, as discussed above, when the reactant Hg(II) concentrations are high, MerA causes preferential reduction of the lighter isotopes leading to the accumulation of heavy isotopes inside the cell (for detailed analysis see (Chapter 5)). However, as Hg(II) concentrations drop, diffusion limitation sets in leading to a slow depletion of the internal pool of heavy isotopes (barred regions in Fig. 4.1-4.3). Under severe Hg(II) limitation (Fig 3.2), after depletion of the internal Hg(II) reserve, no fractionation is observed because the rate limiting step (i.e. diffusion) does not cause any fractionation. I have not considered the role of MerP is contributing to the fractionation observed in my studies. I have discussed the potential role of Hg(II) binding to MerP in contributing to fractionation elsewhere (Chapter 5) and have also listed the reasons I think it is more likely to be a dominant contributor to the net extent of fractionation observed in my studies.

Fractionation by *Anoxybacillus* sp. FB 9:

Since preliminary data showed that MerA specific reduction activities in crude extracts from various strains, including *Bacillus cereus* R607, increased with temperatures up to 50-60 ºC and suggested that MerA might be a thermophilic enzyme[140], one might expect that Hg fractionation will decrease with increased incubation

temperature. However, we observed similar alpha values for the two Gram-positive strains, Strain 5 (a mesophile) and FB9 (a thermophile), when tested at their respective optimal growth temperatures of 30 ºC and 60 ºC, respectively (Table 3.4). It has been reported that there was no significant difference between fractionation of sulfur during sulfate reduction by a thermophilic bacterium growing at 60^0 C as compared to fractionation by mesophilic organisms[141]. This result also gives support to the hypothesis that Hg fractionation during Hg(II) reduction is due to an enzymatic process because equilibrium fractionation is known to be quite temperature dependent[71]. These preliminary results of a similar extent of fractionation during Hg(II) reduction by a mesophile and a thermophile imply that one could expect that *mer* mediated biological Hg(II) reduction in geothermal environments will lead to fractionation that is similar to those environments where ambient temperatures dominate .

Isotopic fractionation during reduction by *S. oneidensis* MR-1:

Mercury reduction by *S. oneidensis* MR-1 is unique in a number of ways. This strain does not posses a *mer* system and thus the starting concentration of Hg(II) in the medium was lower than those used in all other experiments, 50 ppb vs. 500-600 ppb, MR-1 is an facultative anaerobe that reduces Hg(II) by an unknown mechanism likely associated with respiratory electron transport chains[108]. Therefore, a range of fractionation ($\alpha_{202/198}$ = 1.0018) during MR-1 mediated reduction similar to the overall range of alpha values (Table 3.4) was unexpected. I have argued (see discussion for *B. cereus* 5 above and similar issues in (Chapter 5)) that the reduction by MerA, the only fractionation contributing step in the mer-mediated Hg(II) reduction, causes kinetic

fractionation of the reactant Hg(II), which is suppressed at lower bioavailable Hg(II)/cell concentrations due to diffusion/uptake limitation[52](Chapter 3). This raises the question about what leads to a similar extent of fractionation during reduction by MR-1 as compared to the MerA mediated reduction.

Under fumarate-reducing conditions as employed in this study, the electron transport chain ends in periplasmic space because fumarate reductase is found in the periplasm. Genes for numerous oxidoreductases[142,143] and cytochromes, transport and other OM proteins, with known and unknown functions, are up-regulated by several folds in MR-1 under anaerobic conditions in general[144] or fumarate reducing conditions in particular[145,146]. Given this information (also see introduction), I think that in MR-1, Hg(II) is not reduced in the cytoplasm as is the case for MerA mediated Hg(II) reduction and I propose that there are three steps involved in MR-1 mediated Hg(II) reduction: 1. diffusion of Hg(II) compounds through the DBL (diffusion boundary layer), 2. passive diffusive uptake across the outer membrane, and 3. transfer of electrons from a member of the electron transport chain to the periplasm and to Hg(II). Below, I examine which of these three steps have the potential to be rate limiting and/or fractionation contributing steps.

Estimates of the rates of the three steps: Two different theoretical estimates indicate that at 25 °C, the diffusion coefficient for mercuric compounds in water lies in the range of $2.8*10^{-5}$ to $3.2*10^{-5}$ cm^2/s[147]. To the best of my knowledge, there is no experimental verification of these diffusion coefficients in water but one study has reported experimentally determined diffusion constant for mercuric compounds in activated carbon at 37 ^{0}C to be $4.54*10^{-6}$ cm^2/sec[148]. Using a conservative value of $5*10^{-6}$ cm^2/sec

as the diffusion constant for neutral Hg(II) species in water based aqueous media at 30 ^{0}C and relation ($J = 4\pi DR(C_\infty - C_{out})$[92] described in detail earlier in Chapter 3), the minimum diffusion rate of the neutral Hg(II) species should be ~$5*10^5$ Hg(II) molecules/sec when C_{out} is 45 ppb. This rate is much higher than the estimated rate of passive diffusive/uptake through the outer membrane (OM) of a Gram-negative cell. Using the value of permeability (P) = $7.4* 10^4$ cm s^{-1}[91] and parameters described earlier (Chapter 3), the uptake rate of $HgCl_2$ molecules across the OM should be ~ $3.2 *10^3$ molecules/second per cell. These calculations imply that the diffusion across DBL is probably not the rate limiting step for the process of Hg(II) reduction by MR-1. In the absence of knowledge about the mechanism of Hg(II) reduction in MR-1, I can not employ the strategy based on the abundance of the reduction causing agent and it's turnover number as used for MerA mediated reduction[149] to estimate the rate of reduction by MR-1, implying that I can not determine if the uptake across MR-1's OM is slower than the reduction step and is the rate limiting step.

***Fractionation during diffusion through the DBL and uptake across OM*:**

It has been shown that diffusion of neutral forms of two heavy metal ions (Fe(II) and Zn(II)) cause significant fractionation only at distances larger than 10^4 μm[109] and as discussed earlier (Chapter 3) this suggests that the diffusion of neutral Hg(II) compounds across distances of the order of 0.5 μm (typical thickness of DBL) should not cause significant fractionation. Additionally, even if the passive diffusive uptake across the OM is rate limiting (see above), this step may also not cause fractionation as argued earlier (Chapter 3).

However, in addition to the anaerobic growth conditions discussed above, there is another important difference between the *E. coli* and MR-1 growth media that could partially account for the extent of fractionation seen in the experiment with MR-1. Equilibrium stability constant based (MINEQL) modeling showed that the majority (~81%) of the added Hg(II) speciated as $Hg(NH_3)_2^{2+}$ [52] in the anaerobic growth medium (detailed results not shown). For comparison, in the growth medium used for the *E. coli* experiments[52] Hg(II) was dominantly present in the neutral forms. Although speciation of Hg(II) as $Hg(NH_3)_2^{2+}$ is known to not affect the rate of uptake of Hg(II) by Gram-negative bacteria[150], it is plausible that $Hg(NH_3)_2^{2+}$ acts as a kinetically labile species[93] that is either converted to a neutral form of Hg(II) in the DBL during diffusion and the neutral form can then pass through the OM via passive diffusion or that binds with an extracellular or OM embedded transport ligand that causes facilitated uptake of Hg(II) ions (as opposed to un-facilitated passive diffusion of neutral forms) across the cell wall[150]. Although the value of the β factor is presently unavailable for $Hg(NH_3)_2^{2+}$, using the values of β factors for $Hg(H_2O)_6^{2+}$ and $HgCl_2$ at 25 ^{0}C as calculated by Schauble[48] and the relationships $(\alpha_{202/198})_{A\text{-}B} = \beta_A / \beta_B$ and $\Delta_{202/198} = \delta^{202}_A - \delta^{202}_B = 1000 \ln((\alpha_{202/198})_{A\text{-}B})$, I estimate that if the conversion of $Hg(H_2O)_6^{2+}$ (a positively charged species), to $HgCl_2$ (a neutral species capable of diffusing through OM), occurs under equilibrium conditions, the extent of equilibrium fractionation possible during conversion of $Hg(H_2O)_6^{2+}$ (a positively charged species), to $HgCl_2$, i.e. $(\Delta_{202/198})_{Hg(H2O)6\text{-}HgCl2}$ would be ~ +0.05 ± 0.04 ‰ implying a slight preference for lighter isotopes in the neutral form. If the uptake of Hg(II) ions in MR-1 medium involves transfer of Hg(II) from kinetically labile $Hg(NH_3)_2^{2+}$ to transport ligands, the range of β factors for various inorganic Hg(II)

species[48] suggest that the maximum extent of fractionation during a process that does not change in redox state will not exceed 0.5 ‰ and therefore, the step of diffusion across the DBL and uptake across OM could account for a significant, but not complete, extent of fractionation seen in the experiment (1.8 ± 0.1 ‰) .

Fractionation during uptake through the OM under anaerobic conditions: As compared to aerobic conditions, speciation[127], bioavailability and hence uptake of Hg(II)[151,152] change significantly under anaerobic conditions. Moreover, toxicity of heavy metals[153] and the metabolic state of all facultative cells in general, and MR-1 in particular[142,143] are also quite different under anaerobic conditions. It is not clear if and how anaerobicity affects the Hg(II) uptake mechanism and outer membrane composition of the strain MR-1 . Moreover, it is not known if in strain MR-1, there is a passive diffusion of neutral forms of Hg(II), or active "accidental" transport as suggested by some groups[150]. If uptake across the OM involves passive diffusion of neutral forms of Hg(II), the chances of fractionation during uptake are low, but if active movement of charged species that involves binding to non specific transporters takes place, it is plausible that this uptake could also add to the overall fractionation. However, as pointed out above, the maximum extent of fractionation during a process that does not change in redox state might not exceed 0.5 ‰. The effect of anaerobicity on the extent of Hg(II) fractionation could be determined by comparing the extent of fractionation by a mercury resistant *E. coli* during growth on alternative electron acceptors.

***Fractionation during electron transfer to Hg(II)*:**

As pointed out earlier, for non specific but significant reduction of Hg(II) as seen in MR-1, I surmise the involvement of a cytochrome that would competitively transfer electrons to the Hg(II) ion in the periplasm before this thiol -avid metal could poison essential proteins in the cytoplasm and within the cytoplasmic membrane. It is possible that the electron transfer to Hg(II) by such a protein leads to the observed fractionation by MR-1. If the reduction of Hg(II) is caused by a protein embedded in the OM or outer side of the cytoplasmic membrane, it is possible that the high extent of fractionation seen in this experiment is caused due to the effect of membrane potential on electron transfer to Hg(II). Electroplating experiments [154] show a voltage dependent fractionation of iron stable isotopes during electron transfer to Fe(II) and it was suggested[154] that voltage dependent fractionation could have applicability in explaining microbial stable isotope fractionation during reduction of Fe(III), because cell membranes have a trans-membrane voltage. However, a significant extent of Fe fractionation was only observed when the applied voltage was ~400 mV while delta psi, the electrical component of the proton motive force, for the OM of a typical Gram-negative cell lies between 30-40 mV (much lower than that of the cytoplasmic membrane potential ~180 mV)[155-157], which is further diminished under anaerobic conditions[158]. Although, it is possible that the net "intra-membrane potential"[159] that includes dipole[160] and inner potential could exceed 400 mV in some cases, in the absence of current evidence for a voltage dependent fractionation of Hg during electron transfer and presence of OM embedded cytochromes capable of reducing Hg(II), I can only speculate on a role for the membrane potential in Hg fractionation as observed in *S. oneidensis* MR-1.

Concentration dependent suppression of fractionation:

The change in the isotopic composition of Hg(II) in the reactors as a function of the extent of reaction completion (plotted as δ^{202}Hg vs. fraction of Hg(II) remaining (f) in Fig. 4.1-4.3 and Fig. 2.1) shows a progressive suppression in the extent of fractionation. I interpret this suppression as evidence for the change in the rate limiting step in the overall multi-step reaction of the *mer* mediated Hg(II) reduction. Comparison of the cell densities and Hg(II) concentrations at which suppression of fractionation ensued (~10^7 CFU/ml and 520 ppb for Strain 5; ~10^9 CFU/ml and ~180 ppb for FB9; and ~5*10^5 CFU/ml and 30 ppb for MR-1), suggests that it was not the absolute cell densities but likely the bioavailability of Hg(II) per cell ([Hg]/cell) in a given medium that controlled the transition in the nature of the rate limiting step (i.e. from MerA catalysis to Hg(II) transport). However, since the distribution coefficients of Hg(II) among the organic constituents of the cell media components are not known, I can not estimate the amount of bioavailable Hg(II) in each of my experiments. I propose that as the concentration of bioavailable Hg(II) became low, cells began to deplete their internal thiol-bound reserves of heavy isotopes in the cytoplasm leading to a slow and progressive suppression in the observed fractionation (see also (Chapter 5)). The cytoplasm contains mM concentrations of low molecular weight thiols[8] that can bind Hg(II) but to confirm the proposition, a determination of how much Hg(II) can be accumulated inside the cells is clearly needed. I propose that when these internal reserves are depleted the Hg(II) system becomes truly diffusion limited, fractionation is no longer observed because significant fractionation might not occur during Hg(II) transport (see above and (Chapter 5)). It is likely that cell

densities and Hg concentrations will affect the extent of fractionation observed in future field studies.

Conclusions

Because the results show an overlapping range of extent of fractionation by four bacterial strains that employ two different pathways for the reduction of Hg(II) to Hg(0) (Table 4.4), the composition of the microbial communities in environments where their activities partake in the Hg(II) reduction should result in Hg isotope fractionation with the values of the fractionation factors ($\alpha_{202/198}$) of 1.0016 ± 0.0004. This conclusion is corroborated by experiments with the Hg(II) resistant natural community with an $\alpha_{202/198}$ of 1.0013 ± 0.0004[52](Chapter 5). The knowledge of the extent of Hg fractionation during Hg(II) reduction by a common soil bacterium, *B. cereus* Strain 5, an isolate from a geothermal spring, *Anoxybacillus* sp. Strain FB9, and a metal reducer common in subsurface environments and lake sediments, *S. oneidensis* MR-1, should assist in the assessment of how much fractionation is expected during volatilization of Hg(II) by these organisms in their respective environments. Evasion of Hg(0) to the atmosphere is an important step in Hg biogeochemistry in these environments. Knowing the constraints on the extent of fractionation during Hg(II) reduction, including in subsurface environments where the *mer* mediated pathway is not likely to function and reduction by metal reducing bacteria may mobilize Hg(0) into ground water[108], could help in deciphering the role of biological activity in removing Hg(II) from the environments where it may be methylated.

This work also supports the earlier suggestions about the role of cell densities and Hg (II) bioavailability in changing the extent of Hg fractionation. It provides a clear framework for interpreting the changing extent of Hg fractionation and suggests why Hg(II) reduction by the *mer* system may produce a clear isotopic signature when catalysis by MerA is the rate limiting step and no such signature when transport is rate limiting.

Additionally, this study highlights the need to have a detailed understanding (mechanism, and kinetics) of the various steps that are involved in Hg transformations for the emergence of a clear Hg isotopic systematics. Knowledge of fractionation during individual steps, i.e., enzyme transformations, transport, adsorption, and diffusion, will further constrain the extent of Hg fractionation possible during biotic processes (see also Chapter 5). In this regard, the framework provided in this study can guide us in future and ongoing experiments on fractionation during other transformations in the Hg biogeochemistry including fractionation during Hg(II) methylation.

Chapter 5: Microbial stable isotope fractionation of mercury: conclusions, conceptual framework and future possibilities

Overview

1. Current state of the understanding of fractionation during biotic processes
    a. Summary of trends seen in microbial studies
    b. Alternative interpretation of results
    c. Detailed examination of experiments with ***E. coli*** JM109/pPB117
        1. MerB vs. MerA
        2. Effect of growth temperature
2. Comparison with abiotic processes
3. Future directions and possible experiments

1. Current understanding of the biotic fractionation of Hg

All the kinetically controlled experimental studies done to determine $\alpha_{202/198}$ values during MMHg degradation and Hg(II) reduction by microbes show a systematic enrichment of the heavier isotopes in the reactant with progression of the reaction indicating preferential degradation/reduction of molecules containing lighter isotopes of Hg (Chapters 2-4)[52].

1a. **Summary of trends seen in microbial studies**

Most of the experiments showed a common trend of a change in δ^{202}Hg vs. the extent of reaction completion (Fig. 5.1). The Hg isotope data from kinetically controlled biological reactions of Hg usually follows a mass dependent Rayleigh-type fractionation (Region 1). However, as the reaction progresses, there is a suppression in fractionation at lower Hg(II) concentrations and higher cell densities (regions 2 and 3 in Fig. 5.1; Chapters 2-4 and see below). All the fractionation factors $(\alpha_{202/198})_{\text{reactant-product}}$ reported in our studies (Table 5.1)[52](Chapters 3 & 4) were calculated using modified Rayleigh equations (see above) as described in[52] and represent the extent of fractionation in region 1. A fractionation factor as calculated in this thesis implies that at any given point of time, instantaneous (but not cumulative) product will be $(\alpha_{202/198} - 1)*1000$ ‰ lighter than the reactant.

The trend observed in this thesis can be explained by considering Hg(II) reduction and MMHg degradation as multi-step processes and considering the observed extent of fractionation as a function of the rates of the various steps involved. All the steps within the multi-step pathway could contribute to fractionation but it is widely accepted that net observable fractionation of any element during a microbiological process will be the net effect of the fractionation at all of the individual steps before, and including, the rate-limiting step[54,57,66,87,161]. Out of all possible steps in a chain of reactions, one reaction will inevitably be slower i.e., more rate-limiting than others.

I have proposed that the steps (Fig. 5.2) involved in the *mer* mediated reduction of Hg(II) by microbes might include: 1) diffusion of neutral Hg(II) species across the

diffusion boundary layer (DBL) with a thickness similar to the cell's radius, 2) uptake of Hg(II) across the cell wall possibly involving MerP, 3) transfer of Hg(II) to MerT (or an alternative trans-membrane transporter), and transport across the cell membrane to –SH rich groups in the cytoplasm or the N-terminal domain of MerA[8,137], 4) MerA mediated Hg(II) reduction, 5) diffusion of the volatile and lipid soluble Hg(0) across the cell membrane, and 6) diffusion of Hg(0) across the liquid medium-gas interface. Figure 5.2 also shows the steps likely to be involved in MMHg degradation (Chapter 3) and Hg(II) reduction by Hg(II) sensitive strains like *Shewanella oneidensis* MR-1 (Chapter 4).

The estimates on the rates of diffusion of Hg compounds in water and passive uptake across outer membrane suggest that when Hg is abundantly bioavailable, catalysis by MerA and MerB are the rate limiting steps. Furthermore, I have proposed that the diffusion and uptake steps do not cause significant fractionation. As mentioned above, since the net extent of Hg fractionation observed biological studies should be the combined effect of fractionation by all steps only up to and including the rate limiting step, I think that MerA (Chapter 4) and MerB catalysis (Chapter 3) are the only fractionation contributing step during Hg(II) reduction and MMHg degradation, respectively.

The decline in the observed extent of fractionation in region 2 (Fig. 5.1) is likely due to a decrease in the reactant, Hg(II), bioavailability in the bulk medium leading to beginning of 1) diffusion limitation and 2) depletion of the intracellular thiol-bound pool of Hg(II), . I think that in region 2, MerA catalysis is technically still the rate limiting step. The complete suppression in fractionation that follows in region 3 (Fig. 5.1) may occur due to a complete depletion of Hg(II) inside the cell and when diffusion of Hg(II)

becoming the rate limiting step (Chapter 3). Region 2 type behavior was not observed in the MMHg degradation experiments (Chapters 3 & 4) might be because MMHg can not be effectively stored intracellularly (like Hg(II); see above) without damaging the cell. These suggestions require rigorous experimental testing and are crucial for the development of Hg isotope systematics (see below).

1b. Alternative explanation for $\alpha_{202/198}$ observed during *mer* mediated Hg(II) reduction

It was suggested that when the cell is not diffusion limited, MerA catalysis is the rate limiting and fractionation causing step in the overall multi-step reaction(Chapter 4). The argument about the absence of fractionation during passive diffusion across diffusion boundary layer (DBL) and passive uptake across outer membranes (OM) was based on the fact that previous studies on other heavy elements[109,162] found that insignificant fractionation occurs during diffusion across distances of the range of a few micrometers. However, I recognize that there are important differences between the rates of passive diffusion of ions and molecules comprising different stable isotopes in water measured by using a diffusion cell[109] or tube[162] and the rates and mechanism of passage of molecules through a microbe's DBL and the lipid bilayer. The DBL is a thin (usually on the scale of micrometers) layer of fluid that is not mixed with the bulk solution and various solutes in the bulk (and well mixed) medium have to diffuse across this layer to reach the cell surface. In the simplified model, I assumed this layer to be entirely composed of water where in reality this layer is a conduit for diffusion of numerous ions, and organic and inorganic molecules which could affect the diffusion of Hg compounds[156]. Also, a bilayer

is a region that not only offers a passing molecule with a changing hydrophobic/hydrophilic environment but also a dynamic "intramembrane" potential and changing dielectric constant[159]. Therefore, in absence of experimental evidence, one can not be sure if passage across DBL and OM do not cause fractionation and that the only fractionation contributing step in the multi-step process of the *mer* mediated reduction of Hg(II), is MerA catalysis[52](Chapter 4).

Even if future experimental approaches prove that diffusion across DBL and OM (or outer cell wall for Gram positive bacteria) does not contribute towards fractionation during *mer* mediated processes, there is another possibility that also has the potential to explain the extent of fractionation seen in the reduction studies. Binding of Hg(II) to MerP, a step other than MerA catalysis, could also explain the observed extent of fractionation in this research work. MerP is referred to as "the extracytoplasmic Hg(II) sponge" and has likely evolved to uptake Hg(II) in specific and high affinity manner from the extracellular/periplasmic space[8]. Since the periplasm is an oxidizing environment lacking low molecular weight thiols, which are abundant (mM concentrations) in the cytoplasm and keep Hg(II) ion from poisoning cytoplasmic proteins, this sponge also helps to keep protected the Hg(II) vulnerable cysteine-rich membrane associated proteins involved in energy generation. Interaction of neutral mercuric compounds with MerP in the periplasm involves displacing the counter anions (Cl^- or OH^-) and binding of the Hg(II) ion with two cysteine residues. If Hg(II) uptake is indeed the rate limiting step as suggested by some groups ([84] and references therein), it is possible that the binding of Hg(II) to MerP, and not MerA catalysis, causes the fractionation at the beginning of the experiments (in Region 1 of Fig. 45.1) and that the suppression in fractionation seen

towards the end of the experiments is due to diffusion limitation (as explained earlier (Chapter 4)). There are a number of the reasons why I suggest that the binding of Hg(II) to MerP is unlikely to be the rate limiting or high extent of fractionation contributing step.

1. Maximum possible extent of fractionation: There is likely to be no change in the oxidation state of Hg(II) during binding to –SH groups in MerP. If this was the rate limiting step in the chain of events and allowed back reaction, given the estimated fractionation factor (β) calculations and covalent nature of Hg-S bonds[48], maximum mass dependent equilibrium fractionation that is likely to occur during this process would 0.5 per mil.

2. Lack of thiols in periplasm: As noted above, low molecular weight reduced thiols are absent in the periplasmic/extracellular space of aerobic microbes and this scarcity of thiols implies that there is little possibility of storage of Hg(II) in the periplasmic space. This in turn implies that if binding of Hg(II) to MerP was the major fractionation contributing step, I can not explain the slow continuous suppression in fractionation in the experiments (see above for explanation regarding role of thiols in allowing storage of heavier Hg isotopes in cytoplasm)(Chapter 4). However, it is also important to note that although the DNA sequences of MerA from *B. cereus* Strain 5 and *Anoxybacillus* sp. FB9 are not available, analysis of MerA sequences from the phyla *Firmicutes* to which both of these strains belong suggest that their MerA sequences should have the N-terminal[137]. If MerT-like membrane bound transporters directly transfer the Hg(II) ion to the N-terminal of MerA instead of transferring them to

cytoplasmic thiols, the chances of accumulation of heavy isotope within the cytoplasm are also lowered.

3. Lack of temperature dependence: MerP is known to be a water-soluble protein present in the periplasmic space in Gram negative cells[8] but might be associated with extracellular side of cytoplasmic membrane in Gram positive cells[128]. Given the temperature sensitivity of membrane permeability and stiffness, if binding of Hg(II) to MerP was the rate limiting step, fractionation factors could have changed with incubation temperatures. However, my experiments show that the change in incubation temperature and bacterial cell wall structures (Gram positive vs. Gram negative) did not have a significant effect of the extent of fractionation during *mer* mediated reduction (see below)[52].

4. Protein abundance: As pointed out earlier (Chapter 4), MerP has been found to be the most abundantly synthesized protein among the three structural Mer proteins (MerP, MerT and MerA) in a Hg resistant cell[8] which makes it improbable for MerP binding to be the rate limiting step. However, the release of MerP's periplasmic form from the cell's cytoplasm is an energy dependent process and the stability of MerP is not known. Therefore, it is difficult to estimate the true rate of Hg(II) uptake by MerP and conclusively argue that this rate will be lower/higher than rate of Hg(II) reduction by MerA.

The only way to know the extent of fractionation during individual steps involved in the *mer* mediated reduction is to determine it experimentally by working with well characterized purified enzymes and membrane vesicles containing *mer* transporters[163].

MerP and MerT transport proteins are absent in Hg(II) resistant *Thiobacillus* spp.[8,137]. Instead, they express MerC, a transporter which serves a function similar to that of MerT, and this strain could be used to determine the extent of Hg fractionation in absence of MerP and shed light on the contribution of Hg(II) binding to MerP to net fractionation by *mer* mediated reduction. In addition, it would help to work with a well characterized Hg(II) reducing bacterial strain so that rates of diffusion, uptake, DNA transcription and mRNA translation and numbers of different enzymatic molecules could be estimated with more confidence (Chapters 3 & 4). Working under conditions where the cytoplasmic thiols are low could also elucidate the possible role of Hg(II) binding to thiols in potential accumulation of heavy isotopes inside the cell. Experiments with purified *mer* proteins would greatly help in constraining the extent of fractionation by the *mer* pathway. However, experimental determination of fractionation during some steps such as: 1. ionic and MMHg transport across cell membranes 2. adsorption to cell surfaces and exudates, and 3. complexation with low molecular weight thiols and DOC with varying Hg binding capacities will be vital for understanding fractionation not just during *mer* mediated processes but during Hg(II) methylation and demethylation as well. Therefore, constraining the extent of fractionation during individual steps could prove to be critical for ascertaining the importance of mass dependent fractionation in differentiating amongst various biological processes that do not cause MIF.

1c. Detailed examination of experiments with *E. coli* JM109/pPB117

1c. i) MerB vs. MerA in *E. coli* JM109/pPB117

Comparison of the *mer* mediated Hg(II) reduction[52] with the *mer* mediated MMHg degradation (Chapter 3) by *E. coli.* JM109/pPB117 at similar "low" cell densities and the same range of total Hg(II) or MMHg concentrations (~30 ppb) (see Fig. 5.3) shows that the fractionation factors for the two processes are similar. However, this similar extent of fractionation does not imply that the fractionation contributing step(s) are similar. If catalysis by MerA were to be the rate limiting step for both the multi-step processes, it would have implied that MerB catalysis doesn't cause fractionation. But as shown in Fig. 5.2 and discussed earlier (Chapter 3), even though the last three steps of the two processes are the same, the rate limiting step (when ample Hg species is bioavailable per unit cell) for Hg(II) reduction is most likely MerA catalysis but for MMHg degradation it is MerB catalysis. Moreover, unlike the uptake of Hg(II), MMHg uptake does not involve specific transporting enzymes (Fig. 5.2).

1c. ii) Effect of growth temperature on fractionation by *E. coli* JM109/pPB117

Equilibrium fractionation factors vary inversely with temperature ($1000\ln(\alpha)$ is proportional to $1/T$ or $1/T^2$)[70,71] but given the overlapping values of fractionation factors which were obtained for *E. coli* Hg(II) reduction studies at different temperatures[52], it is hard to conclude that there is a clear effect of incubation temperature on the extent of fractionation (Table 5.1; Fig. 5.4). Moreover, the fractionation factors for the

experiments done at 22 ^{0}C were based on only two reactor data points and, in my opinion, are not completely reliable. No change in fractionation factors with changing incubation temperature has been reported earlier for a non-traditional heavy metal. There is no change in the extent of fractionation of selenium during reduction of selenate to elemental selenium by resting cell suspensions of *Sulfurosprillum barnesii* between 15 ^{0}C and 30 ^{0}C[57]. Together with the results of experiments with two Gram positive strains (Table 5.1) studied at very different temperatures (30 ^{0}C and 60 ^{0}C), in the contest of Hg biogeochemical cycling, the non-dependence of fractionation factors on temperature suggests that the seasonal variation in temperatures and composition of microbial community might not change the isotopic composition of Hg(0) being emitted into the atmosphere due to *mer* mediated Hg(II) reduction.

2. Fractionation during dark abiotic Hg(II) reduction processes

Hg isotope ratio measurement can be used successfully if the extent of fractionation during different Hg(II) reduction mechanisms (abiotic photo-reduction vs. reduction by dark abiotic processes vs. biotic *mer* mediated reduction vs. biotic non-*mer* mediated reduction) is discernibly different from each other. Photo processes impart a distinctive MIF signal[51] which might be absent in biological processes (Chapter 3) and therefore photo-reduction could be differentiated from the other three kinds of reduction on the basis of presence of MIF. The studies with a variety of Hg(II) reducing strains suggest that it might be difficult to differentiate between *mer* mediated and non-*mer* mediated reduction (Chapter 4).

With regards to differences between dark abiotic processes and biological reduction, the extent of fractionation of Hg during dark abiotic Hg(II) reduction occurring in all three kinds of defined growth media (M9 based media for *E. coli* JM109/pPB117 and *B. cereus* Strain 5; thiosulfate containing defined medium for chemolithohetrotrophic *Anoxybacillus* sp. FB9 and fumarate containing anaerobic medium for *S. oneidensis* MR-1) used in my studies[52](Chapter 4) was negligible even when significant extent of Hg(II) reduction had occurred. However, two dark abiotic controls containing 1 mg C/L DOC described by Bergquist and Blum[51] lead to high extent of fractionation, $^{202/198}\alpha_{\text{reactant/product}}$ of 1.0013 (outdoor incubation with aluminum foil wrapped on the reactor) and 1.0020 (incubation at room temperature in light insulation box), respectively.

I would like to point out important differences between the two kinds of dark abiotic reduction studies. All the three types of defined media mentioned above contained organic carbon molecules like pyruvate, acetate, lactate, and fumarate, all of which have small molecular weights and well-defined structures with very low chance of forming any radicals. M9 based medium had 1300 mg-C/L (in the form of pyruvate); thiosulfate containing medium had 240 mg C/L as acetate, and ultra trace amounts of thiamine (100 μg/L) and biotin (10 μg/L); and fumarate containing anaerobic medium had a total of 1200 mg-C/L as fumarate and lactate (none of the amino acids added to the anaerobic medium at μg levels had –SH group.

On the contrary, the DOC used by Bergquist and Blum[51] consisted of high molecular weight Suwannee River fulvic acids (SRFA) which are known to cause dark abiotic reduction of Hg(II)[14] and have strong affinity for Hg(II) (see below). Elemental

analysis of SRFA shows that 52% of the total weight is carbon (http://www.ihss.gatech.edu/). The total reactive site content of SRFA was found to be 13.9 mmol/g, of which 57% were carboxylic acids, and 43% hydroxyl and amino groups[164]. Based on these numbers, it implies that 1 mg C/L SRFA used by Bergquist and Blum[51] will have ~10^{19} reactive sites/L (Estimates are based on the following sequence of calculations: If DOC content is 100 mg C/L, it implies 200 mg DOC/L and 2.8 mmol total reactive sites[164] which in turn is equal to~ 1 *10^{21} reactive sites/L (using Avogadro's number(N) = 6.023*10^{23} molecules/mole)).

The abundance of ligands in DOC that are capable of binding to Hg is much less than reduced thiol groups in DOC pool. However, it has been estimated that on average, ~1-60 out of 10^6 organic carbon atoms in DOC are associated with Hg binding equivalents[7]. (If DOC content is 100 mg C/L, it implies 8.3 mmol C/L (using a molecular weight of 12 for carbon) and ~1*10^{22} organic carbon molecules per L (using N, see above) and 5*10^{16} – 3*10^{18} Hg(II) binding equivalents per L[7]). This implies that 1 mg C/L SRFA is likely to have between 5*10^{14} – 3*10^{16} Hg(II) binding equivalents /L. These numbers imply that, for a reactor containing ~100 ppb Hg(II), there are at least 1000 fold more Hg(II) binding equivalents than Hg(II) molecules and 10^5 times more reactive sites per unit volume of the solution. Given the high number of expected Hg(II) binding equivalents in SRFA (see estimates above), it is reasonable to wonder if the fractionation seen by Bergquist and Blum (2007) was indeed due to preferential reduction of lighter isotopes of Hg(II) or it was due to preferential adsorption of heavier isotopes to DOC. Fractionation of Hg during its adsorption to various surfaces and complexation with different organic ligands has not yet been studied. However, if the Fe(II) adsorption

studies are indicative of a trend[74], heavier isotopes of Hg(II) should get preferentially adsorbed and could explain, at least partially, why the heavier isotopes of Hg are preferentially left behind in the reactor in the dark abiotic control containing complex DOC molecules.

Given the high distribution coefficients of Hg compounds, the study of Hg fractionation during adsorption of various inorganic and organo-mercurial compounds to surfaces with differing Hg(II) binding equivalents requires serious attention. Thus far, I do not think that adsorption of Hg compounds and their preferential partitioning to cell surfaces, which is well documented especially for Hg(II) species[85,108], causes any isotope fractionation of Hg. But if the adsorption of Hg compounds to cell surfaces and organic contents exuded by the cells causes preferential binding of heavy isotopes to the surfaces, I would need to revisit my interpretation of the steps which cause fractionation during *mer* mediated Hg(II) reduction and MMHg degradation. I suggest that all Hg isotope studies with pure microbial cultures, in addition to simple uninoculated or heat-killed defined medium controls reported earlier (Chapters 2-4), should include several controls containing varying amounts of well characterized DOC (i.e. with Hg(II) binding equivalents of known affinities) and incubations in light-exposed and dark environments. This will help to suggest the relative roles of Hg's microbial transformation vs. adsorption vs. complexation to Hg fractionation in natural systems.

3. Additional future directions and suggestions for future studies

In addition to the future implications already suggested throughout this thesis (This chapter and discussion sections of chapters 2-5), pointed below are some other

important factors that could be considered for a more rigorous development of Hg isotope systematics.

Choice of strains, experimental conditions and controls: The initial aim of microbial Hg isotopic studies done in this research study was to find if biotic processes cause fractionation and the choice of strains depended on their ability to grow well in a defined medium without access complex organic contents such that reduction and fractionation by the abiotic controls did not complicate interpretation of results. Undefined and complex media could have lead to abiotic fractionation. It was not realized that interpretation of results would be facilitated by using well-characterized strains. However, now I would like to recommend that future experiments for studying Hg fractionation during biological transformations be done with well characterized genetic biochemical and microbial systems such that the rates of gene induction, mRNA expression, turnover number of enzymes are well known. To illustrate the problem: it is known that different functional MerB occurring within a single bacteria species on a single transposon have different substrate specificities[165] and it is very likely that values of k_{cat} vary significantly between enzymes from different bacterial species. Therefore, the use of 0.7 per minute as the turnover number for MerB in Chapter 3 could be misplaced. At some point it would be essential to move away from exponentially growing planktonic pure cultures of bacteria and study how naturally occurring constantly evolving mixed microbes in different stages of growth fractionate mercury. As pointed out earlier, both the growth environment of the cell and cell's physiology affect the extent of

fractionation. Therefore, continued emphasis needs to be paid to the metabolic state and growth phase and growth rate of the bacterial cultures.

Role of supersaturation in changing observable extent of fractionation

Marine waters are frequently supersaturated with Hg(0)[7] and even if *mer* mediated biological fractionation is an important Hg(0) forming process in marine systems, fractionation factors implied by my kinetically controlled studies might not be totally relevant to marine ecosystems if equilibrium control and supersaturation changes the extent of fractionation. Therefore, we should also consider measuring fractionation without bubbling the reactors and check the effect of supersaturation of Hg(0) on extent of difference between isotopic composition of the Hg(II) in the reactor and Hg(0) dissolved in the reactor.

For isotopic studies involving pure enzymes

The break down of the chain of events in the multi-step *mer*-mediated reaction into various steps is not very precise. For example, for the step of "catalysis by MerA", I haven't clearly defined what is meant by "catalysis". As outlined by a number of workers ([116] and references therein), there are a number of micro-steps involved in transfer of electrons to Hg(II) by MerA and the net amount of fractionation by a single enzyme will also depend on the contribution from all the micro-steps up to and including the rate limiting step. In fact, in enzyme catalyzed reactions, the step involving transition state formation is seldom the only slow step, so rate expressions for the enzyme catalyzed reactions are usually much more complex (Karsten and Cook in [49]).

If MerA catalysis is indeed the rate limiting step (see above), the catalysis is itself composed of a many mini-steps. Such mini-steps may involve reversible binding of the enzyme to the substrate, reversible conversion of substrate to the product via the formation of transition state and irreversible release of the product from the enzyme.

$$E + Hg(II) \underset{k2}{\overset{k1}{\leftrightarrow}} [E - Hg(II)] \underset{k4}{\overset{k3}{\leftrightarrow}} [E - Hg(0)] \overset{k5}{\rightarrow} E + Hg(0)$$

Galimov[166] and Lewis and Schramm[167] both elegantly show in their relatively similar but semantically different treatments that the net fractionation during an enzymatic process can be mathematically shown to be a combination of reduced kinetic effect (due to differences in k_L3 and k_H3) and reduced equilibrium effects (due to reversible binding of E and S) where the extent of "reduction" of the effects will depend on the ratio of the rate constants k1 to k5. Therefore, in order to interpret the results from purified enzyme studies and know the relevance of fractionation during the interaction of Hg with *mer* enzymes to Hg fractionation during other processes that might involve similar interactions, it would be crucial to work with well characterized MerA and MerB enzymes for which rate constants for all the steps are known.

Overall significance of the thesis

This thesis provides clear evidence of presence of mass dependent and absence of non-mass dependent fractionation of Hg isotopes during biological reduction of Hg(II) and degradation of methylmercury by *mer* mediated processes. Hg is one of the heaviest

elements for which significant, reproducibly measurable and systematic biological fractionation has been observed.

The fractionation factors for all the reduction experiments (Table 5.1 and Fig. 5.5) lie in an overlapping range 1.0016 ± 0.0005 in spite of variations in cell wall structures (Gram positive vs. Gram negative species), incubation temperature and growth media. There might be a small inverse temperature dependence on the extent of fractionation and Gram positive bacteria might cause a slightly lower fractionation than Gram negative bacteria. *Shewanella oneidensis* MR-1 lacks the *mer* operon but the extent of fractionation during reduction by MR-1 is in the same range as observed during *mer* mediated reduction.

The analysis also suggests that mass independent fractionation might not happen during biological transformations and interactions of mercury but this suggestion (Chapter 3) needs to be confirmed experimentally especially by doing experimental studies in presence of varying strength of external magnetic fields.

It strongly suggests that Hg isotope ratios have the potential for distinguishing between different sources of Hg(0) emissions, cause of Hg(II) reduction and degradation of MMHg (biotic vs. abiotic) based on the extent of mass dependent and mass independent isotope fractionation. This work is an important initial step in the development of Hg isotope systematics for the purpose of identifying Hg sources and sinks in the environment, for determining in situ pathways affecting Hg toxicity, and for investigating the nature and evolution of Hg redox reactions in both modern and paleo environments.

Tables

Table 1.1

Isotope	Abundance (%)	Nuclear Spin
^{196}Hg	0.15	0
^{198}Hg	9.97	0
^{199}Hg	16.87	1/2
^{200}Hg	23.10	0
^{201}Hg	13.18	3/2
^{202}Hg	29.86	0
^{204}Hg	6.87	0

Table 2.1

Table 1 Summary of $\alpha_{202/198}$ values obtained from linear regression of isotope data from all experiments

Conditions		**Based on reactor (Eq. 1)♦**			**Based on trap (Eq. 2)♦**				
Temperature	Reactor size	Slope	2 SD	N*	Slope	2 SD	Intercept	2 SD	N*
Pure culture: *E. coli* JM109/pPB117									
37^{0}C	1 L	1.0016	± 0.0005	5	1.0020	± 0.0002	1.0020	± 0.0002	5
	1 L	1.0014	± 0.0001	5	1.0017	± 0.0002	1.0020	± 0.0002	5
	100 ml	NA[#]		2	1.0020	± 0.0006	1.0020	± 0.0004	5
30^{0}C	1 L	1.0017	± 0.0003	10	1.0023	± 0.0002	1.0020	± 0.0001	9
22^{0}C	100 ml	1.0018	± 0.0004	2	1.0026	± 0.0014	1.0019	± 0.0004	6
	100 ml	1.0020	± 0.0002	2	1.0032	± 0.0009	1.0028	± 0.0005	10
Natural microbial consortium									
Adapted Hg(II) resistant	1 L	1.0013	± 0.0004	6					
Un-adapted Hg(II) sensitive	1 L	1.0004	± 0.0002	4					

♦ Refer to Methods and Materials

* N is the number of data points used for regression (see methods for details).

[#] Not applicable; One of the two data points available corresponds to f = 0.08

Table 3.1

Reactor description	Time (Hours)	Conc. (ng/g)	f	n	δ^{202}Hg (‰)	1SD	δ^{201}Hg (‰)	1SD	δ^{200}Hg (‰)	1SD	δ^{199}Hg (‰)	1SD	Δ^{199}Hg (‰)	Δ^{201}Hg (‰)	Cell conc. (CFU/ml)
	0	32.1	1.000	3	-0.50	0.09	-0.42	0.08	-0.22	0.16	-0.18	0.10	-0.05	-0.04	1.0E+06 ± 4.5E+05
	3	27.2	0.845	3	-0.42	0.09	-0.37	0.09	-0.20	0.05	-0.15	0.05	-0.04	-0.05	
MeHg	6	24.8	0.772	3	-0.37	0.05	-0.33	0.06	-0.19	0.02	-0.16	0.03	-0.07	-0.05	
degradation at	8.5	22.6	0.703	3	-0.38	0.11	-0.34	0.13	-0.16	0.09	-0.16	0.07	-0.06	-0.06	
Low starting	10.5	19.2	0.598	3	-0.31	0.02	-0.27	0.03	-0.14	0.06	-0.11	0.04	-0.03	-0.04	
cell density	12	16.9	0.525	3	-0.27	0.03	-0.27	0.08	-0.13	0.04	-0.10	0.07	-0.03	-0.07	
	18.5	12.6	0.393	3	-0.28	0.07	-0.26	0.07	-0.14	0.04	-0.11	0.04	-0.04	-0.04	2.0E+07 ± 1.0E+07
	0	28.1	1.000	3	-0.39	0.09	-0.36	0.07	-0.23	0.11	-0.18	0.08	-0.08	-0.06	4.0E+06 ± 1.5E+06
MeHg	3	24.1	0.856	3	-0.29	0.07	-0.28	0.04	-0.14	0.02	-0.11	0.02	-0.04	-0.06	
degradation at	6	21.7	0.773	3	-0.31	0.08	-0.27	0.07	-0.12	0.07	-0.13	0.04	-0.05	-0.04	
High starting	8	19.8	0.705	3	-0.31	0.01	-0.26	0.07	-0.19	0.06	-0.13	0.05	-0.05	-0.03	
cell density	12	17.3	0.618	3	-0.30	0.11	-0.30	0.08	-0.19	0.08	-0.12	0.05	-0.04	-0.07	
	18.5	11.8	0.419	3	-0.33	0.08	-0.24	0.04	-0.17	0.05	-0.13	0.04	-0.05	0.00	7.0E+07 ± 2.0E+07
Reactor description	**Time** (min)	**Conc.** (ng/g)	**f**	**n**	δ^{202}Hg (‰)	**1SD**	δ^{201}Hg (‰)	**1SD**	δ^{200}Hg (‰)	**1SD**	δ^{199}Hg (‰)	**1SD**	Δ^{199}Hg (‰)	Δ^{201}Hg (‰)	**Cell conc.** (CFU/ml)
	0	28.0	1.000	3	0.05	0.04	0.02	0.08	0.01	0.07	-0.04	0.03	-0.05	-0.02	4.0E+06 ± 2.0E+06
Reduction at	25	24.4	0.871	2	0.25	0.06	0.22	0.03	0.14	0.02	0.02	0.02	-0.04	0.03	
High Cell	45	22.6	0.805	2	0.27	0.09	0.16	0.11	0.12	0.06	0.00	0.08	-0.07	-0.04	
density	60	22.3	0.794	2	0.28	0.11	0.23	0.12	0.17	0.03	0.08	0.07	0.01	0.02	
	90	20.0	0.714	2	0.21	0.04	0.13	0.10	0.09	0.10	-0.02	0.05	-0.07	-0.03	
	110	18.3	0.654	3	0.27	0.06	0.21	0.07	0.16	0.05	0.04	0.04	-0.03	0.01	
	140	17.8	0.633	3	0.27	0.05	0.23	0.06	0.16	0.01	0.04	0.04	-0.03	0.02	
	1110														7.0E+09 ± 2.0E+09

Table 4.1

Reactor	Time (Hours)	Conc. (ng/g)	f	n	δ^{202}Hg (‰)	1SD	δ^{201}Hg (‰)	1SD	δ^{200}Hg (‰)	1SD	δ^{199}Hg (‰)	1SD	Cell conc. (CFU/ml)
Exponentially growing cells	0.0	599.3	1.000	6	0.02	0.08	0.01	0.06	0.00	0.05	0.01	0.02	5.E+05 ± 5.E+04
	1.2	572.5	0.955	2	0.09	0.03	0.08	0.05	0.04	0.01	0.03	0.04	
	2.7	535.3	0.893	3	0.16	0.03	0.11	0.02	0.08	0.01	0.02	0.01	
	2.9	525.8	0.877	3	0.18	0.02	0.12	0.02	0.08	0.01	0.03	0.02	
	3.2	492.2	0.821	3	0.20	0.01	0.16	0.03	0.10	0.02	0.03	0.02	
	3.3	456.9	0.762	3	0.25	0.05	0.17	0.04	0.12	0.03	0.03	0.01	
	3.7	414.7	0.692	3	0.28	0.07	0.20	0.04	0.14	0.02	0.05	0.02	
	4.0	382.9	0.639	3	0.30	0.02	0.20	0.01	0.14	0.00	0.05	0.01	7.E+07 ± 1.E+07
	6.5	217.4	0.363	3	0.40	0.04	0.28	0.03	0.19	0.03	0.07	0.03	
No cell Abiotic control	0.0	584.7	1.000	3	-0.02	0.03	-0.02	0.01	-0.01	0.00	-0.02	0.00	
	2.7	580.8	0.993	3	0.07	0.05	0.04	0.04	0.03	0.03	0.01	0.01	
	4.0	578.6	0.990	3	0.12	0.05	0.09	0.03	0.06	0.02	0.03	0.03	
	6.5	576.3	0.986	2	0.10	0.03	0.06	0.01	0.03	0.02	0.01	0.00	
	7.5	573.8	0.981	3	0.09	0.01	0.07	0.04	0.05	0.02	0.01	0.03	
	8.5	569.3	0.974	2	0.05	0.02	0.03	0.02	0.03	0.02	0.00	0.02	

Table 4.2

Reactor	Time (Hours)	Conc. (ng/g)	f	n	δ^{202}Hg (‰)	1SD	δ^{201}Hg (‰)	1SD	δ^{200}Hg (‰)	1SD	δ^{199}Hg (‰)	1SD	Cell conc. (CFU/ml)
Growing cells	0.0	487.3	1.000	3	-0.85	0.01	-0.58	0.10	-0.41	0.01	-0.18	0.02	1.4E+08 ± 1.E+07
	1.0	461.6	0.947	3	-0.62	0.01	-0.48	0.03	-0.40	0.17	-0.16	0.04	
	2.0	370.7	0.761	3	-0.38	0.07	-0.32	0.05	-0.18	0.05	-0.12	0.04	
	3.0	248.7	0.510	3	0.14	0.09	0.03	0.07	0.06	0.05	-0.04	0.01	3.E+08 ± 3.E+07
	4.0	185.7	0.381	3	0.50	0.10	0.28	0.04	0.17	0.20	0.02	0.02	
	6.0	151.6	0.311	3	0.59	0.05	0.36	0.05	0.30	0.03	0.04	0.04	7.E+09 ± 2.E+08
	7.3	147.2	0.302	3	0.59	0.02	0.35	0.00	0.28	0.01	0.01	0.01	
	8.2	139.0	0.285	3	0.60	0.04	0.37	0.03	0.28	0.04	0.04	0.02	
	9.0	138.9	0.285	3	0.67	0.08	0.41	0.08	0.31	0.04	0.04	0.03	TNTC
Heat Killed Abiotic control	0	491.1	1.000	3	-0.83	0.08	-0.64	0.07	-0.40	0.04	-0.18	0.02	
	1.3	485.9	0.989	3	-0.74	0.18	-0.59	0.11	-0.38	0.06	-0.18	0.03	
	5.3	463.9	0.945	3	-0.71	0.06	-0.54	0.06	-0.33	0.04	-0.16	0.03	
	8	449.4	0.915	3	-0.71	0.05	-0.54	0.04	-0.34	0.02	-0.15	0.00	
	8.5	450.8	0.918	3	-0.71	0.05	-0.54	0.05	-0.34	0.03	-0.16	0.01	
				Av.	**-0.74**								
No cell Abiotic control	0	871.4	1.000	3	-0.86	0.04	-0.62	0.03	-0.40	0.03	-0.18	0.01	
	1.5	856.3	0.983	3	-0.81	0.17	-0.61	0.09	-0.40	0.04	-0.18	0.02	
	3	874.2	1.003	3	-0.74	0.16	-0.55	0.12	-0.36	0.09	-0.16	0.04	
	4	847.1	0.972	3	-0.76	0.05	-0.57	0.04	-0.35	0.00	-0.17	0.02	
	6	865.8	0.994	3	-0.78	0.14	-0.60	0.12	-0.39	0.06	-0.18	0.06	
	20	790.6	0.907	3	-0.70	0.03	-0.50	0.07	-0.36	0.00	-0.13	0.01	
				Av.	**-0.78**								

Table 4.3

Reactor description	Time (min)	Conc. (ng/g)	f	n	δ^{202}Hg (‰)	1SD	δ^{201}Hg (‰)	1SD	δ^{200}Hg (‰)	1SD	δ^{199}Hg (‰)	1SD
Inoculum OD 0.07 Protein conc. at time zero = 0.27 μg/ml	0	47.7	1.000	3	0.01	0.06	0.03	0.03	0.00	0.03	0.01	0.01
	15	49.2	1.031	3	-0.03	0.03	-0.03	0.01	-0.05	0.04	-0.01	0.03
	60	47.5	0.996	6	0.07	0.08	0.05	0.07	0.03	0.06	0.03	0.02
	90	45.0	0.944	6	0.09	0.06	0.07	0.02	0.03	0.03	0.02	0.02
	150	42.1	0.883	3	0.25	0.04	0.16	0.01	0.11	0.01	0.05	0.02
	240	37.3	0.783	3	0.53	0.09	0.34	0.02	0.22	0.05	0.07	0.04
	323	30.3	0.637	3	0.79	0.12	0.54	0.11	0.37	0.07	0.13	0.03
	433	28.2	0.592	3	0.78	0.14	0.52	0.09	0.35	0.05	0.10	0.03
	553	27.1	0.569	3	0.98	0.11	0.68	0.06	0.45	0.05	0.17	0.04
	773	25.3	0.530	3	0.75	0.08	0.52	0.05	0.35	0.05	0.13	0.04
Heat killed Abiotic control	0	39.5	1.000	3	-0.17	0.04	-0.11	0.04	-0.08	0.03	0.00	0.00
	60	38.8	0.983	3	0.02	0.04	0.03	0.04	0.00	0.01	0.04	0.03
	433	38.2	0.965	3	-0.03	0.01	-0.03	0.03	-0.01	0.02	0.01	0.02
	750	37.6	0.952	3	-0.05	0.06	-0.04	0.05	-0.05	0.04	0.00	0.03

Table 4.4

Strain	Optimum growth temp.	Common Habitat	Cell Wall	Used e- acceptor	Used e- donor	Reduction pathway	Added Hg(II) (ppb)	n[1]	Fractionation factor ($\alpha_{202/198}$)
Escherichia coli JM109/pPB117	37 ^{0}C	Soil/water[2]	Gram -ve	Oxygen	Pyruvate	*mer*	600	5	(1.0014 ± 0.0001)[3]
replicate								5	(1.0016 ± 0.0005)[3]
Bacillus cereus Strain 5	30 ^{0}C	Soil	Gram +ve	Oxygen	Pyruvate	*mer*	600	4	1.0012 ± 0.0001
Anoxybacillius spp. Strain FB9	60 ^{0}C	Geothermal areas	Gram +ve	Oxygen	Acetate	*mer*	500	5	1.0014 ± 0.0001
Shewanella oneidensis MR-1	30 ^{0}C	Sediment/Subsurface	Gram -ve	Fumarate	Lactate	Unknown	50	7	1.0018 ± 0.0003

[1] Number of data points used for regression analysis

[2] Plasmid inserted under laboratory settings

[3] Best estimate of fractionation factor based on reactor data (Kritee *et al, 2007)*

Table 5.1

Conditions		Based on reactant Hg(II)			Based on product Hg(0)				
Temperature	Reactor size	Slope	2 SD	N*	Slope	2 SD	Intercept	2 SD	N*
Pure cultures									
***E. coli* JM109/pPB117**									
37^{0}C	1 L	1.0016	± 0.0005	5	1.0020	± 0.0002	1.0020	± 0.0002	5
	1 L	1.0014	± 0.0001	5	1.0017	± 0.0002	1.0020	± 0.0002	5
	100 ml	NA[#]		2	1.0020	± 0.0006	1.0020	± 0.0004	5
30^{0}C	1 L	1.0017	± 0.0003	10	1.0023	± 0.0002	1.0020	± 0.0001	9
22^{0}C	100 ml	1.0018	± 0.0004	2	1.0026	± 0.0014	1.0019	± 0.0004	6
	100 ml	1.0020	± 0.0002	2	1.0032	± 0.0009	1.0028	± 0.0005	10
***B. Cereus S*train 5**									
30^{0}C	1L	1.0012	± 0.0001	4					
***Anoxybacillus* spp. FB9**									
60^{0}C	1L	1.0014	± 0.0001	5					
Shewanella MR-1									
30^{0}C	1L	1.0018	± 0.0003	7					
Natural microbial consortium									
Adapted Hg(II) resistant	1 L	1.0013	± 0.0004	6					
Un-adapted Hg(II) sensitive	1 L	1.0004	± 0.0002	4					

♦ Refer to Methods and Materials in Kritee et al, 2007

* N is the number of data points used for regression (see methods in Kritee et al, 2007 for details).

[#] Not applicable; One of the two data points available corresponds to f = 0.08

Figures

Fig 1.1

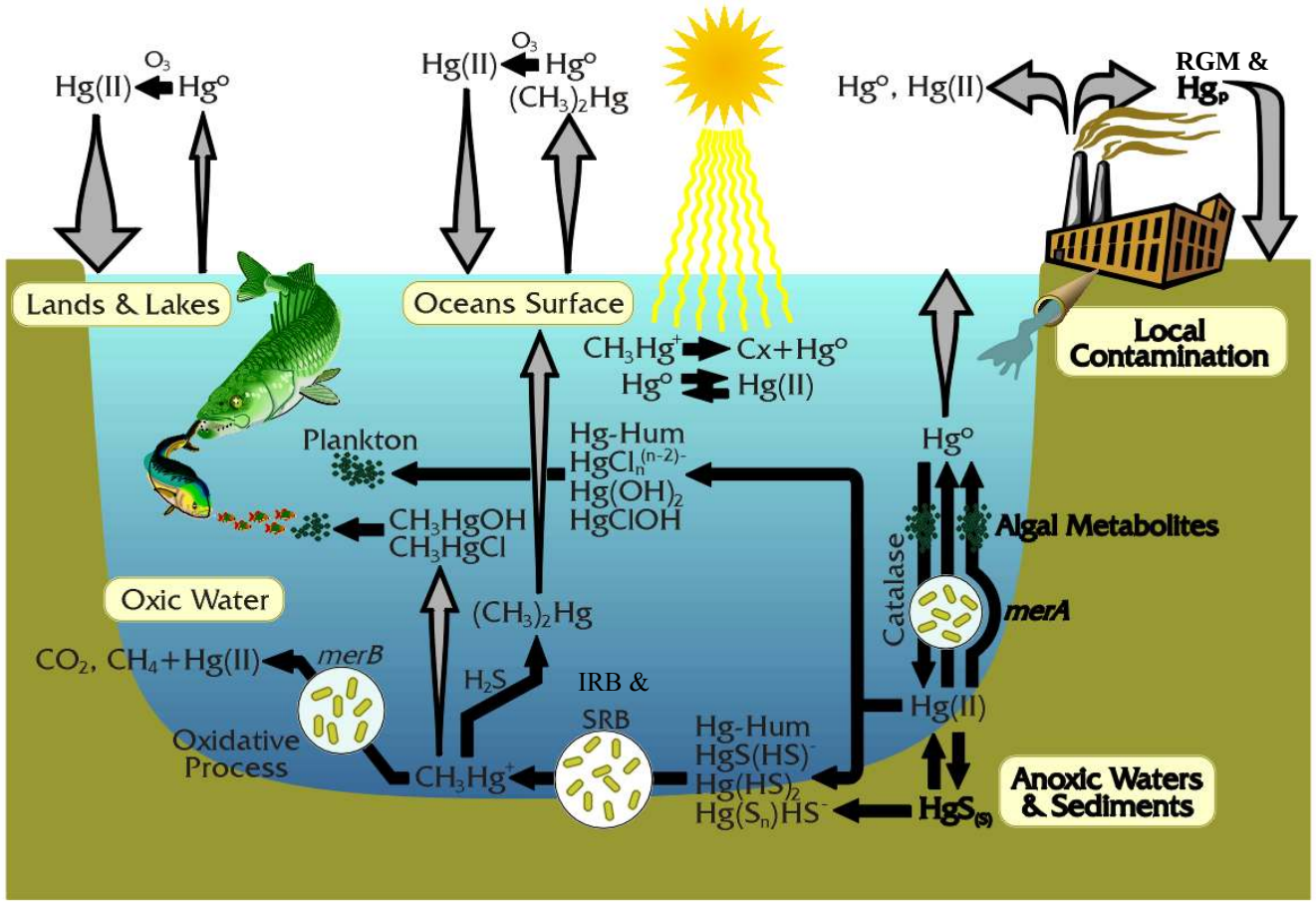

Fig. 1.2

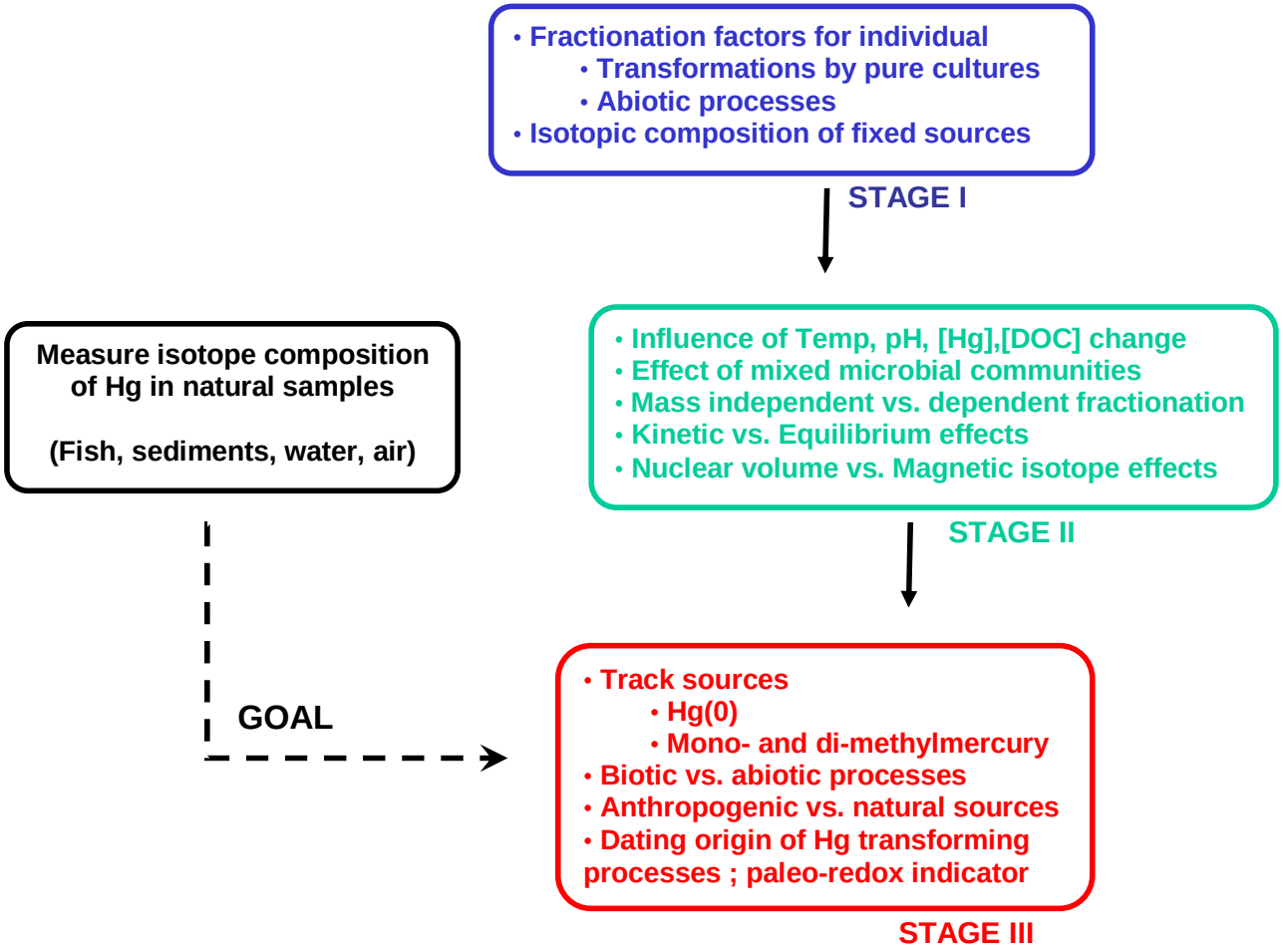
• Fractionation factors for individual
• Transformations by pure cultures
• Abiotic processes
• Isotopic composition of fixed sources
STAGE I
Measure isotope composition of Hg in natural samples
(Fish, sediments, water, air)
• Influence of Temp, pH, [Hg],[DOC] change
• Effect of mixed microbial communities
• Mass independent vs. dependent fractionation
• Kinetic vs. Equilibrium effects
• Nuclear volume vs. Magnetic isotope effects
STAGE II
GOAL
• Track sources
• Hg(0)
• Mono- and di-methylmercury
• Biotic vs. abiotic processes
• Anthropogenic vs. natural sources
• Dating origin of Hg transforming processes ; paleo-redox indicator
STAGE III

Fig. 2.1

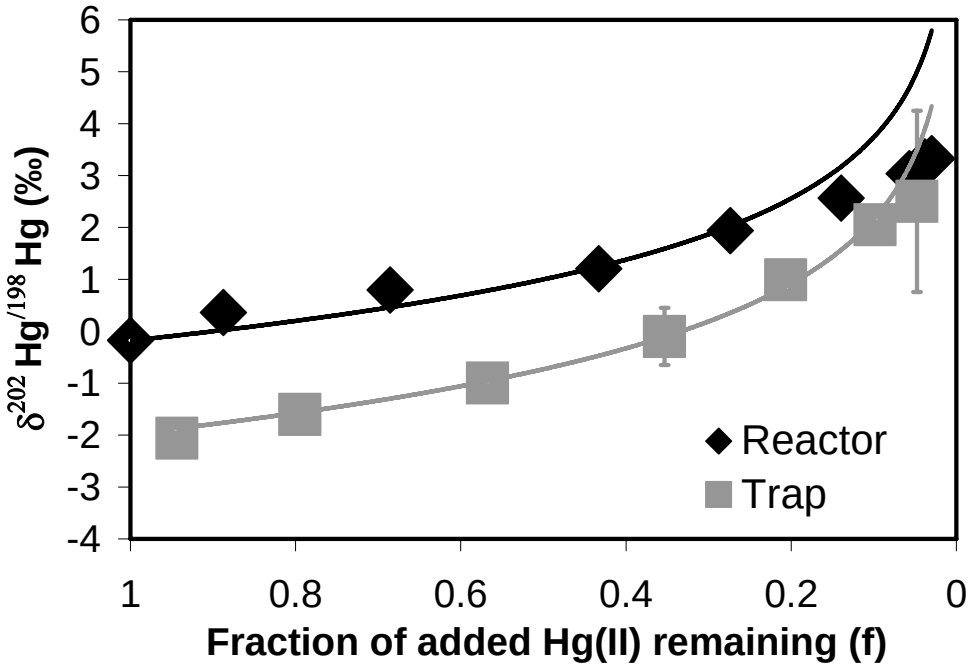
6
5
4
3
2
1
0
-1
-2
-3
-4
1
0.8
0.6
0.4
0.2
0
δ202 Hg/198 Hg (‰)
Fraction of added Hg(II) remaining (f)
Reactor
Trap

Fig. 2.2

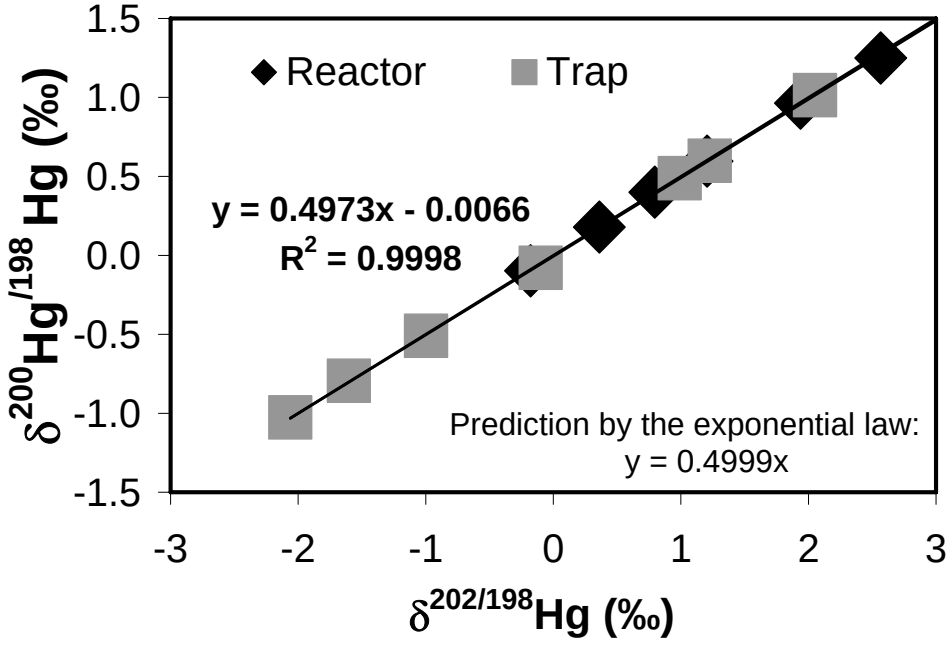
1.5
1.0
0.5
0.0
-0.5
-1.0
-1.5
-3
-2
-1
0
1
2
3
δ200Hg/198 Hg (‰)
δ202/198Hg (‰)
Reactor
Trap
y = 0.4973x - 0.0066
R2 = 0.9998
Prediction by the exponential law:
y = 0.4999x

Fig. 2.3

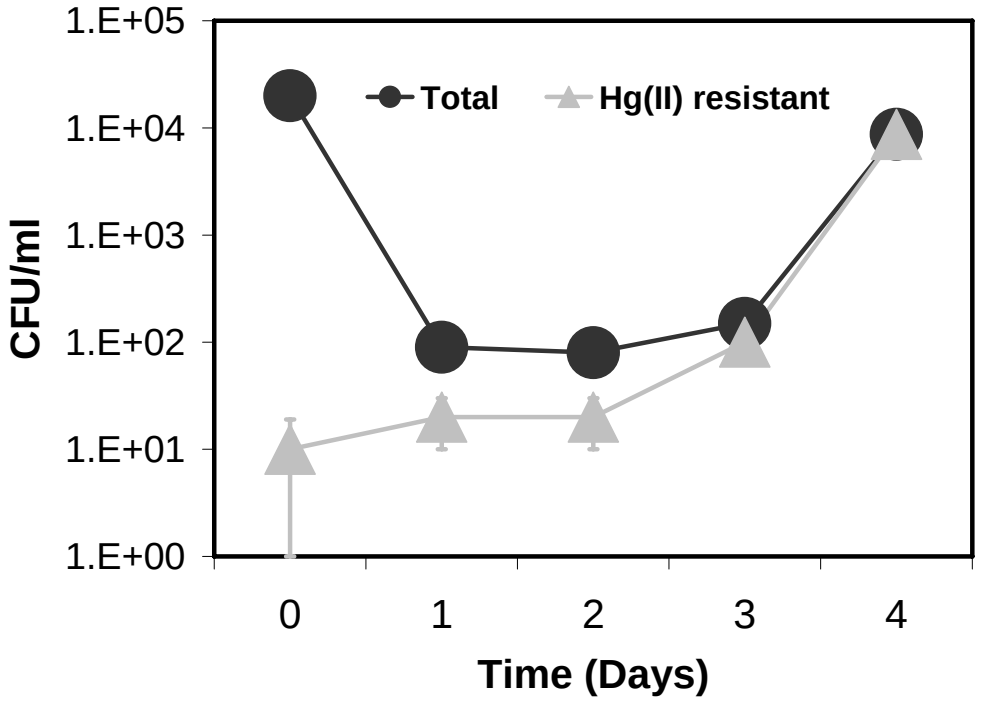
1.E+05
1.E+04
1.E+03
1.E+02
1.E+01
1.E+00
CFU/ml
Total
Hg(II) resistant
0
1
2
3
4
Time (Days)

Fig. 2.4

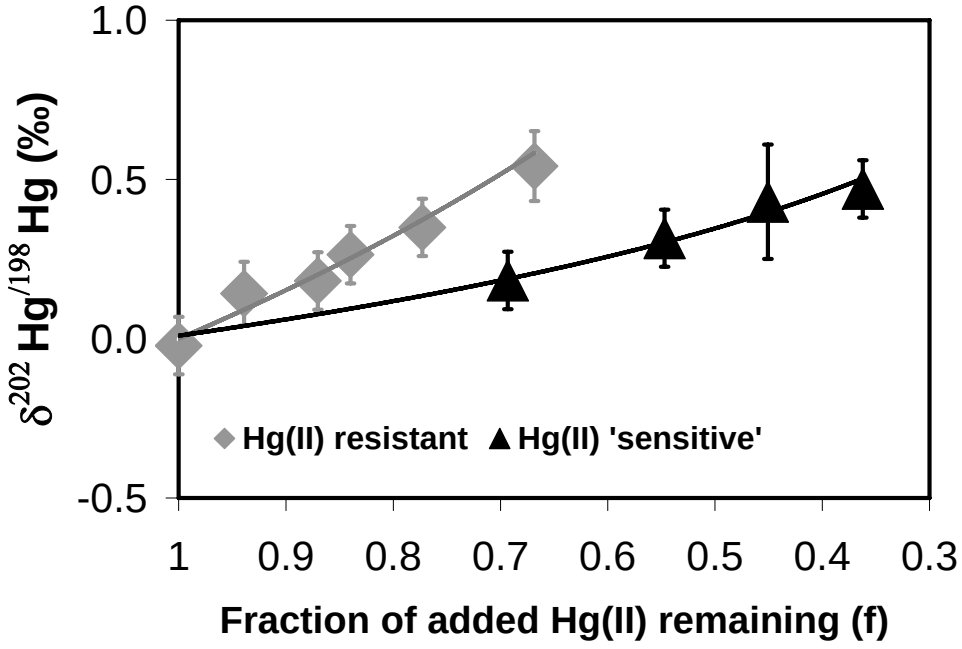
1.0
0.5
0.0
-0.5
δ202 Hg/198 Hg (‰)
Hg(II) resistant
Hg(II) 'sensitive'
1
0.9
0.8
0.7
0.6
0.5
0.4
0.3
Fraction of added Hg(II) remaining (f)

Fig 3.1A

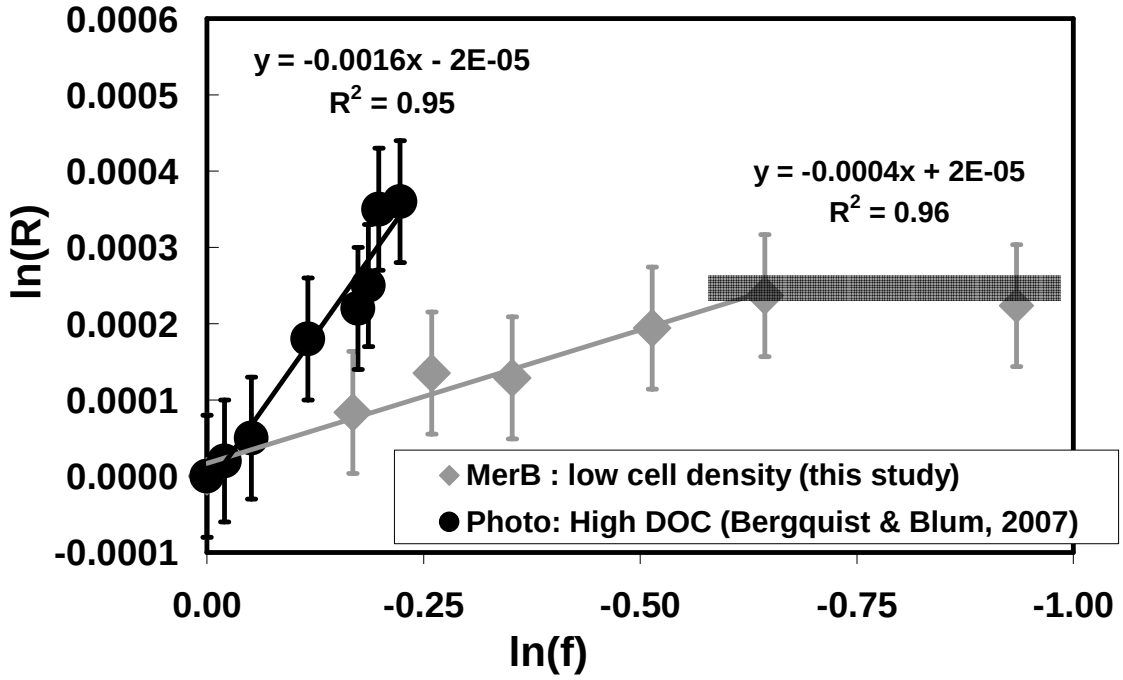

Fig. 3.1B

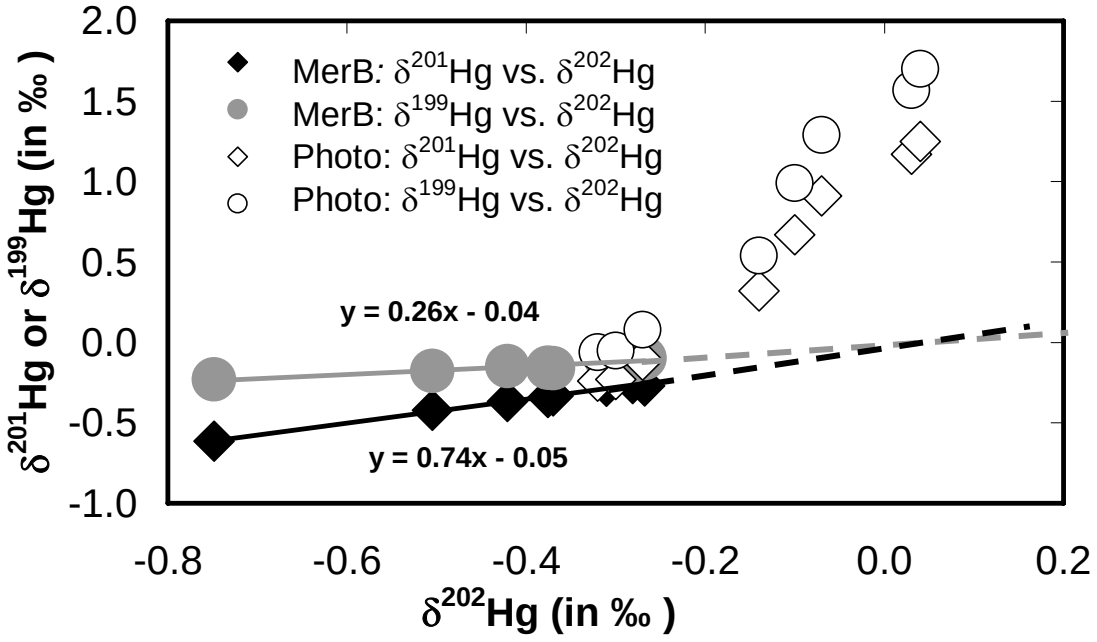

Fig. 3.2

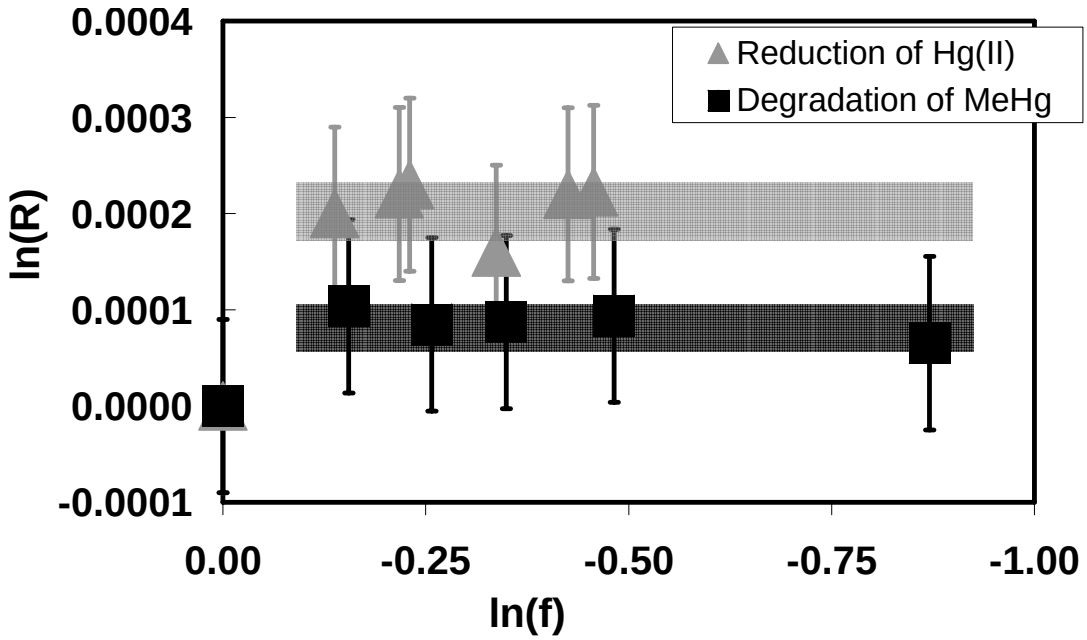
0.0004
0.0003
0.0002
0.0001
0.0000
-0.0001
ln(R)
0.00
-0.25
-0.50
-0.75
-1.00
ln(f)
Reduction of Hg(II)
Degradation of MeHg

Fig. 3.3

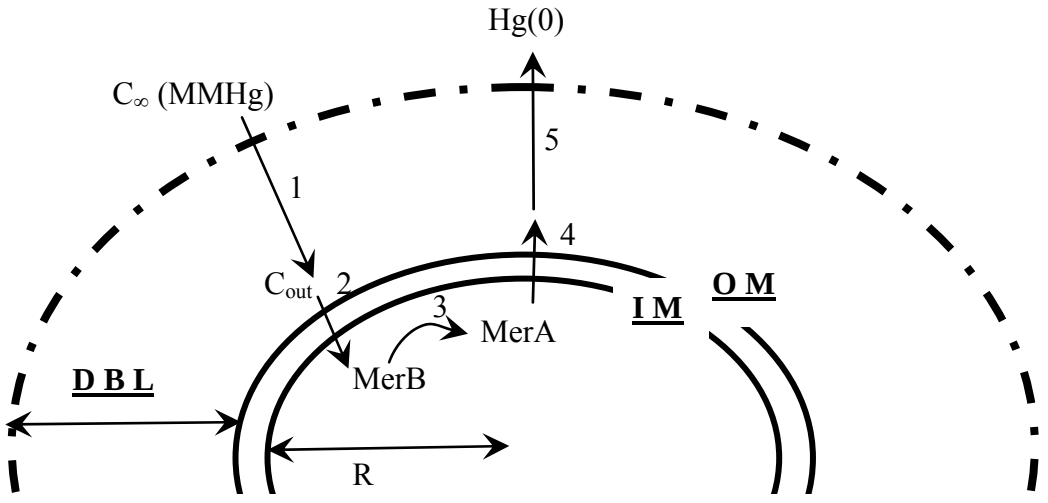
Hg(0)
C∞ (MMHg)
1
5
4
Cout
2
3
MerA
MerB
O M
I M
D B L
R

Fig. 4.1

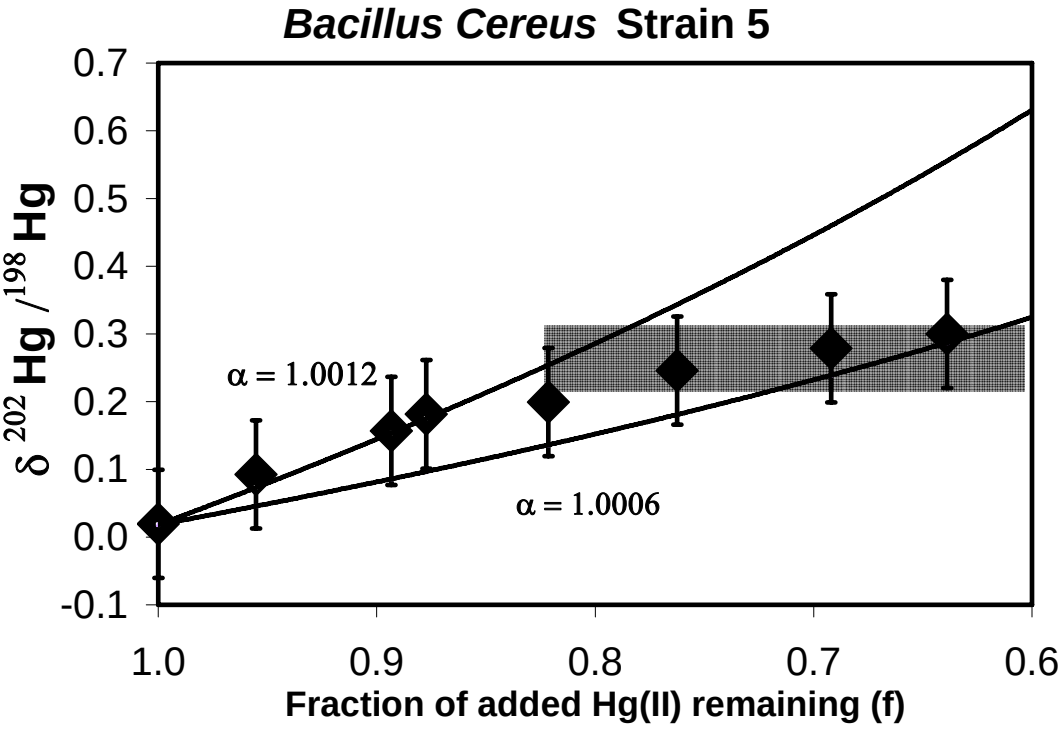
Bacillus Cereus Strain 5
0.7
0.6
0.5
0.4
0.3
0.2
0.1
0.0
-0.1
δ 202 Hg /198 Hg
α = 1.0012
α = 1.0006
1.0
0.9
0.8
0.7
0.6
Fraction of added Hg(II) remaining (f)

Fig. 4.2

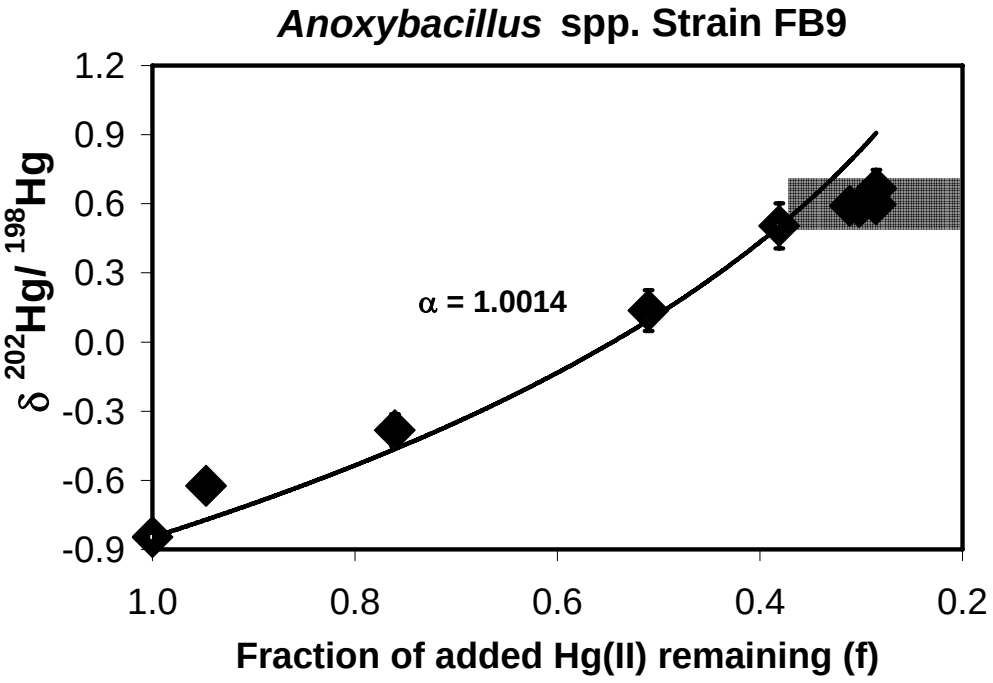
Anoxybacillus spp. Strain FB9
1.2
0.9
0.6
0.3
0.0
-0.3
-0.6
-0.9
δ 202Hg/ 198Hg
α = 1.0014
1.0
0.8
0.6
0.4
0.2
Fraction of added Hg(II) remaining (f)

Fig. 4.3

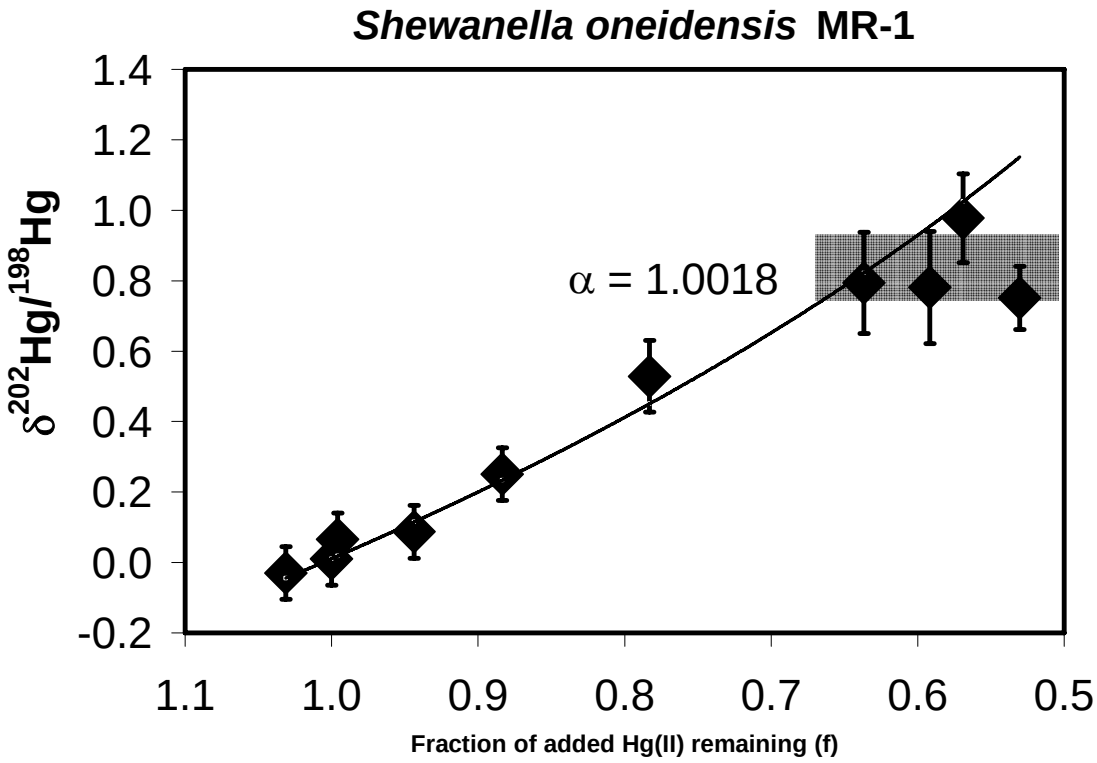
Shewanella oneidensis MR-1
α = 1.0018
δ202Hg/198Hg
1.4
1.2
1.0
0.8
0.6
0.4
0.2
0.0
-0.2
1.1
1.0
0.9
0.8
0.7
0.6
0.5
Fraction of added Hg(II) remaining (f)

Fig. 5.1

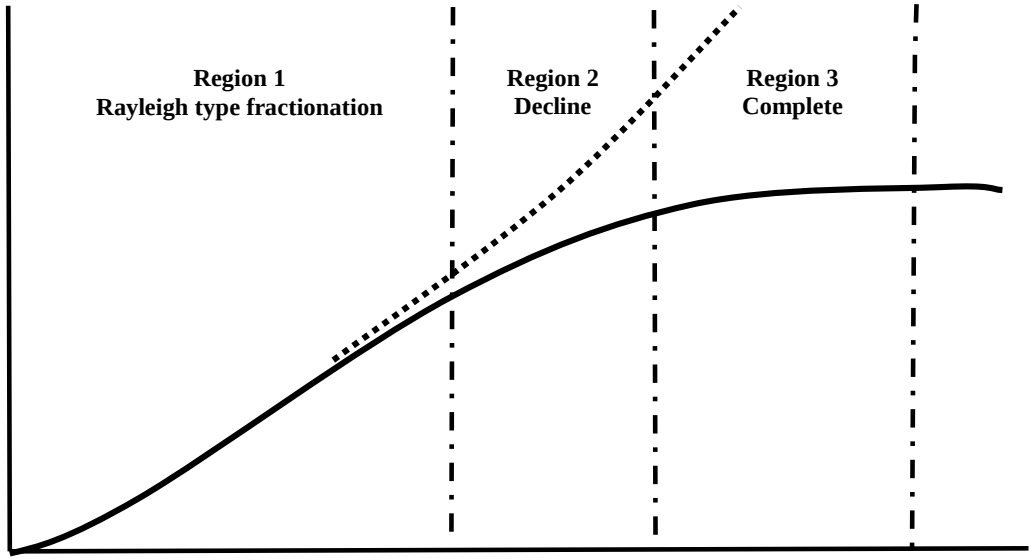
Region 1
Rayleigh type fractionation
Region 2
Decline
Region 3
Complete

Fig. 5.2

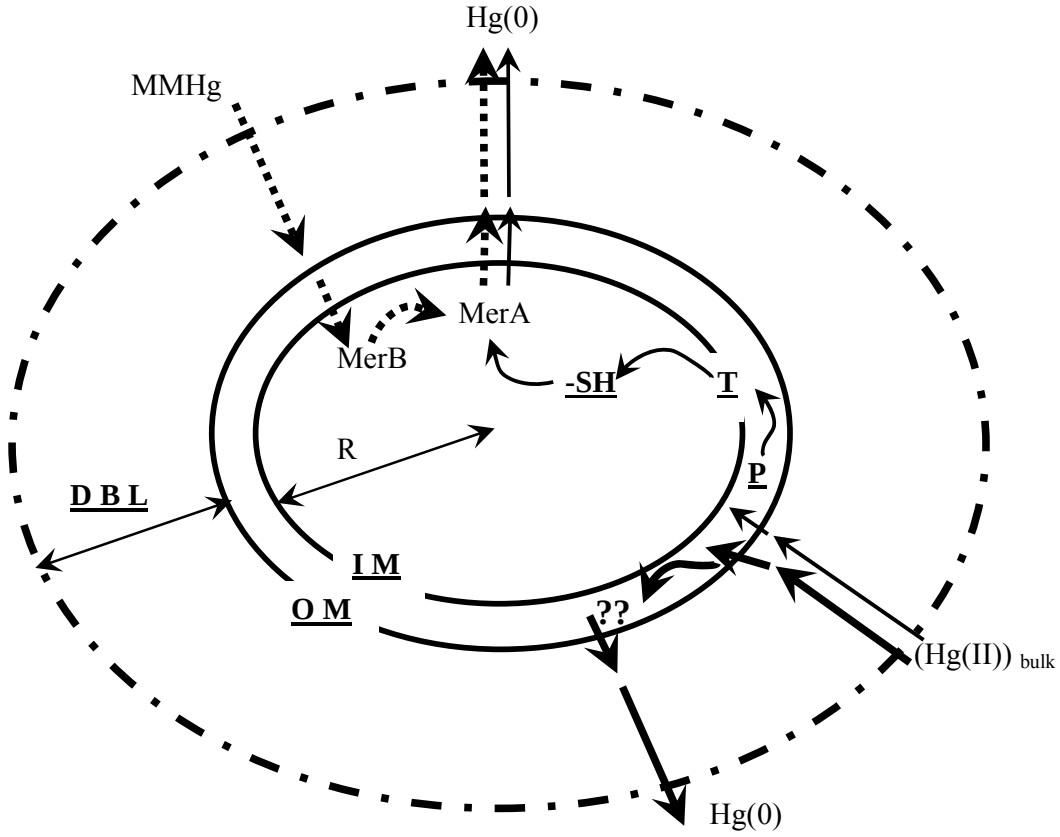
Hg(0)
MMHg
MerA
MerB
-SH
T
R
P
D B L
I M
O M
??
(Hg(II)) bulk
Hg(0)

Fig. 5.3

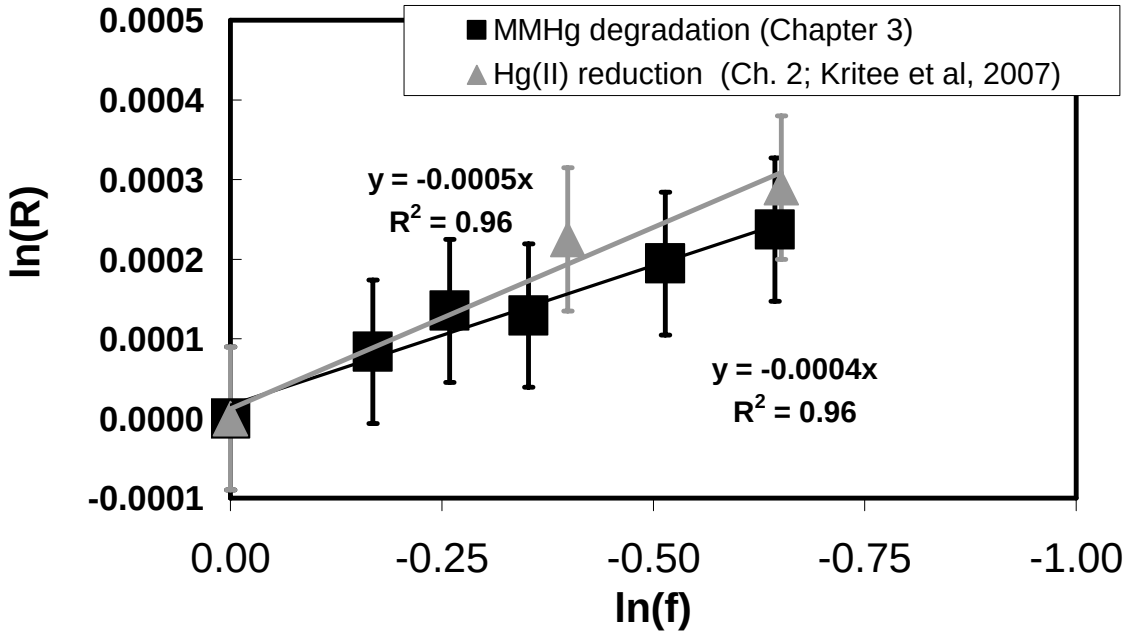
MMHg degradation (Chapter 3)
Hg(II) reduction (Ch. 2; Kritee et al, 2007)
y = -0.0005x
R2 = 0.96
y = -0.0004x
R2 = 0.96
ln(R)
0.0005
0.0004
0.0003
0.0002
0.0001
0.0000
-0.0001
0.00
-0.25
-0.50
-0.75
-1.00
ln(f)

Fig. 5.4

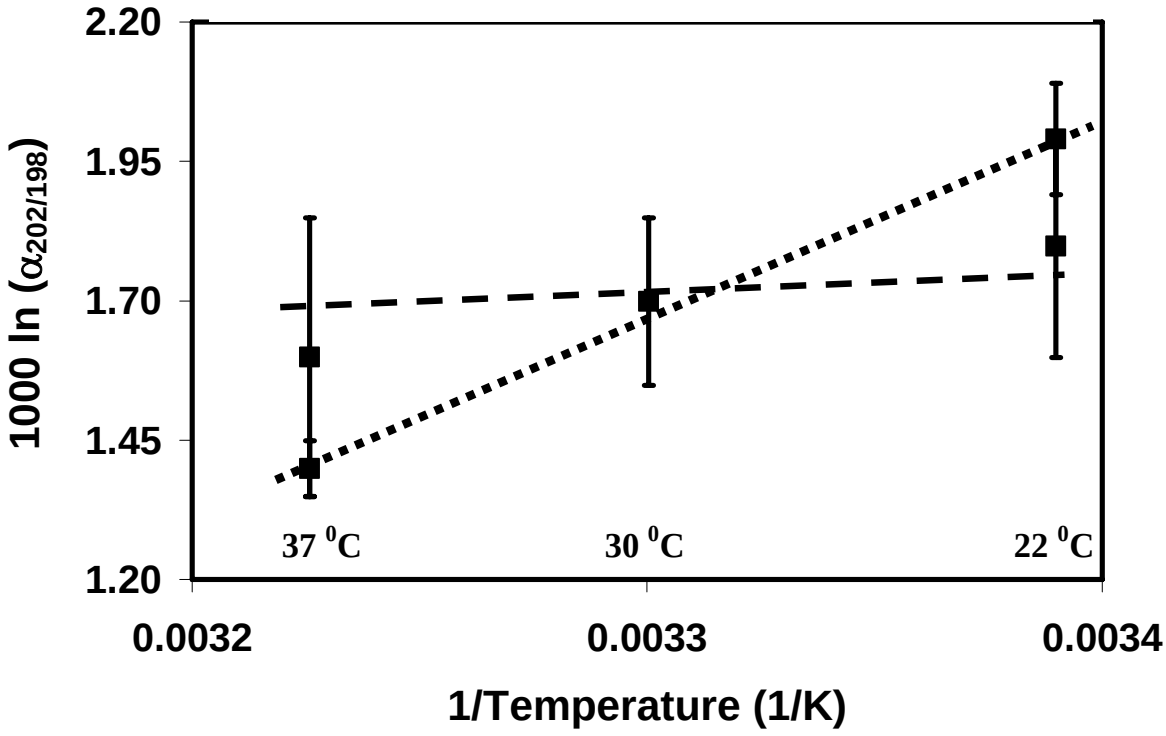
1000 ln (α202/198)
2.20
1.95
1.70
1.45
1.20
37 0C
30 0C
22 0C
0.0032
0.0033
0.0034
1/Temperature (1/K)

Fig. 5.5

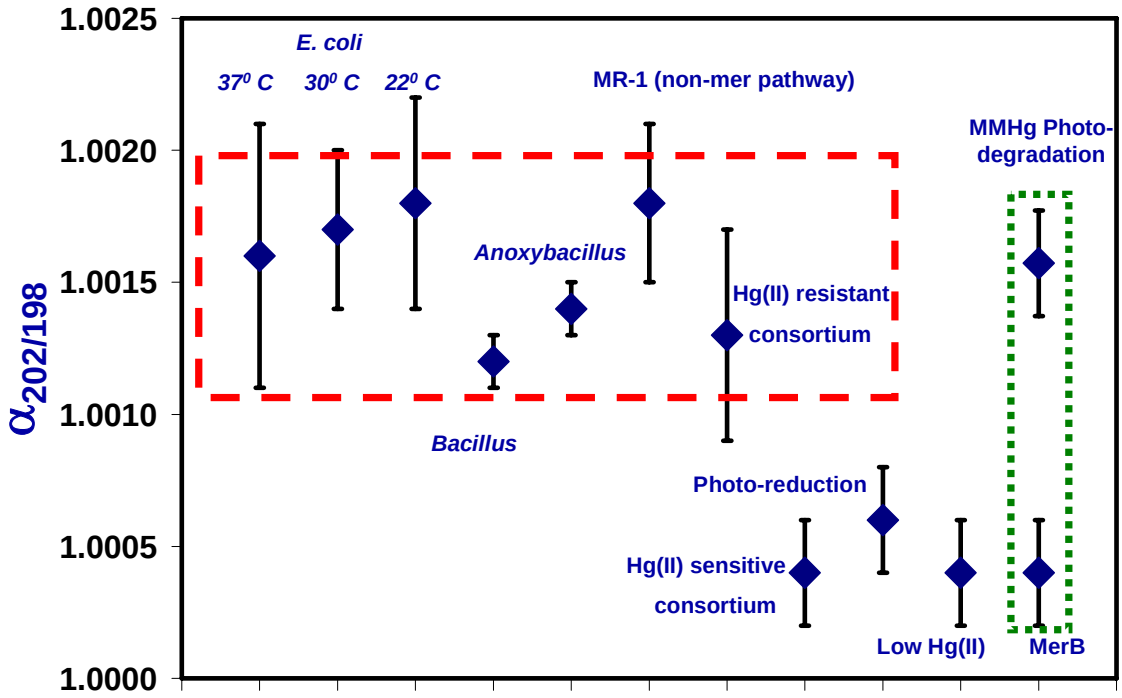
1.0025
1.0020
1.0015
1.0010
1.0005
1.0000
α202/198
E. coli
37⁰ C
30⁰ C
22⁰ C
MR-1 (non-mer pathway)
MMHg Photo-degradation
Anoxybacillus
Hg(II) resistant consortium
Bacillus
Photo-reduction
Hg(II) sensitive consortium
Low Hg(II)
MerB

Appendices

Supplement to Chapter 1

Fractionation is not absolute separation: Energy distribution & Concept of partition function

Fractionation: a partial not absolute separation

If the energy required to break or change bonds made of a lighter isotope is lesser, why is there not a complete separation of the light isotope from heavier isotope during any reaction? For example, If the bond strength of ^{12}C-O bond is always less than ^{13}C-O, why is not that during the fixation of CO_2 by phytoplankton or cyanobacteria, all carbon dioxide molecules made of ^{12}C (hereafter $^{12}CO_2$) are fixed before the molecules made of ^{13}C are utilized at all? The answer lays moving away from classical mechanics towards quantum mechanics and taking a statistical view of any system under consideration.

Statistical distribution of 'quantized' energy

One of the basic tenets of quantum mechanics is that a collection of molecules, with their wavelike character, have their total energy, *distributed* over numerous 'quantized' energy levels[168]. At a given temperature, total energy (translational, rotational, vibrational and electronic components) of all the molecules is constant. However, this total energy is not distributed equally to all the constituting molecules and

over the different energy components and instead follows what is called Boltzmann distribution[168]. Partition functions (described below) indicate how unequally the energy is distributed in a collection of molecules made of a single isotope. Any single molecule could have its total energy distributed over any possible combination of discrete energy levels of translational, rotational, vibrational and electronic components. Therefore, although the average bond strength of ^{12}C-O bond is less than that of ^{13}C-O, because of the distribution, there are a lot of $^{12}CO_2$ molecules whose bond strength is higher than that of $^{13}CO_2$ and there is not a constant difference between the bond strength (vibrational force constant) of the two kinds of bonds.

Similarly, at a given temperature, average translational energy of all the molecules in a system is constant but the speeds of individual molecules vary in accordance with Maxwell distribution[168].

Among all energy components, vibrational energy levels and among all possible vibrational energy levels, the first 'quantum' vibrational energy level corresponding to zero point energy (ZPE) is the most sensitive to the changes in isotopic mass. ZPE (=1 /2hν) is the energy every molecule has even at a temperature of absolute zero (0^0 K), where ν (=$1/2\pi\sqrt{(k/\mu)}$) is the fundamental vibrational frequency; h = Plank's constant; k = vibrational force constant for the bond in question and μ is the reduced mass of the molecule ($1/\mu = 1/m_1 + 1/m_2$). Lighter molecules have less reduced mass and therefore have higher fundamental frequency and ZPE at absolute zero. Therefore, the concept of zero point energy is frequently used to explain differences in bond strengths and free energy contents of light and heavy molecules.

Statistical thermodynamics has provided us a central concept called partition function (Z) that is employed to describe fractionation, both qualitatively and quantitatively[50,53,69-71].

Concept and significance of partition function

Partition function (Z) is a very large dimensionless number which is based on the energies of individual molecules (or microstates) and is a function of the temperature *T*. *Importantly for isotope biogeochemists, the energy of individual microstate or molecule in turn is a function of its mass.* The letter *Z* stands for the German word *Zustands-summe* meaning "sum over states" and encodes how the probabilities of finding the individual molecules in a system with a particular energy or finding the whole system in a particular microstate are partitioned among the different microstates where a microstate is the state of a system in which the location and momentum of each molecule and atom are specified in great detail. Basically, the value of the partition function (a very large dimensionless number) for any system indicates how widely is the energy of the whole system distributed among a total number of possibilities. A higher value of the partition function suggests that there are more ways to distribute the total energy in a system with a given total number of molecules or microstates. Therefore, higher value of partition function implies higher value of entropy and free energy. For more detailed mathematical description of partition functions corresponding to electronic, vibrational, rotational and translational energy levels are calculated, the reader may refer elsewhere[50].

Supplement to Chapter 2

Legends to supplementary figures and Tables for Chapter 2

Fig. S1.1 and 1.2: Rayleigh Plot (ln[R] vs. ln[f]) for the two independent experiments with *E. coli* JM109/pPB117 at 37 ^{0}C in 1L reactors. Error bars represent external precision as mentioned in the main text.

Fig. S1.3: Rayleigh Plot (ln[R] vs. ln[f]) for the experiment done with *E. coli* JM109/pPB117 at 37 ^{0}C in 100 ml reactor.

Fig. S2: Rayleigh Plot (ln[R] vs. ln[f]) for the experiment with *E. coli* JM109/pPB117 at 30 ^{0}C in 1L reactors. Error bars represent external precision as stated in the main text.

Fig. S3.1 and S3.2: Rayleigh Plots (ln[R] vs. ln[f]) for two experiments done with *E. coli* JM109/pPB117 at 22 ^{0}C in 100 ml reactor.

Fig. S4: Rayleigh Plot (ln[R] vs. ln[f]) for the experiments with naturally occurring microbes at 30 ^{0}C in 1L reactors. Error bars represent external precision.

Table S1 Hg isotopic data for the reactor and trap samples for the two experiments done with *E. coli* JM109/pPB117 at 37 ^{0}C in a 1L reactor and a typical experiment done in a 100 ml reactor. For the experiment with the 1L reactor, isotopic ratios are the averages of "n" duplicate isotopic analyses and errors in the δ values reflect ± 2SE based on duplicates (for n > 1). For the experiment done with the 100 ml reactor, because n was equal to 1, no errors are reported.

Table S2 Hg isotopic data for the reactor and trap samples for the experiment done with *E. coli* JM109/pPB117 at 30 ^{0}C in 1L reactor. For details see legend to Table S1.

Table S3 Hg isotopic data for the trap samples for the experiment done with *E. coli* JM109/pPB117 at 22 ^{0}C in the 100 ml reactor. For details see legend to Table S1.

Table S4 Hg isotopic data for samples from the experiments done with an Hg(II) resistant natural microbial consortium and an Hg(II) sensitive natural community at 30 ^{0}C in 1 L reactors.

Supplementary figures (Chapter 2)

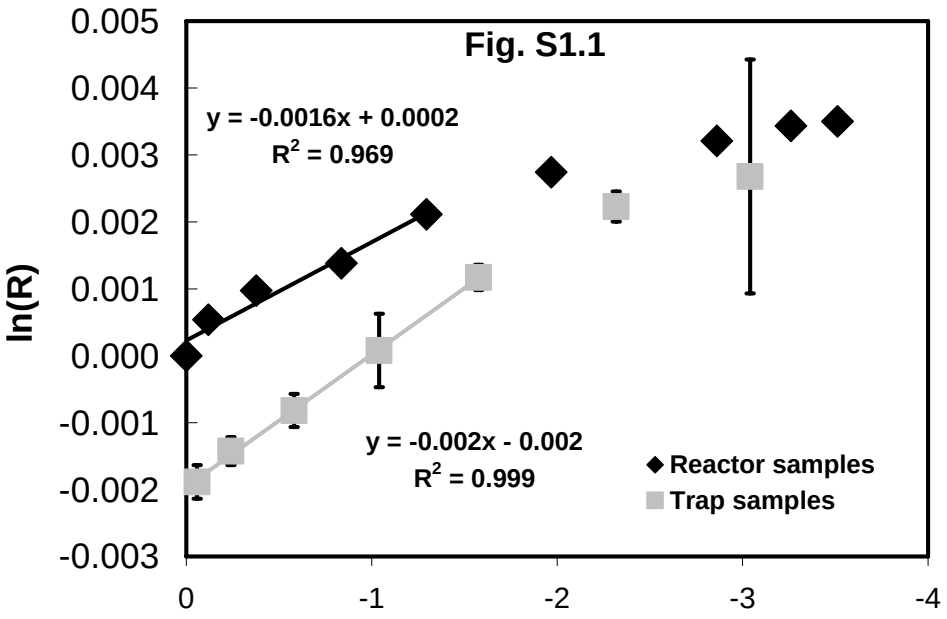

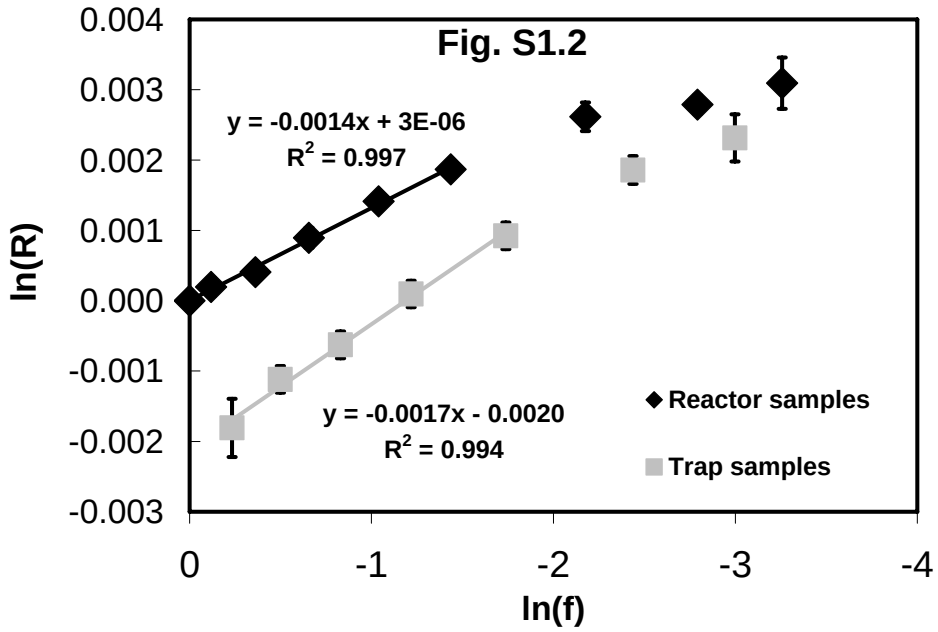

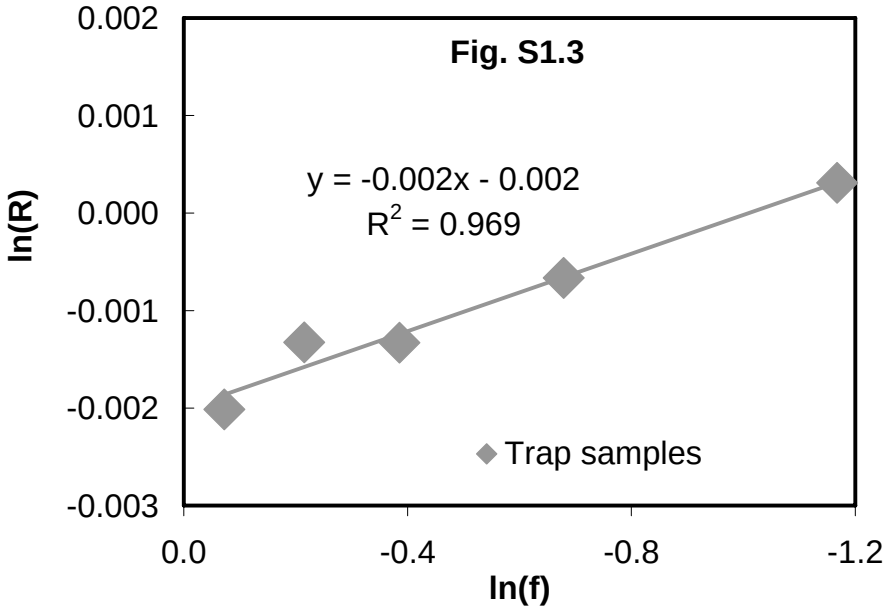
Fig. S1.3
y = -0.002x - 0.002
R2 = 0.969
Trap samples
ln(R)
ln(f)
0.002
0.001
0.000
-0.001
-0.002
-0.003
0.0
-0.4
-0.8
-1.2

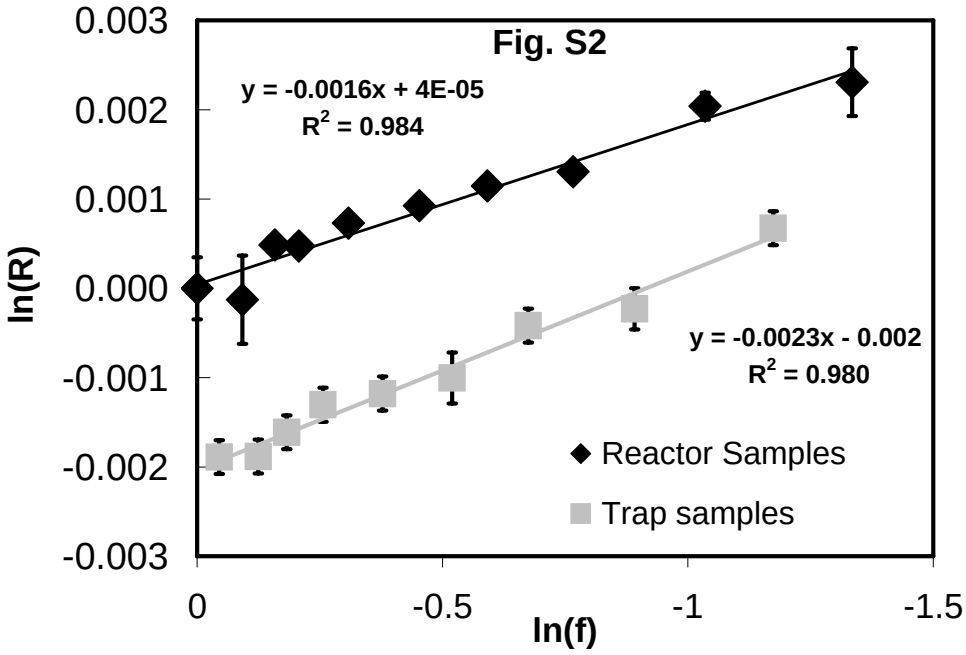
Fig. S2
y = -0.0016x + 4E-05
R2 = 0.984
y = -0.0023x - 0.002
R2 = 0.980
Reactor Samples
Trap samples
ln(R)
ln(f)
0.003
0.002
0.001
0.000
-0.001
-0.002
-0.003
0
-0.5
-1
-1.5

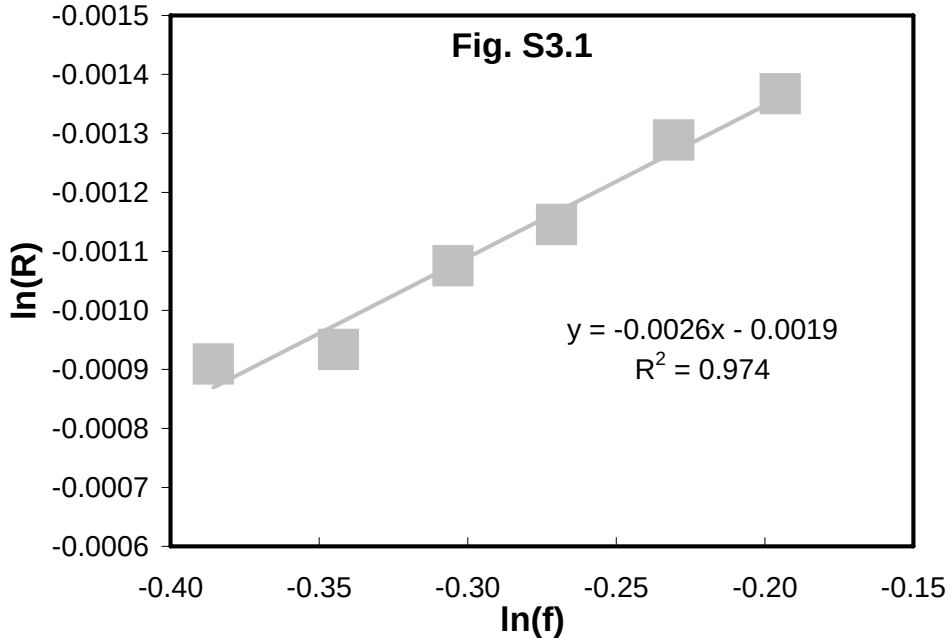
Fig. S3.1
-0.0015
-0.0014
-0.0013
-0.0012
-0.0011
-0.0010
-0.0009
-0.0008
-0.0007
-0.0006
ln(R)
y = -0.0026x - 0.0019
R2 = 0.974
-0.40
-0.35
-0.30
-0.25
-0.20
-0.15
ln(f)

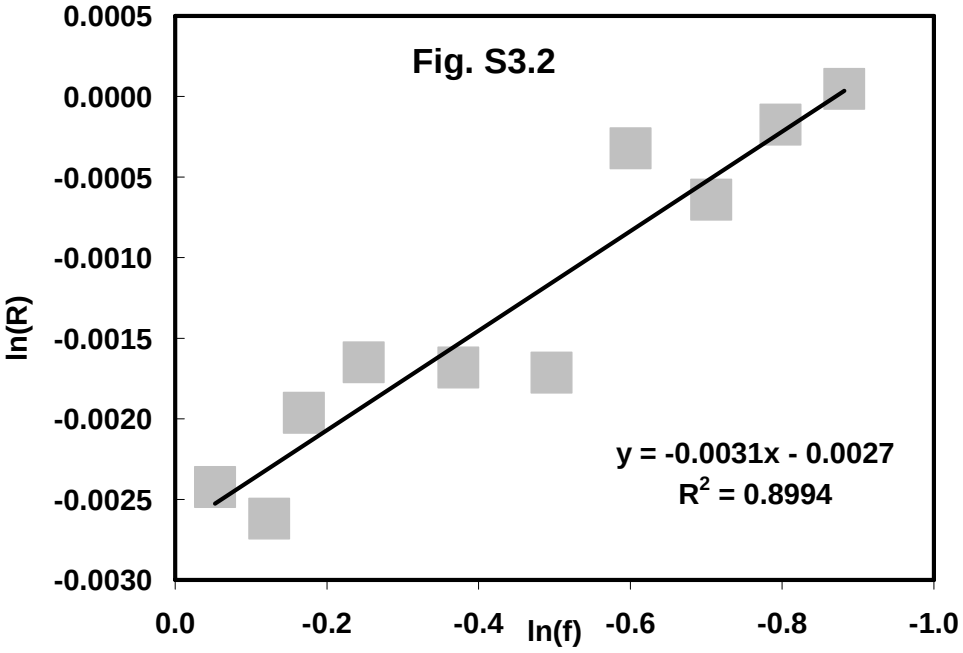
Fig. S3.2
0.0005
0.0000
-0.0005
-0.0010
-0.0015
-0.0020
-0.0025
-0.0030
ln(R)
y = -0.0031x - 0.0027
R2 = 0.8994
0.0
-0.2
-0.4
-0.6
-0.8
-1.0
ln(f)

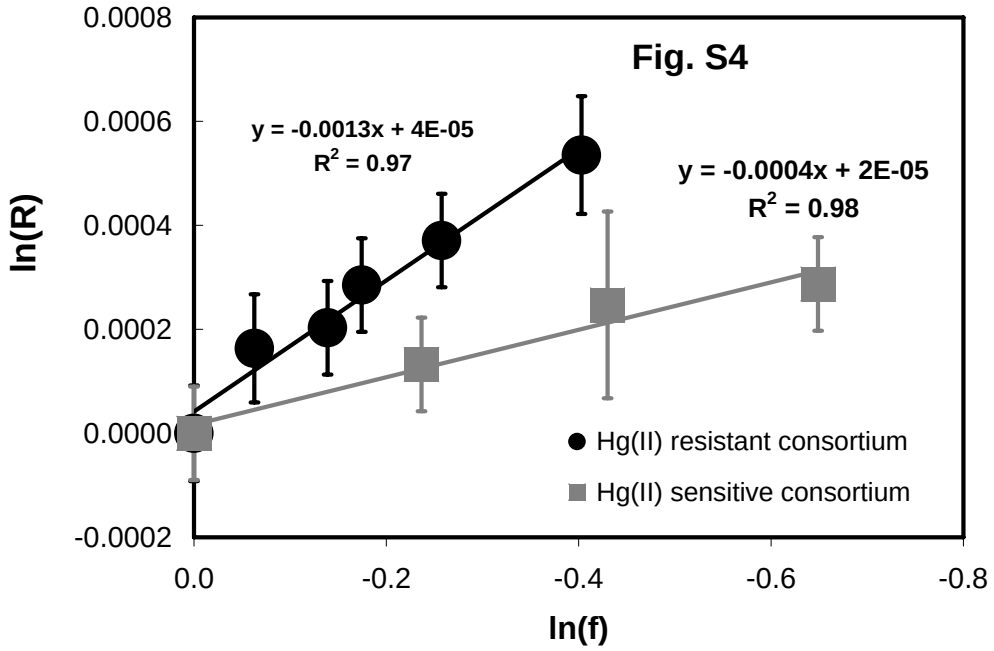
Fig. S4
y = -0.0013x + 4E-05
R2 = 0.97
y = -0.0004x + 2E-05
R2 = 0.98
Hg(II) resistant consortium
Hg(II) sensitive consortium
ln(R)
ln(f)
0.0008
0.0006
0.0004
0.0002
0.0000
-0.0002
0.0
-0.2
-0.4
-0.6
-0.8

Supplementary Tables (Chapter 2)

Table S1 **Experiments done with *E.coli* JM109/pPB117 at 37^{0}C**

Reactor Size	Reactor Data				Trap Data				Calculation of 'f'				
	Time (min)	δ^{202}Hg (‰)	n	2SE	Time (min)	δ^{202}Hg (‰)	n	2SE	Weight[1] (g)	Conc[2] (ng/g)	Total[3] Hg (μg)	f[4]	f[5]
1 L	0	-0.18	4	0.03					241.0	599	131	1.000	
	35	0.36	3	0.20	0-35	-2.06	2	0.25	218.9	532	116	0.887	0.944
	70	0.80	3	0.12	35-70	-1.60	2	0.21	204.1	411	89.6	0.686	0.787
	105	1.20	3	0.13	70-105	-1.00	3	0.25	189.1	259	56.6	0.433	0.559
	140	1.94	3	0.02	105-140	-0.10	2	0.55	173.9	164	35.8	0.274	0.353
	175	2.57	3	0.07	140-175	0.99	3	0.08	158.5	83.7	18.2	0.140	0.207
	210	3.04	2	0.18	175-210	2.05	3	0.23	143.8	34.3	7.47	0.057	0.098
	245	3.26	2	0.01	210-245	2.50	3	1.75	128.6	23.0	5.01	0.038	0.048
	280	3.33	1		245-280	1.23	2	1.01	113.7	17.9	3.90	0.030	0.034
1 L	0	0.05	3	0.06					236.1	637	136	1.000	
	35	0.25	3	0.13	0-35	n.a[6]		n.a	213.3	565	120	0.888	0.944
	70	0.46	3	0.10	35-70	-1.76	2	0.41	197.9	443	94.4	0.696	0.792
	105	0.95	3	0.14	70-105	-1.07	3	0.17	184.9	330	70.3	0.519	0.607
	140	1.46	4	0.07	105-140	-0.58	2	0.03	168.7	225	48.0	0.354	0.436
	175	1.92	3	0.12	140-175	0.15	3	0.05	154.2	152	32.3	0.238	0.296
	210	2.67	3	0.20	175-210	0.97	3	0.02	141.1	72.3	15.4	0.114	0.176
	245	2.84	2	0.13	210-245	1.91	3	0.20	124.2	39.0	8.31	0.061	0.087
	280	3.15	2	0.36	245-280	2.37	3	0.33	109.1	24.5	5.22	0.039	0.050
100 ml	0	0.03	1								15.20	1.000	
					0-40	-1.98	1		19.2	111	2.14		0.930
					40-70	-1.30	1		19.8	83.2	1.65		0.806
					70-100	-1.30	1		17.9	124	2.21		0.680
					100-130	-0.63	1		20.6	149	3.08		0.507
					130-160	0.34	1		20.9	140	2.92		0.311
					160-190	1.92	1		21.5	35.9	0.772		0.190
					190-220	3.00	1		20.7	26.2	0.543		0.147
					220-250	2.98	1		18.8	22.6	0.426		0.116
					250-280	3.74	1		17.6	14.3	0.252		0.093
					280-320	4.57	1		19.7	9.5	0.188		0.080
	320	6.16	1								0.350	0.023	

[1] Weight of the 1L reactor contents before sample withdrawl or of the trap attached to 100 ml reactor.
[2] Hg concentration in the 1L Reactor sample or in the trap attached to 100 ml reactor
[3] Total Hg(II) in 1L reactor assuming no loss of Hg(II) due to sampling or in a trap attached to 100 ml reactor)
[4] Fraction of Hg(II) remaining in the reactor as used for linear regression using Eq. 1
[5] Average fraction of Hg(II) remaining in the reactor as used for linear regression using Eq. 2 (see methods)
[6] Hg conc. was < 0.5 ppb and trap was found disconnected from the reactor at the end of 35 min.

Table S2 **Experiment done with *E. coli* JM109/pPB117 *at 30 ^{0} C***

Reactor Data				Trap Data				Calculation of 'f'				
Time (min)	δ^{202}Hg (‰)	n	2 SE	Time (min)	δ^{202}Hg (‰)	n	2 SE	Weight[1] (g)	Conc[2] (ng/g)	Total[3] Hg (μg)	f[4]	f[5]
0	-0.17	2	0.35					258.6	640	155	1.000	
60	-0.30	2	0.49	0-60	-2.05	3	0.12	241.7	584	141	0.912	0.956
120	0.32	3	0.04	60-120	-2.05	3	0.10	225.5	546	132	0.854	0.883
180	0.31	3	0.11	120-180	-1.78	3	0.11	207.7	520	126	0.813	0.833
240	0.56	3	0.10	180-240	-1.47	3	0.16	191.3	470	114	0.735	0.774
300	0.76	3	0.07	240-300	-1.35	3	0.14	173.9	407	98.4	0.636	0.685
360	0.98	3	0.10	300-360	-1.17	3	0.28	157.3	354	85.6	0.554	0.595
420	1.14	3	0.08	360-420	-0.59	3	0.02	140.9	297	71.9	0.465	0.509
480	1.87	3	0.15	420-480	-0.40	4	0.23	123.9	227	54.9	0.355	0.410
540	2.14	4	0.38	480-540	0.51	3	0.16	106.8	168	40.7	0.263	0.309

[1] Weight of the 1L reactor contents before sample withdrawl

[2] Hg concentration in the 1L Reactor sample

[3] Total Hg(II) in 1L reactor assuming no loss of Hg(II) due to sampling

[4] Fraction of Hg(II) remaining ($[Hg]_{Li}/[Hg]_{Lo}$) as used in Eq. 1 (see methods)

[5] Average fraction of Hg(II) remaining ($[Hg]_{Li}/[Hg]_{Lo}$) as used in Eq. 2 (see methods)

Table S3. Experiments with *E. coli* JM109/pPB117 at 22^{0}C in 100ml reactor

Reactor Data			Trap data			Calculation of 'f'				
Time (min)	δ^{202}Hg (‰)	n	Time (min)	δ^{202}Hg (‰)	n	Weight[1] (g)	Conc[2] (ng/g)	Total[3] Hg (μg)	f[4]	f[5]
First Experiment[6]										
0	-0.01	1				21.3	660	14.05	1.000	
			0-90	-2.15	1	17.5	38	0.666		0.976
			90-180	-2.40	1	18.6	17	0.317		0.941
			180-270	-2.00	1	19.6	51	0.998		0.895
			270-360	-2.17	1	17.1	19	0.324		0.847
			360-450	-1.37	1	19.1	19	0.363		0.823
			450-540	-1.30	1	18.0	25	0.450		0.794
			540-630	-1.15	1	18.8	22	0.414		0.763
			630-720	-1.08	1	20.7	16	0.321		0.737
			720-810	-0.94	1	18.8	25	0.462		0.709
			810-900	-0.92	1	18.5	20	0.360		0.680
900	0.76	1				21.3	432	9.20	0.655	
Second experiment										
0	0.05	1				16.3	420	6.84	1.000	
			0-90	-2.37	1	17.5	40	0.700		0.949
			90-180	-2.56	1	19.5	10	0.195		0.883
			180-270	-1.91	1	19.1	18	0.344		0.844
			270-360	-1.60	1	19.6	27	0.530		0.780
			360-450	-1.63	1	18.0	40	0.722		0.688
			450-540	-1.66	1	18.3	20	0.366		0.609
			540-630	-0.27	1	18.2	25	0.456		0.549
			630-720	-0.59	1	20.1	15	0.302		0.493
			720-810	-0.12	1	19.0	15	0.286		0.450
			810-900	0.10	1	20.9	10	0.209		0.414
900	1.98	1	810-900			16.3	160	2.61	0.382	

[1] Weight of liquid in the trap or reactor [2] Hg concentration in the sample

[3] Total Hg(II) in a trap attached to the reactor or Total Hg(II) remaining in the reactor

[4] Fraction of Hg(II) remaining in the reactor as used for linear regression using Eq. 1

[5] Average fraction of Hg(II) remaining in the reactor as used for linear regression using Eq. 2 (methods)

[6] For this experiment, data from first four traps was not used for regression analysis. This improved the R^2 value from 0.86 to 0.97

Table S4. Experiment done with natural microbial community

	Reactor Data				Calculation of 'f'			
	Time (hours)	δ^{202}Hg (‰)	n	2 SE	Weight[1] (g)	Conc[2] (ng/g)	Total[3] Hg (μg)	f[4]
Hg(II) resistant Adapted Consortium	0	-0.02	4	0.09	210.6	224	43.5	1.000
	12	0.14	2	0.10	194.0	210	40.8	0.939
	24	0.18	3	0.01	175.5	195	37.8	0.870
	36	0.26	4	0.02	154.8	188	36.5	0.840
	48	0.35	3	0.08	135.4	173	33.6	0.773
	60	0.51	3	0.11	115.0	150	29.1	0.668
Control[5] Hg(II) sensitive community	0	-0.41	2	0.07	209.9	27.9	5.86	
	10	0.18	2	0.07	189.1	19.3	3.66	1.000
	19	0.32	2	0.06	167.5	15.3	2.56	0.789
	26	0.43	2	0.18	145.6	12.6	1.83	0.650
	48	0.47	1		121.4	10.1	1.23	0.523

[1] Weight of the reactor contents before sample withdrawl

[2] Hg concentration in the 1L Reactor sample

[3] Total Hg(II) in 1L reactor assuming no loss of Hg(II) due to sampling

[4] Fraction of Hg(II) remaining as used in Eq. 1 (methods)

[5] The low δ value at time = 0 minutes for the unenriched control experiment is either an artifact resulting from equilibration of Hg(II) with ligands in the natural water sample (Barkay et al., 1997) and transient loss of isotopically heavy Hg (i.e., adsorption) or contamination. Preliminary experiments in our laboratory suggest that adsorption of Hg(II) to particulate matter in natural waters might lead to fractionation. This point was not used for analysis. Isotope data from the sample collected at 10 hours was considered to be R_0.

Table S5. Comparison* of the extent of fractionation observed for Hg with other redox-sensitive elements undergoing fractionation.

	Avg. Mol. Weight	% mass spread	Maximum Range of δ (‰/amu)	Maximum reported α/amu
Fe	56	7	2**	1.0015**
Mo	96	8	1.7##	1.002##
Hg	**200**	**4**	**1.5**	**1.0015**

* This is a crude comparison & does not include fractionation due to amplifying processes such as iterative distillation or chromatography (Johnson C. M. et al, 2004)

** Maximum range of isotopic variation (relative to standard) reported for low temperature processes occurring either in nature & under laboratory conditions. Eg. $\delta^{56/54}$Fe in natural samples varies from ~-3 to +1 making the max. range ~2 ‰/amu. Max. α for $^{56/54}$Fe is 1.003 for non biological redox eqm. of Fe(III) and Fe(II).

$\delta^{97/95}$Mo varies between -0.9 to +2.5 for natural samples.

Supplementary Text

Reliability of individual datasets

Uncertainties associated with the alpha values (as reported in Table 2.1) are a good estimate of the reliability of the data from a particular experiment. Moreover, all 1 L reactor experiments are more reliable than the 100 ml reactor experiments because isotope analysis was not replicated for 100 ml reactor experiments. As noted in the main manuscript, alpha values based on the reactor data are more reliable than the trap data.

Additional notes on the calculations of 'f'

For the experiments done in 100 ml reactors, the smaller reactor size did not allow for withdrawal of multiple samples from the reactor, and thus calculation of f^R was not feasible. In these experiments, close to complete trapping of Hg(0) was verified and f^T could be used reliably. However, the trapping efficiency was non-quantitative when using the larger 1 L reactors. For example, I determined that the amount of Hg collected in traps at each stage ranged between 65 to 95% of the total amount of Hg(II) lost from the reactor during one of the experiments with the large 1 L reactor (data not shown). The non-quantitative trapping efficiency could be due to small gas leaks from the apparatus, adsorption of Hg(0) to soda lime in the drying tube, and/or Hg(0) trapping by condensed water vapor in the transfer tubing between the reactor and trap. (There was no detectable carry-over of Hg from the first trap to a connected second trap). Since $\alpha_{202/198}$ values inferred from the isotopic ratios of the trap and reactor samples are very similar for experiments done at both 37 ^{0}C and 30 ^{0}C (Table 2.1), the loss of Hg(0) between the

reactor and the trap appears not to have significantly changed the isotopic composition of the trapped volatilized Hg(0).

I note that for all the experiments done using 1 L reactor, the slopes (and therefore alpha values) obtained from linear regression of the reactor isotope data are always lower than the slopes obtained from the regression of the trap isotope data. This might be partially due to time averaging of the trap data. As reported in the methods section, the value of effective 'f' for the traps was calculated as the average of 'f^R' before and after the internal of time during which a particular trap accumulated the product Hg(0). It is possible that this averaging under-estimates the value of effective 'f^T'.

Additional notes about experiments done at 22 ^{0}C

The comparison of the isotopic composition of the traps with the prediction of the Rayleigh model yielded a weaker correlation (R^2 = 0.86 for the first experiment done at 22 ^{0}C when N =10; see Table S3) compared to higher temperature experiments (R^2 = 0.97 to 0.99). This apparent weaker correlation might be a consequence of lack of replicate isotopic analysis for the samples (Table S3) and/or inconsistent Hg(II) uptake and reduction rates at 22 ^{0}C, possibly due to low metabolic rates or other responses to lower growth temperature, including changes in the cell membrane fluidity of the bacterium[67,87].

I did not perform replicate analysis for the samples from two experiments done at 22 ^{0}C. I chose not to repeat the experiments at 22 ^{0}C in order to obtain replicate isotopic data because this temperature is low enough to impair normal physiological activity of *E. coli* (a mesophilic organism with optimum growth temperature of 37 ^{0}C) and the noise in

the data could be simply due to impairment and not necessarily due to lack of replicate analysis for samples.

Implications for scientists using 'enriched' Hg stable isotopes as biogeochemical tracers

The use of single or multiple 'enriched' Hg stable isotope spikes as biogeochemical tracers has become common in recent years[169-172]. During the course of their investigations, authors have been repeatedly asked if the fractionation of Hg stable isotopes by processes similar to those investigated in this study can affect the application of 'enriched' stable isotopes as tracers. I would like to point out that the corrections for mass dependent fractionation can easily be applied, and that my estimates based on isotope dilution equations show that even if uncorrected, mass dependent Hg isotope fractionation would introduce much smaller uncertainties in the 'spike experiments' than existing uncertainties in spike isotopic composition, ambient concentrations of various Hg species and blank corrections[169,170,173] .

Supplement to Chapter 3

<u>Supplementary Figure</u>: **Rate of degradation of MMHg**

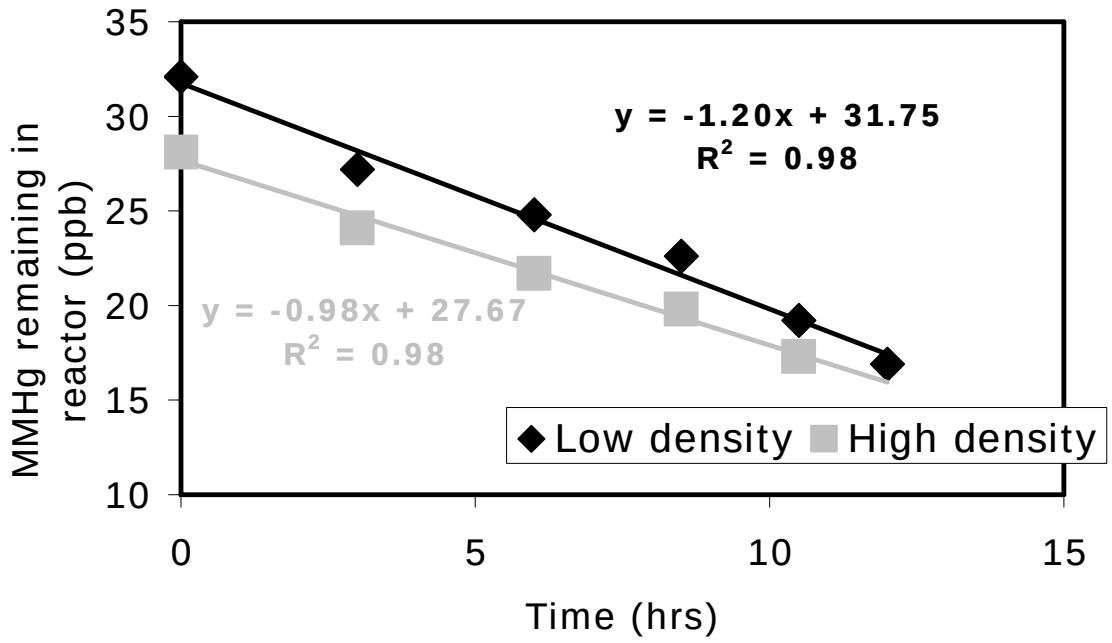

<u>Supplementary Text</u>

Notes on pre-exposure to MMHg: I did not perform any experiments to check the level of *mer* transcripts with and without pre-exposure. Although it is not widely accepted, at least one previous study claims induction of *mer* operon by methylmercury chloride[174]. Usually, induction by MMHg is considered to be an artifact arising either due to generation of Hg(II) following the initial cleavage of the Hg-C bond by the basal level of MerB which is present even in repressed systems or due to small but significant quantities of Hg(II) present in all laboratory MMHg stocks.

Difficulties in estimating exact number of MerB molecules per cell in absence of experimental data: *E. coli* JM109 cells containing a pUC19 based multi copy plasmids, such as pPB117, can have 40-250 copies per cell depending on the host strain and temperature[175,176]. Moreover even if the exact copy number is known, it doesn't necessarily translate to a known number of functional enzyme molecules[106]. It is also not precisely known how actively the *mer* genes on this plasmid are transcribed and translated in *E. coli* JM109 and how stable is the MerB protein. mRNA stability depends on a number of factors including growth rates and extent of synchronization between RNA polymerase and the translating ribosomes during transcription[177-179] and none of these are known for JM109/pPB117.

Fractionation during uptake of MMHg: If the MMHg uptake is not through passive diffusion but instead through "accidental" (as has been suggested for Hg(II) by Golding et al[150,152] but in my opinion unlikely) transport of MMHg with other transporters which would require binding to transporters, uptake could also contribute to fractionation.

Unit conversions

1 ppb = 1 ng/g = 1 ng/ml = 5 Nm; 1 ppm = 1000 ppb = 5000 nM = 5 μM

Bibliography

1. Mergler, D. et al. Methylmercury Exposure and Health Effects in Humans: A Worldwide Concern. *AMBIO: A Journal of the Human Environment*, 3-11 (2007).
2. Scheuhammer, A.M., Meyer, M.W., Sandheinrich, M.B. & Murray, M.W. Effects of Environmental Methylmercury on the Health of Wild Birds, Mammals, and Fish. *AMBIO: A Journal of the Human Environment*, 12-19 (2007).
3. Barnes, H.L. & Seward, T.M. Geothermal systems and mercury deposits. in *Geochemistry of Hydrothermal Ore Deposits.* (ed. Barnes, H.L.) 699-736 (John Wiley & Sons, Inc., New York, 1997).
4. Morel, F.M.M., Kraepiel, A.M.L. & Amyot, M. The chemical cycle and bioaccumulation of mercury. *Annual Reviews in Ecology and Systematics* 29, 543-566 (1998).
5. Mason, R.P. & Sheu, G.-R. Role of the ocean in the global mercury cycle. *Global Biogeochemical Cycles* 16, 1093-2007 (2002).
6. Lindberg, S. et al. A synthesis of progress and uncertainties in attributing the sources of mercury in deposition. *Ambio* 36, 19-32 (2007).
7. Fitzgerald, W.F., Lamborg, C.H. & Hammerschmidt, C.R. Marine biogeochemical cycling of mercury. *Chem Rev* 107, 641-62 (2007).
8. Barkay, T., Miller, S.M. & Summers, A.O. Bacterial mercury resistance from atoms to ecosystems. *FEMS Microbiol. Rev.* 27, 355-384 (2003).
9. Mason, R.P., Morel, F.M.M. & Hemond, H.F. The role of microorganisms in elemental mercury formation in natural waters. *Water Air Soil Poll.* 80, 775-787 (1995).
10. Pacyna, E.G., Pacyna, J.M., Steenhuisen, F. & Wilson, S. Global anthropogenic mercury emission inventory for 2000. *Atmospheric Environment* 40, 4048-4063 (2006).
11. Wilson, S.J., Steenhuisen, F., Pacyna, J.M. & Pacyna, E.G. Mapping the spatial distribution of global anthropogenic mercury atmospheric emission inventories. *Atmospheric Environment* 40, 4621-4632 (2006).
12. Nriagu, J.O. Mechanistic steps in the photoreduction of mercury in natural waters. *The Science of the Total Environment* 154, 1-8 (1994).
13. Zhang, H. & Lindberg, S.E. Sunlight and iron(III)-induced photochemical production of dissolved gaseous mercury in freshwater. *Environmental Science and Technology* 35, 928-935. (2001).
14. Skogerboe, R.K. & Wilson, S.A. Reduction of ionic species by fulvic acid. *Analytical Chemistry* 53, 228-232 (1981).
15. Baltisberger, R.J., A., H.D., Grieble, D. & Ballintine, T.A. A study of the disproportionation of mercury (I) induced by gas sparging in acidic aqueous solutions for cold-vapor atomic absorption septrometery. *Analytica Chimica Acta* 111, 111-122 (1979).
16. Pitts, K.E. & Summers, A.O. The roles of thiols in the bacterial organomercurial lyase (MerB). *Biochemistry* 41, 10287-96 (2002).

17. Schaefer, J.K. et al. The role of the bacterial organomercury lyase (MerB) in controlling methylmercury accumulation in mercury contaminated natural waters. *Environ. Sci. Technol.* 38, 4304-4311 (2004).
18. Oremland, R.S., Culbertson, C.W. & Winfrey, M.R. Methylmercury decomposition in sediments and bacterial cultures: involvement of methanogens and sulfate reducers in oxidative demethylation. *Applied and Environmental Microbiology* 57, 130-137 (1991).
19. Suda, I., Suda, M. & Hirayama, K. Degradation of methyl and ethyl mercury by singlet oxygen generated from sea water exposed to sunlight or ultraviolet light. *Archives of Toxicology* 67, 365-368 (1993).
20. Sellers, P., Kelly, C.A., Rudd, J.W.M. & MacHutchon, A.R. Photodegradation of methylmercury in lakes. *Nature* 380, 694-697 (1996).
21. Compeau, G.C. & Bartha, R. Sulfate-reducing bacteria: principle methylators of mercury in anoxic estuarine sediment. *Applied and Environmental Microbiology* 50, 498-502 (1985).
22. Gilmour, C.C., Henry, E.A. & Mitchell, R. Sulfate stimulation of mercury methylation in freshwater sediments. *Environmental Science and Technology* 26, 2281-2287 (1992).
23. King, J.K., Kostka, J.E., Frischer, M.E. & Saunders, F.M. Sulfate-reducing bacteria methylate mercury at variable rates in pure culture and in marine sediments. *Applied and Environmental Microbiology* 66, 2430-7 (2000).
24. Benoit, J.M., Gilmour, C.C., Mason, R. & Hayes, A. Sulfide controls on mercury speciation and bioavailability to methylating bacteria in sediment pore waters. *Environmental Science and Technology* 33, 951-957 (1999).
25. Benoit, J.M., Gilmour, C.C. & Mason, R.P. Aspects of bioavailability of mercury for methylation in pure cultures of Desulfobulbus propionicus (1pr3). *Applied and Environmental Microbiology* 67, 51-58 (2001a).
26. Benoit, J.M., Gilmour, C.C. & Mason, R.P. The influence of sulfide on solid-phase mercury bioavailability for methylation by pure cultures of *Desulfobulbus propionicus* (1pr3). *Environmental Science and Technology* 35, 127-132 (2001b).
27. Fleming, E.J., Mack, E.E., Green, P.G. & Nelson, D.C. Mercury methylation from unexpected sources: molybdate-inhibited freshwater sediments and an iron-reducing bacterium. *Applied and Environmental Microbiology* 72(2006).
28. Kerin, E.J. et al. Mercury Methylation by Dissimilatory Iron-Reducing Bacteria. *Applied and Environmental Microbiology* 72, 7919-7921 (2006).
29. Weber, J.H. Review of possible paths for abiotic methylation of mercury(II) in the aquatic environment. *Chemosphere* 26, 2063-2077 (1993).
30. Falter, R. Experimental study on the unintentional abiotic methylation of inorganic mercury during analysis: part 1: localisation of the compounds effecting the abiotic mercury methylation. *Chemosphere* 39, 1051-1073 (1999).
31. Cerrati, G., Bernhard, M. & Weber, J.H. Model reactions for abiotic mercury(II) methylation: kinetics of methylation of mercury(II) by mono-, di-, and tri-methylation in seawater. *Applied Organometallic chemistry* 6, 587-595 (1992).

32. Lindberg, S.E. et al. Dynamic oxidation of gaseous mercury in the Arctic troposphere at polar sunrise. *Environmental science and Technology* 36, 1245-1256. (2002).
33. Siciliano, S.D., O'Driscoll, N.J. & Lean, D.R. Microbial reduction and oxidation of mercury in freshwater lakes. *Environmental Science and Technology* 36, 3064-3068. (2002).
34. Thoming, J., Kliem, B.K. & Ottosen, L.M. Electrochemically enhanced oxidation reactions in sandy soil polluted with mercury. *Science of the Total Environment* 261, 137-147. (2000).
35. Smith, T., Pitts, K., McGarvey, J.A. & Summers, A.O. Bacterial Oxidation of Mercury Metal Vapor, Hg(0). *Appl. Environ. Microbiol.* 64, 1328-1332 (1998).
36. de Magalhaes, M.E. & Tubino, M. A possible path for mercury in biological systems: the oxidation of metallic mercury by molecular oxygen in aqueous solutions. *Science of the Total Environment* 170, 229-239. (1995).
37. Munthe, J. The aqueous oxidation of elemental mercury by ozone. *Atmospheric Environment* 26A, 1461-1468 (1992).
38. Yamamoto, M. Possible mechanism of elemental mercury oxidation in the presence of SH compounds in aqueous solution. *Chemosphere* 31, 2791-2798 (1995).
39. Ebinghaus, R. et al. Antarctic springtime depletion of atmospheric mercury. *Environmental Science and Technology* 36, 1238-1244. (2002).
40. Lalonde, J.D., Amyot, M., Kraepiel, A.M. & Morel, F.M. Photooxidation of Hg(0) in artificial and natural waters. *Environmental Science and Technology* 35, 1367-1372. (2001).
41. Amyot, M., Gill, G.A. & Morel, F.M. Production and loss of dissolved gaseous mercruy in coastal seawater. *Environmental Science and Technology* 31, 3606-3611 (1997).
42. Bigeleisen, J. Theoretical basis of isotope effects from an autobiographical perspective. in *Isotope effects in Chemistry and Biology* (eds. Kohen, A. & Limbach, H.) (Taylor and Francis Group, Florida, 2006).
43. Hayes, J.M. An introduction to isotopic calculations. (Woods Hoel Oceanographic Institute, Woods Hole, MA, 2004).
44. Blum, J.D. & Bergquist, B.A. Reporting of variations in the natural isotopic composition of mercury. *Anal Bioanal Chem* 388, 353-9 (2007).
45. Johnson, C.M., Beard, B.L. & Albarède, F. *Geochemistry of Non-traditional Stable isotopes*, 454 (The Mineralogical Society of America, Washington, 2004).
46. Jackson, T.A., Whittle, D.M., Evans, M.S. & Muir, D.C.G. Evidence for mass-independent and mass-dependent fractionation of the stable isotopes of mercury by natural processes in aquatic ecosystems, *in press*. *Applied Geochemistry* (2008).
47. Turro, N.J. Influence of Nuclear Spin on Chemical Reactions: Magnetic Isotope and Magnetic Field Effects (A Review). *Proceedings of the National Academy of Sciences of the United States of America* 80, 609-621 (1983).

48. Schauble, E.A. Role of nuclear volume in driving equilibrium stable isotope fractionation of mercury, thallium, and other very heavy elements. *Geochimica et Cosmochimica Acta* 71, 2170-2189 (2007).
49. Kohen, A. & Limbach, H. *Isotope effects in Chemistry and Biology*, (Taylor and Francis Group, Florida, 2006).
50. Schauble, E.A. Applying stable isotope fractionation theory to new systems. in *Geochemistry of Non-traditional Stable isotopes*, Vol. 55 (eds. Johnson, C.M., Beard, B.L. & Albarède, F.) 65-111 (The Mineralogical Society of America, Washington, 2004).
51. Bergquist, B.A. & Blum, J.D. Mass-dependent and mass-independent fractionation of Hg isotopes by photo-reduction in aquatic systems. *Science* 318, 417-420 (2007).
52. Kritee, K., Blum, J.D., Johnson, M.W., Bergquist, B.A. & Barkay, T. Mercury Stable Isotope Fractionation during Reduction of Hg(II) to Hg(0) by Mercury Resistant Microorganisms. *Environ. Sci. Technol.* 41, 1889-1895 (2007).
53. Cook, P.F. *Enzyme mechanism from isotope effects*, (CRC Press, Inc., Florida, 1991).
54. Brunner, B. & Bernasconi, S.M. A revised isotope fractionation model for dissimilatory sulfate reduction in sulfate reducing bacteria. *Geochimica et Cosmochimica Acta* 69, 4759-4771 (2005).
55. Kendall, C. & McDonnell, J.J. *Isotope Tracers in Catchment Hydrology.*, (Elsevier Science B.V., Amsterdam, 1998).
56. Wellman, R.P., Cook, F.D. & Krouse, H.R. Nitrogen-15: Microbiological Alteration of Abundance. *Science* 161, 269-270 (1968).
57. Johnson, T.M. & Bullen, T.D. Mass-dependent fractionation of Selenium and Chromium isotopes in low temperature environments. in *Geochemistry of non-traditional stable isotopes*, Vol. 55 (eds. Johnson, C.M., Beard, B.L. & Albarede, F.) (The Mineralogical Society of America, Washington, DC, 2004).
58. Mariotti, A. et al. Experimental determination of nitrogen kinetic isotope fractionation: Some principles; illustration for the denitrification and nitrification processes. *Plant and Soil* 62, 413-430 (1981).
59. Albarede, F. & Beard, B.L. Analytical methods for non-traditional isotopes. in *Geochemistry of non-traditional stable isotopes*, Vol. 55 (eds. Johnson, C.M., Beard, B.L. & Albarede, F.) (The Mineralogical Society of America, Washington, DC, 2004).
60. Rademacher, L.K. et al. Experimentally determined uranium isotope fractionation during reduction of hexavalent U by bacteria and zero valent iron. *Environ Sci Technol* 40, 6943-8. (2006).
61. Rehkamper, M. et al. Thallium isotope variations in seawater and hydrogenetic, diagenetic, and hydrothermal ferromanganese deposits. *Earth and Planetary Science Letters* 197, 65-81 (2002).
62. Lauretta, D.S., Klaue, B., Blum, J.D. & Buseck, P.R. Mercury abundances and isotopic compositions in the Murchison (CM) and Allende (CV) carbonaceous chondrites. *Geochim. Cosmochim. Acta* 65, 2807-2818 (2001).

63. Smith, C.N., Kesler, S.E., Klaue, B. & Blum, J.D. Mercury isotope fractionation in fossil hydrothermal systems. *Geology* 33, 825-828 (2005).
64. Johnson, C.M. & Beard, B.L. Fe isotopes: An emerging technique for understanding modern and ancient biogeochemical cycles. *GSA Today* 16, 4-10 (2006).
65. Hintelmann, H. & Lu, S.Y. High precision isotope ratio measurements of mercury isotopes in cinnabar ores using multi-collector inductively coupled plasma mass spectrometry. *Analyst* 128, 635-639 (2003).
66. Rees, C.E. A steady state model for sulfur isotope fractionation in bacterial reduction processes. *Geochim. Cosmochim. Acta* 37, 1141-1162 (1973).
67. Canfield, D.E. Biogeochemistry of sulfur isotopes. in *Stable Isotope Geochemistry*, Vol. 43 (eds. Valley, J.W. & Cole, D.R.) (The Mineralogical Society of America, Washington, DC, 2001).
68. Foucher, D. & Hintelmann, H. High-precision measurement of mercury isotope ratios in sediments using cold-vapor generation multi-collector inductively coupled plasma mass spectrometry. *Anal. Bioanal. Chem.* 384, 1470-8 (2006).
69. Bigeleisen, J. The relative velocities of isotopic molecules. *The journal of chemical physics* 17, 675-678 (1949).
70. Valley, J.W. & Cole, D.R. *Stable Isotope Geochemistry*, (The Mineralogical Society of America, Washington, DC, 2001).
71. Hoefs, J. *Stable Isotope Geochemistry*, (Springer-Verlag, Berlin Heidelberg, 2004).
72. Melander, L. *Isotope effects on reaction rates*, (The Ronald Press Company, New York, 1960).
73. Fitzgerald, W.F., Mason, R.P. & Vandal, G.M. Atmospheric cycling and air-water exchange of Hg over mid-continental lacustrine regions. *Water Air Soil Poll.* 56, 745-767. (1991).
74. Johnson, C.M., Beard, B.L., Roden, E.E., Newman, D.K. & Nealson, K.H. Isotopic contraints on biogeochemical cycling of Fe. in *Geochemistry of non-traditional stable isotopes*, Vol. 55 (eds. Johnson, C.M., Beard, B.L. & Albarede, F.) (The Mineralogical Society of America, Washington, DC, 2004).
75. Jackson, T.A., Muir, D.C. & Vincent, W.F. Historical variations in the stable isotope composition of mercury in Arctic lake sediments. *Environ. Sci. Technol.* 38, 2813-21 (2004).
76. Mason, R.P., Fitzgerald, W.F. & Morel, F.M.M. Aquatic biogeochemical cycling of elemental mercury: anthropogenic influence. *Geochim. Cosmochim. Acta.* 58, 3191-3198. (1994).
77. Fitzgerald, W.F., Mason, R.P., Vandal, G.M. & Dulac, F. Air-water cycling of mercury in lakes. in *Mercury as a Global pollutant: Toward Integration and Synthesis* (eds. Watras, C.J. & Huckabee, J.W.) 203-220 (Lewis Press, Boca Raton, FL, 1994).
78. Reniero, D., Galli, E. & Barbieri, P. Cloning and comparison of mercury- and organomercurial-resistance determinants from a Pseudomonas stutzeri plasmid. *Gene* 166, 77-82 (1995).

79. Sambrook, J., Fritsch, E.F. & Maniatis, T. *Molecular Cloning: A Laboratory Manual*, (Cold Spring Harbor Laboratory Press, New York, 1989).
80. Selifonova, O., Burlage, R. & Barkay, T. Bioluminescent sensors for detection of bioavailable Hg(II) in the environment. *Applied and Environmental Microbiology* 59, 3083-3090 (1993).
81. Barkay, T. Adaptation of aquatic microbial communities to Hg^{2+} stress. *Appl. Environ. Microbiol.* 53, 2725-2732 (1987).
82. York, D. Least-squares fitting of a straight line. *Can. J. Phys.* 44, 1076-1086 (1966).
83. Scott, K.M., Lu, X., Cavanaugh, C.M. & Lu, J.S. Optimal methods for estimating kinetic isotope effects from different forms of the Raleigh distillation equation. *Geochim. Cosmochim. Acta* 68, 433-442 (2004).
84. Wilson, J.R., Leang, C., Morby, A.P., Hobman, J.L. & Brown, N.L. MerF is a mercury transport protein: Different structures but a common mechanism for mercuric ion transporters? *FEBS letters* 472, 78-82 (2000).
85. Barkay, T., Gillman, M. & Turner, R.R. Effects of dissolved organic carbon and salinity on bioavailability of mercury. *Appl. Environ. Microbiol.* 63, 4267-71 (1997).
86. Vetriani, C. et al. Mercury adaptation among bacteria from a deep-sea hydrothermal vent. *Appl. Environ. Microbiol.* 71, 220-6 (2005).
87. Canfield, D.E. Isotope fractionation by natural populations of sulfate-reducing bacteria. *Geochim. Cosmochim. Acta* 65, 1117 - 1124 (2001).
88. Barkay, T. & Wagner-Dobler, I. Microbial transformations of mercury: potentials, challenges, and achievements in controlling mercury toxicity in the environment. *Adv. Appl. Microbiol.* 57, 1-52 (2005).
89. Gehrke, G.E., Blum, J.D. & Meyers, P.A. The geochemical behavior and isotopic composition of Hg in a mid-Pleistocene Mediterranean sapropel (*submitted*). *Geochim. Cosmochim. Acta.* (2008).
90. Zheng, W., Foucher, D. & Hintelmann, H. Mercury isotope fractionation during volatilization of Hg(0) from solution into the gas phase. *Journal of Analytical Atomic Spectrometry* 22, 1097 - 1104 (2007).
91. Mason, R.P., Reinfelder, J.R. & Morel, F.M.M. Uptake, Toxicity, and Trophic Transfer of Mercury in a Coastal Diatom. *Environ. Sci. Technol.* 30, 1835-1845 (1996).
92. Schulz, H.N. & Jorgensen, B.B. Big bacteria. *Annu Rev Microbiol* 55, 105-37 (2001).
93. Hudson, R.J.M. Which aqueous species control the rates of trace metal uptake by aquatic biota? Observations and predictions of non-equilibrium effects. *Science of The Total Environment* 219, 95-115 (1998).
94. Bienvenue, E. et al. Transport of mercury compounds across bimolecular lipid membranes: Effect of lipid composition, pH and chloride concentration. *Chemico-Biological Interactions* 48, 91-101 (1984).
95. Kiyono, M., Omura, T., Fujimori, H. & Pan-hou, H. Lack of involvement of merT and merP in methylmercury transport in mercury resistant *Pseudomonas K-62*. *FEMS Microbiology Letters* 128, 301-306 (1995).

96. Kiyono, M., Omura, T., Fujimori, H. & Pan-Hou, H. Organomercurial resistance determinants in *Pseudomonas* K-62 are present on two plasmids. *Arch Microbiol* 163, 242-7 (1995).
97. Kiyono, M. & Pan-hou, H. The merG Gene Product Is Involved in Phenylmercury Resistance in *Pseudomonas* Strain K-62. *Journal of Bacteriology* 181, 726-730 (1999).
98. Benison, G.C. et al. A Stable Mercury-Containing Complex of the Organomercurial Lyase MerB: Catalysis, Product Release, and Direct Transfer to MerA. *Biochemistry* 43, 8333-8345 (2004).
99. Moore, M.J., Miller, S.M. & Walsh, C.T. C-Terminal cysteines of Tn501 mercuric ion reductase. *Biochemistry* 31, 1677-1685 (1992).
100. Sandstrom, A. & Lindskog, S. Activation of mercuric reductase by the substrate NADPH. *European Journal of Biochemistry* 164, 243-249 (1987).
101. Begley, T.P., Walts, A.E. & Walsh, C.T. Bacterial organomercurial lyase: overproduction, isolation, and characterization. *Biochemistry* 25, 7186-7192 (1986).
102. Holmes, J. & Lean, D. Factors that influence methylmercury flux rates from wetland sediments. *Science of The Total Environment (Selected papers from the 7th International Conference on Mercury as a Global Pollutant, Ljubljana, Slovenia June 27 - July 2, 2004)* 368, 306-319 (2006).
103. Fox, B. & Walsh, C. Mercuric reductase. Purification and characterization of a transposon- encoded flavoprotein containing an oxidation-reduction-active disulfide. *J. Biol. Chem.* 257, 2498-2503 (1982).
104. Madigan, M.T. & Martinko, J.M. *Brock Biology of Microorganisms*, (Prentice Hall, Upper Saddle River, NJ, 2006).
105. Lu, P., Vogel, C., Wang, R., Yao, X. & Marcotte, E.M. Absolute protein expression profiling estimates the relative contributions of transcriptional and translational regulation. *Nature Biotechnology* 25, 117-124 (2007).
106. Nakahara, H. et al. Gene copy number effects in the *mer* operon of plasmid NR1. *J Bacteriol* 138, 284-7 (1979).
107. Hammerschmidt, C.R. & Fitzgerald, W.F. Methylmercury cycling in sediments on the continental shelf of southern New England. *Geochimica et Cosmochimica Acta* 70, 918-930 (2006).
108. Wiatrowski, H.A., Ward, P.M. & Barkay, T. Novel Reduction of Mercury(II) by Mercury-Sensitive Dissimilatory Metal Reducing Bacteria. *Environ. Sci. Technol.* 40, 6690-6696 (2006).
109. Rodushkin, I., Stenberg, A., Andren, H., Malinovsky, D. & Baxter, D.C. Isotopic Fractionation during Diffusion of Transition Metal Ions in Solution. *Anal. Chem.* 76, 2148-2151 (2004).
110. Kritee, K., Blum, J.D. & Barkay, T. Chapter 3: Variation in the extent of mercury stable isotope fractionation during reduction of Hg(II) to Hg(0) by different microbial species (Submitted). (2008).
111. Grissom, C.B. Magnetic Field Effects in Biology: A Survey of Possible Mechanisms with Emphasis on Radical-Pair Recombination. *Chem. Rev.* 95, 3-24 (1995).

112. Begley, T.P., Walts, A.E. & Walsh, C.T. Mechanistic studies of a protonolytic organomercurial cleaving enzyme: bacterial organomercurial lyase. *Biochemistry* 25, 7192-7200 (1986).
113. DiLello, P. et al. NMR Structural Studies Reveal a Novel Protein Fold for MerB, the Organomercurial Lyase Involved in the Bacterial Mercury Resistance System. *Biochemistry* 43, 8322-8332 (2004).
114. Melnick, J.G. & Parkin, G. Cleaving Mercury-Alkyl Bonds: A Functional Model for Mercury Detoxification by MerB. *Science* 317, 225-227 (2007).
115. Brown, N.L. et al. Mercury transport and resistance. *Biochem. Soc. Trans.* 30, 715-718 (2002).
116. Miller, S.M. Bacterial detoxification of Hg(II) and organomercurials. in *Essays in Biochemistry*, Vol. 34 (ed. Ballou, D.P.) 14-30 (Portland Press, London, 1999).
117. Khudyakov, I.V., Serebrennikov, Y.A. & Turro, N.J. Spin-orbit coupling in free-radical reactions: on the way to heavy elements. *Chem. Rev.* 93, 537-570 (1993).
118. Koziar, J.C. & Cowan, D.O. Photochemical heavy-atom effects. *Accounts of Chemical Research* 11, 334-341 (1978).
119. Anderson, M.A., Xu, Y. & Grissom, C.B. Electron Spin Catalysis by Xenon in an Enzyme. *J. Am. Chem. Soc.* 123, 6720-6721 (2001).
120. Anderson, M.A. & Grissom, C.B. Increasing the Heavy Atom Effect of Xenon by Adsorption to Zeolites: Photolysis of 2,3-Diazabicyclo[2.2.2]oct-2-ene. *J. Am. Chem. Soc.* 118, 9552-9556 (1996).
121. Omary, M.A., Kassab, R.M., Haneline, M.R., Elbjeirami, O. & Gabbai, F.P. Enhancement of the Phosphorescence of Organic Luminophores upon Interaction with a Mercury Trifunctional Lewis Acid. *Inorg. Chem.* 42, 2176-2178 (2003).
122. Jalilehvand, F., Leung, B.O., Izadifard, M. & Damian, E. Mercury(II) Cysteine Complexes in Alkaline Aqueous Solution. *Inorg. Chem.* 45, 66-73 (2006).
123. Buchachenko, A. et al. Magnetic isotope effect for mercury nuclei in photolysis of bis(p-trifluoromethylbenzyl) mercury. *Doklady Physical Chemistry* 413, 39-41 (2007).
124. Buchachenko, A.L., Kouznetsov, D.A. & Shishkov, A.V. Spin Biochemistry: Magnetic Isotope Effect in the Reaction of Creatine Kinase with CH_3HgCl. *J. Phys. Chem. A* 108, 707-710 (2004).
125. Izaki, K. Enzymatic reduction of mercurous and mercuric ions in Bacillus cereus. *Can J Microbiol* 27, 192-7 (1981).
126. Chatziefthimiou, A.D., Crespo-Medina, M., Wang, Y., Vetriani, C. & Barkay, T. The isolation and initial characterization of mercury resistant chemolithotrophic thermophilic bacteria from mercury rich geothermal springs. *Extremophiles* 11, 469-79 (2007).
127. Irving, P.L., Kritee, K. & Barkay, T. Intra and extracellular constraints on substrate's chemical speciation drive evolution of the mercuric ion reductase. *submitted* (2008).
128. Hsieh, J.L., Chen, C.Y., Chang, J.S., Endo, G. & Huang, C.-C. Overexpression of a Single Membrane Component from the *Bacillus mer* Operon Enhanced Mercury Resistance in an *Escherichia coli* Host. *Bioscience, Biotechnology, and Biochemistry* 71, 1494-1499 (2007).

129. Belliveau, B.H. & Trevors, J.T. Mercury resistance determined by a self-transmissible plasmid in *Bacillus cereus* 5. *Biometals* 3, 188-196 (1990).
130. Schecher, W.D. & Mcavoy, D. MINEQL+: A Chemical Equilibrium Program for Personal Computers. *Environmental Research Software: Hollowell, ME.* (1994).
131. Martell, A.E., Smith, R.M. & Motekaitis, R.J. NIST Critical Stability Constants of 21 Metal Complexes Database. in *U. S. Department of Commerce: Gaithersburg, MD.* (1998).
132. Huang, C.-C., Narita, M., Yamagata, T., Itoh, Y. & Endo, G. Structure analysis of a class II transposon encoding the mercury resistance of the Gram-positive bacterium *Bacillus megaterium* MB1, a strain isolated from Minamata Bay, Japan. *Gene* 234, 361-369 (1999).
133. Huang, C.-C. et al. Polypeptides for heavy-metal biosorption: capacity and specificity of two heterogeneous MerP proteins. *Enzyme and Microbial Technology: The 8th Symposium of Young Asian Biochemical Engineers' Community (YABEC 2002)* 33, 379-385 (2003).
134. Yamaguchi, A., Tamang, D. & Saier, M. Mercury Transport in Bacteria. *Water, Air, & Soil Pollution* 182, 219-234 (2007).
135. Lund, P.A. & Brown, N.L. Role of the merT and merP gene products of transposon Tn501 in the induction and expression of resistance to mercuric ions. *Gene* 52, 207-214 (1987).
136. Nakahara, H., Silver, S., Miki, T. & Rownd, R.H. Hypersensitivity to Hg^{2+} and hyperbinding activity associated with cloned fragments of the mercurial resistance operon of plasmid NR1. *J Bacteriol* 140, 161-6 (1979).
137. Lu-Irving, P., Kritee, K. & Barkay, T. Intra and extracellular constrains on substrate's chemical speciation drive the evolution of mercuric reductase (submitted). (2008).
138. Yu, H., Chu, L. & Misra, T.K. Intracellular inducer Hg^{2+} concentration is rate determining for the expression of the mercury-resistance operon in cells. *J Bacteriol* 178, 2712-4 (1996).
139. Gambill, B.D. & Summers, A.O. Synthesis and degradation of the mRNA of the Tn21 *mer* operon. *Journal of Molecular Biology* 225, 251-259 (1992).
140. Crespo-Medina, M., Barkay, T. & Vetriani, C. Mercuric reductase enzymes from mesophilic bacteria are optimally active at a moderately thermophilic to thermophilic temperature range. in *Extremophiles 2004: 5th International Conference on Extremophiles.* (Cambridge, MD., 2004).
141. Bottcher, M.E., Sievert, S.M. & Kuever, J. Fractionation of sulfur isotopes during dissimilatory reduction of sulfate by a thermophilic gram-negative bacterium at 60 degrees C. *Arch Microbiol* 172, 125-8 (1999).
142. Fang, R. et al. Differential Label-free Quantitative Proteomic Analysis of *Shewanella oneidensis* Cultured under Aerobic and Suboxic Conditions by Accurate Mass and Time Tag Approach. *Mol Cell Proteomics* 5, 714-725 (2006).
143. Frank Vanrobaeys et al. Proteomics of the dissimilatory iron-reducing bacterium *Shewanella oneidensis* MR-1, using a matrix-assisted laser desorption/ionization-tandem-time of flight mass spectrometer. *PROTEOMICS* 3, 2249-2257 (2003).

144. Maier, T.M. & Myers, C.R. The outer membrane protein Omp35 affects the reduction of Fe(III), nitrate, and fumarate by *Shewanella oneidensis* MR-1. *BMC MICROBIOLOGY* 4, 23 (2004).
145. Beliaev, A.S. et al. Microarray Transcription Profiling of a *Shewanella oneidensis* etrA Mutant. *J Bacteriol* 184, 4612-4616 (2002).
146. Beliaev, A.S. et al. Global Transcriptome Analysis of *Shewanella oneidensis* MR-1 Exposed to Different Terminal Electron Acceptors. *J. Bacteriol.* 187, 7138-7145 (2005).
147. Technologies, A. Recovery of Mercury from Contaminated Liquid Wastes: Topical Report Covering Base Contract (ADA Project Number 4446). (ed. Prepared by: ADA Technologies, I.E., CO) Page 41 (For Federal Energy Technology Center - Morgantown, Morgantown, WV, 1998).
148. Mohan, D., Gupta, V.K., Srivastava, S.K. & Chander, S. Kinetics of mercury adsorption from wastewater using activated carbon derived from fertilizer waste. *Colloids and Surfaces A: Physicochemical and Engineering Aspects* 177, 169-181 (2000).
149. Kritee, K., Blum, J.D. & Barkay, T. Chapter 2: Mercury stable isotope fractionation during *mer* mediated degradation of methylmercury. (In preparation). (2008).
150. Golding, G.R. et al. Evidence for facilitated uptake of Hg(II) by *Vibrio anguillarum* and *Escherichia coli* under anaerobic and aerobic conditions. *Limnol. Oceanogr.* 47, 967-975 (2002).
151. Golding, G.R., Kelly, C.A., Sparling, R., Loewen, P.C. & Barkay, T. Evaluation of mercury toxicity as a predictor of mercury bioavailability. *Environ Sci Technol* 41, 5685-92 (2007).
152. Golding, G.R., Sparling, R. & Kelly, C.A. Effect of pH on Intracellular Accumulation of Trace Concentrations of Hg(II) in *Escherichia coli* under Anaerobic Conditions, as Measured Using a *mer-lux* Bioreporter. *Appl. Environ. Microbiol.* 74, 667-675 (2008).
153. Viamajala, S., Peyton, B.M., Sani, R.K., Apel, W.A. & Petersen, J.N. Toxic Effects of Chromium(VI) on Anaerobic and Aerobic Growth of *Shewanella oneidensis* MR-1. *Biotechnol. Prog.* 20, 87-95 (2004).
154. Kavner, A., Bonet, F., Shahar, A., Simon, J. & Young, E. The isotopic effects of electron transfer: An explanation for Fe isotope fractionation in nature. *Geochimica et Cosmochimica Acta* 69, 2971-2979 (2005).
155. Felle, H., Porter, J.S., Slayman, C. & Kaback, H. Quantitative measurements of membrane potential in *Escherichia coli*. *Biochemistry* 19, 3585-3590 (1980).
156. Nikaido, H. Molecular Basis of Bacterial Outer Membrane Permeability Revisited. *Microbiol. Mol. Biol. Rev.* 67, 593-656 (2003).
157. Delcour, A.H. Solute uptake through general porins. *Front Biosci.* 8, 1055-1071 (2003).
158. Kashket, E.R. Effects of aerobiosis and nitrogen source on the proton motive force in growing *Escherichia coli* and *Klebsiella pneumoniae* cells. *J Bacteriol* 146, 377-384 (1981).

159. Honig, B.H., Hubbell, W.L. & Flewelling, R.F. Electrostatic Interactions in Membranes and Proteins. *Annual Review of Biophysics and Biophysical Chemistry* 15, 163-193 (1986).
160. Flewelling, R.F. & Hubbell, W.L. The membrane dipole potential in a total membrane potential model. Applications to hydrophobic ion interactions with membranes. *Biophys. J.* 49, 541-552 (1986).
161. Comstock, J.P. Steady-state isotopic fractionation in branched pathways using plant uptake of NO3- as an example. *Planta* 214, 220-34 (2001).
162. Richter, F.M. et al. Kinetic isotopic fractionation during diffusion of ionic species in water. *Geochimica et Cosmochimica Acta* 70, 277-289 (2006).
163. Sahlman, L., Wong, W. & Powlowski, J. A mercuric ion uptake role for the integral inner membrane protein, MerC, involved in bacterial mercuric ion resistance. *Journal of Biological Chemistry* 272, 29518-29526 (1997).
164. Yates III, L.M. & von Wandruszka, R. Functional group analysis of Suwannee River fulvic acid with reactive fluorescent probes. *Fresenius' Journal of Analytical Chemistry* 364, 746-748 (1999).
165. Huang, C.-C., Narita, M., Yamagata, T. & Endo, G. Identification of three merB genes and characterization of a broad-spectrum mercury resistance module encoded by a class II transposon of Bacillus megaterium strain MB1. *Gene* 239, 361-366 (1999).
166. Galimov, E.M. *The Biological Fractionation of Isotopes*, 261 (Academic Press, Inc., Orlando, Florida, 1985).
167. Lewis, B.E. & Schramm, V.L. Enzymatic binding isotope effects and the interaction of glucose with hexokinase. in *Isotope effects in Chemistry and Biology* (eds. Kohen, A. & Limbach, H.) 1020-1048 (Taylor and Francis Group, Florida, 2006).
168. Atkins, P. *Physical Chemistry*, (W. H. Freeman and Company, New York, 1998).
169. Hintelmann, H. & Evans, R.D. Application of stable isotopes in environmental tracer studies - Measurement of monomethylmercury (CH3Hg+) by isotope dilution ICP-MS and detection of species transformation. *Fresenius J. Anal. Chem.* 358, 378-85 (1997).
170. Pickhardt, P.C., Folt, C.L., Chen, C.Y., Klaue, B. & Blum, J.D. Algal blooms reduce the uptake of toxic methylmercury in freshwater food webs. *PNAS Biological Sciences: Ecology* 99, 4419-4423 (2002).
171. Hintelmann, H. et al. Reactivity and mobility of new and old mercury deposition in a boreal forest ecosystem during the first year of the METAALICUS study. Mercury Experiment To Assess Atmospheric Loading In Canada and the US. *Environ Sci Technol* 36, 5034-40 (2002).
172. Eckley, C.S. & Hintelmann, H. Determination of mercury methylation potentials in the water column of lakes across Canada. *Sci. Total Environ.* 368, 111-125 (2006).
173. Hintelmann, H. & Ogrinc, N. Determination of stable mercury isotopes by ICP/MS and their application in the environmental studies. in *Biogeochemistry of environmentally important trace elements* (eds. Cai, Y. & Braids, O.) (American Chemical Society, Washigton, DC, 2003).

174. Kiyono, M., Omura, T., Inuzuka, M., Fujimori, H. & Pan-Hou, H. Nucleotide sequence and expression of the organomercurial-resistance determinants from a *Pseudomonas* K-62 plasmid pMR26. *Gene* 189, 151-157 (1997).
175. Lin-Chao, S., Chen, W.-T. & Wong, T.-T. High copy number of the pUC plasmid results from a Rom/Rop-suppressible point mutation in RNA II. *Molecular Microbiology* 6, 3385-3393 (1992).
176. Pogliano, J., Ho, T.Q., Zhong, Z. & Helinski, D.R. Multicopy plasmids are clustered and localized in *Escherichia coli*. *Proceedings of the National Academy of Sciences* 98, 4486-4491 (2001).
177. Bernstein, J.A., Khodursky, A.B., Lin, P.-H., Lin-Chao, S. & Cohen, S.N. Global analysis of mRNA decay and abundance in *Escherichia coli* at single-gene resolution using two-color fluorescent DNA microarrays. *Proceedings of the National Academy of Sciences* 99, 9697-9702 (2002).
178. Nilsson, G., Belasco, J.G., Cohen, S.N. & von Gabain, A. Growth-rate dependent regulation of mRNA stability in Escherichia coli. 312, 75-77 (1984).
179. Iost, I. & Dreyfus, M. The stability of Escherichia coli lacZ mRNA depends upon the simultaneity of its synthesis and translation. *EMBO Journal* 14, 3252-3261 (1995).

Curriculum Vita

Kritee

Education

2001- 2008	Doctoral Candidate, Microbiology and Molecular Genetics Program, Department of Biochemistry and Microbiology **Rutgers University, New Brunswick, New Jersey**
2007	Microbial Diversity Summer Course **Marine Biological Laboratory, Woods Hole, Massachusetts**
1996-2001	Five year Integrated Bachelors and Masters of Technology Department of Biochemical Engineering & Biotechnology **Indian Institute of Technology, New Delhi (IITD), India**

Publications

1. **Kritee K.,** Joel. D. Blum and Tamar Barkay (2008), A review on microbial stable isotope fractionation framework (under preparation).

2. **Kritee K.,** Joel. D. Blum and Tamar Barkay (2008), Contraints on the extent of mercury stable isotope fractionation during reduction of Hg(II) to Hg(0) by different microbial species (under preparation for *Applied and Environmental Microbiology*).

3. **Kritee K.,** Joel. D. Blum and Tamar Barkay (2008), Mercury stable isotope fractionation during *mer* mediated degradation of methylmercury (under preparation for *Geochimica et Cosmochimica Acta*).

4. Patricia Lu-Irving**, Kritee K.** and Tamar Barkay (2008), Distribution and characteristics of amino acids sequences of the enzyme mercuric reductase (MerA) among bacteria and archaea and the implications on evolution of the *mer* operon (submitted to *Proceeding of the National Academy of Sciences*).

5. **Kritee K.,** Joel. D. Blum, Marcus. W. Johnson, Bridget. A. Bergquist and Tamar Barkay (2007), Mercury stable isotope fractionation during reduction of Hg(II) to Hg(0) by mercury resistant microorganisms. *Environmental Science and Technology.* **41:**1889-1895

6. **Kritee K.**, Bjorn Klaue, Joel D. Blum and Tamar Barkay (2005), Biological mercury isotope fractionation. *Geochimica et Cosmochimica Acta.* **69** (10) Supplement 1: 708

7. **Kritee K**., Bjorn Klaue, Tamar Barkay & Joel Blum (2004), Mercury isotopic fractionation observed during the reduction of Hg(II) to Hg(0) by the bacterial mercuric reductase. *RMZ – Materials and Geoenvironment.* **51**(2): 1154-55.

8. Samrat Dutta*, Poonam Singhal*, Praveen Agarwal*, Raju Tomer*, **Kritee K**.*, Ekta Khurana and B. Jayaram (2006), A Physicochemical Model for analyzing DNA sequences. *Journal of Chemical Information and Modeling* **46**: 78-85 * equal contributors